

EMISSIONS, EFFICIENCY,  
AND COMBUSTION CHAMBER CONDITIONS  
OF A SMOKELESS, HAND-FIRED COAL HEATER

by

Daniel Waslo

Thesis submitted to the Graduate Faculty of the  
Virginia Polytechnic Institute and State University  
in partial fulfillment of the requirements for the degree of

MASTER OF SCIENCE

in

Mechanical Engineering

APPROVED:

---

D. R. Jaasma, Chairman

---

A. M. Squires

---

C. L. Yates

April, 1982

Blacksburg, Virginia

## ACKNOWLEDGMENTS

The author would like to thank Dr. Dennis R. Jaasma for his advice and guidance throughout the course of this project. Dr. Arthur Squires and Dr. Charles Yates are thanked for their advice and service on the graduate committee. Special thanks are extended to the Department of Health, Education, and Welfare for providing a fellowship for graduate studies which made this work possible. The coal analyses provided by R. A. Rice of the Westmoreland Coal Company are greatly appreciated. The Aga-Rayburn Division of Glynwed Appliances, Ltd. is gratefully thanked for their donation of the test heater.

The author is indebted to his lovely fiancée, Jennifer Mackend, for her support and encouragement throughout his graduate work. His parents are sincerely thanked for their encouragement during his academic career.

## TABLE OF CONTENTS

	<u>Page</u>
Acknowledgments . . . . .	ii
Table of Contents . . . . .	iii
List of Figures . . . . .	vi
List of Tables . . . . .	ix
Nomenclature . . . . .	x
1. Introduction . . . . .	1
2. Literature Review . . . . .	3
2.1 Smoke Formation and Measurement . . . . .	3
2.2 Secondary Combustion and Smokeless Furnaces . . . . .	7
2.3 Efficiency Measurement Techniques . . . . .	12
2.4 Probe Sampling Techniques . . . . .	13
3. Experimental Apparatus and Procedures . . . . .	17
3.1 Experimental Apparatus . . . . .	17
3.1.1 Description of Test Heater . . . . .	17
3.1.2 Description of Probe Sampling Apparatus . . . . .	19
3.1.3 Description of Emissions and Efficiency Measurement Apparatus . . . . .	25
3.2 Description of Test Coals . . . . .	34
3.3 Experimental Procedures . . . . .	36
3.3.1 Axial Probe Sampling Test Procedure . . . . .	36
3.3.2 Axial and Radial Probe Sampling Test Procedure . . . . .	37
3.3.3 Temperature Variation Test Procedure . . . . .	37

# TABLE OF CONTENTS (Continued)

	<u>Page</u>
3.3.4 Emissions and Efficiency Test Procedure -- Maximum Burning Rate . . . . .	38
3.3.5 Emissions and Efficiency Test Procedure -- Low Burning Rate . . . . .	40
3.3.6 Particulate Sizing Procedure . . . . .	41
4. Data Reduction . . . . .	42
4.1 Emission Factor Calculations . . . . .	42
4.2 Efficiency Calculations . . . . .	46
4.3 Calculation of Gas Residence Time in Secondary Combustion Chamber . . . . .	48
5. Results and Discussion . . . . .	51
5.1 Species Concentration and Temperature Measurements in Secondary Combustion Zone . . . . .	51
5.2 Emissions Tests . . . . .	63
5.2.1 Emission Factors for High Burning Rate Tests .	63
5.2.2 Emission Factors for Low Burning Rate Tests .	78
5.2.3 Particulate Sizing . . . . .	85
5.3 Efficiency Test Results . . . . .	87
5.4 Uncertainty Analysis . . . . .	94
6. Conclusions . . . . .	97
7. Recommendations . . . . .	99
8. References . . . . .	101

# TABLE OF CONTENTS (Continued)

	<u>Page</u>
Appendices . . . . .	104
A. Heat Transfer in Water-Cooled Probe . . . . .	104
B. Conversion of Species Concentrations from Dry to Wet Basis . . . . .	106
C. Data Reduction Program Listing . . . . .	109
D. Measured Axial Species Concentrations in Secondary Combustion Zone for the High, Intermediate, and Low Burning Rate Tests . . . . .	115
E. Calculation of Diluted CO <sub>2</sub> Concentrations . . . . .	119
Vita . . . . .	121
Abstract	

## LIST OF FIGURES

<u>Figure</u>		<u>Page</u>
1	Cross-Section of Rayburn Prince 76 . . . . .	18
2	Orientation of Water-Cooled Sampling Probe and Fast Response Suction Pyrometer in Secondary Combustion Chamber . . . . .	20
3	Water-Cooled Gas Sampling Probe . . . . .	21
4	Two-Dimensional Stainless Steel Water-Cooled Gas Sampling Probe . . . . .	23
5	Probe Sampling Train . . . . .	24
6	Fast Response Suction Pyrometer . . . . .	26
7	Flue Gas Handling System for Emissions and Efficiency Tests . . . . .	27
8	Boiler Water Flow Path . . . . .	29
9	Stack Gas Sampling Train . . . . .	31
10	Smoke Sampling Train . . . . .	32
11	Cascade Impactor Sampling Train . . . . .	33
12	Axial Gas Temperature Measurements in Secondary Combustion Zone for Intermediate Burning Rate Test .	52
13	Axial Species Concentration Measurements in Secondary Combustion Zone for Intermediate Burning Rate Test . . . . .	53
14	Species Concentrations over Six Cross-Sections in Secondary Combustion Zone for Intermediate Burning Rate Test . . . . .	60
15	Position of Two-Dimensional Probe in Secondary Combustion Chamber . . . . .	61
16	Oscilloscope Trace Displaying Temperature Variation At a Point Near the Entrance of the Secondary Combustion Chamber . . . . .	64

LIST OF FIGURES  
(Continued)

<u>Figure</u>		<u>Page</u>
17	Instantaneous CO Emission Factor for the High Burning Rate Clinchfield Test . . . . .	65
18	Instantaneous CO Emission Factor for the High Burning Rate Pocahontas Test . . . . .	66
19	Instantaneous NO <sub>x</sub> Emission Factor for the High Burning Rate Clinchfield Test . . . . .	67
20	Instantaneous NO <sub>x</sub> Emission Factor for the High Burning Rate Pocahontas Test . . . . .	68
21	Instantaneous SO <sub>x</sub> Emission Factor for the High Burning Rate Clinchfield Test . . . . .	69
22	Instantaneous SO <sub>x</sub> Emission Factor for the High Burning Rate Pocahontas Test . . . . .	70
23	Instantaneous CO Emission Factor for the Low Burning Rate Clinchfield Test . . . . .	79
24	Instantaneous CO Emission Factor for the Low Burning Rate Pocahontas Test . . . . .	80
25	Instantaneous NO <sub>x</sub> Emission Factor for the Low Burning Rate Clinchfield Test . . . . .	81
26	Instantaneous NO <sub>x</sub> Emission Factor for the Low Burning Rate Pocahontas Test . . . . .	82
27	Instantaneous SO <sub>x</sub> Emission Factor for the Low Burning Rate Clinchfield Test . . . . .	83
28	Instantaneous Efficiency for the High Burning Rate Clinchfield Test . . . . .	88
29	Instantaneous Efficiency for the High Burning Rate Pocahontas Test . . . . .	89
30	Instantaneous Efficiency for the Low Burning Rate Clinchfield Test . . . . .	90

LIST OF FIGURES  
(Continued)

<u>Figure</u>		<u>Page</u>
31	Instantaneous Efficiency for the Low Burning Rate Pocahontas Test . . . . .	91
32	Sample Gas Temperature vs. Distance and Time from Tip of Water-Cooled Sampling Probe . . . . .	105



## LIST OF TABLES

<u>Table</u>		<u>Page</u>
I	Test Coal Data . . . . .	35
II	Comparison of Measured and Calculated CO <sub>2</sub> Concentrations (Based on Dilution) in Secondary Combustion Chamber . . . . .	58
III	CO, NO <sub>x</sub> , SO <sub>x</sub> , and Smoke Emission Factors for High and Low Burning Rate Tests with Comparison to Other's Results . . . . .	71
IV	Smoke Emission Rates for High and Low Burning Rate Tests with Comparison to British Results and Standards . . . . .	77
V	Particulate Size Distributions for the Rayburn Prince 76 Operating on Pocahontas and Clinchfield Coals . . . . .	86
VI	Energy Loss Distributions, Efficiencies, and Average Useful Heat Outputs for High and Low Burning Rate Tests . . . . .	92
VII	Measured Axial Species Concentrations (Wet Basis) in Secondary Combustion Zone for High Burning Rate Test . . . . .	116
VIII	Measured Axial Species Concentrations (Wet Basis) in Secondary Combustion Zone for Intermediate Burning Rate Test . . . . .	117
IX	Measured Axial Species Concentrations (Wet Basis) in Secondary Combustion Zone for Low Burning Rate Test . . . . .	118

## NOMENCLATURE

$a$	molar ratio of water to hydrogen in coal
$A$	area, $m^2$
$C$	correction factor
$C_d$	orifice discharge coefficient, 0.608
$\bar{C}_p$	molar constant pressure specific heat of air, 30 J/mol K
$d$	distance between inlet and outlet of secondary combustion chamber, m
$\dot{E}$	energy release or loss rate, kW
$EF$	emission factor, g/kg
$\dot{H}$	average useful heat output from stove, kW
$\bar{h}_{fg}$	enthalpy of vaporization of water, 43,740 J/mol
$HV$	heating value, kJ/kg
$\dot{m}$	instantaneous burning rate of coal, kg/s
$M$	total mass
$\dot{M}$	mass emission rate, g/s
$MW$	molecular weight, g/mol
$n$	number of moles
$\dot{n}$	molar flow rate, kg mol/s
$P$	pressure, kPa
$\Delta P$	pressure drop across orifice, kPa
$\dot{Q}$	volumetric flow rate, $m^3/s$
$r$	molar ratio of carbon to hydrogen in coal
$R$	universal gas constant, 8.314 J/mol K
$t$	time, s

## NOMENCLATURE (Continued)

T	temperature, K
V	velocity, m/s
W	maximum permitted smoke emission rate, g/h
X	mole fraction
y	mass fraction
$\eta$	instantaneous efficiency, %
$\phi$	relative humidity, %

### Subscripts

A	average
C	carbon
ch	chemical loss due to gas phase species
col	collected
com	combustion generated
D	dry basis
DT	dilution tunnel
DW	dry to wet basis
em	emitted from stove
h	humidity
i	inlet
l	latent
m	moisture
o	outlet

NOMENCLATURE  
(Continued)

or	orifice
p	probe
r	room
rs	residence
s	stack
sc	secondary combustion zone
sen	sensible
sm	smoke
sr	saturated moisture at room temperature
w	wet basis

## 1. INTRODUCTION

As late as 1950, the majority of American homes were using coal as a primary heating fuel. However, in the 1950's Americans switched to oil and natural gas as heating fuels, as they were cheaper, cleaner, and more convenient to burn than coal. Presently, only about 1% of the nation's homes are heated with coal. However, as oil and natural gas reserves diminish, there is renewed interest in the use of coal as a residential heating fuel.

Some research on coal stoves was done in the U.S. from 1920 to 1950 in an attempt to reduce smoke emissions. Indeed, it seemed that substantial progress had been made toward the development of smokeless coal stoves. However, the decline of the coal stove industry essentially ended all research efforts.

Although coal stove research ended in the U.S., British research continued, spurred on by the Clean Air Act of 1956. Today their work is considered state-of-the-art. As coal stove research is being revived in the U.S. today, it would be wise to learn what the British have already learned in the area of reducing smoke emissions from coal burning appliances.

The object of this research is to quantify the emissions and efficiency of the Rayburn Prince 76, a clean-burning, hand-fired coal heater developed by the British and which utilizes staged combustion. In order to gain an understanding of how the Prince operates, probe sampling was conducted in this unit's secondary combustion chamber. This work is of importance since very little is known concerning

emissions from hand-fired coal stoves and their combustion chamber conditions. The findings from this project significantly augment present knowledge in these areas. It was also desired to determine if the Prince's design would lead to low smoke emissions when operated on American bituminous coals. If so, effective emissions-reducing features of the unit could possibly be incorporated into future American coal stove designs.

## 2. LITERATURE REVIEW

The first section of this literature review discusses the formation of smoke from coal and how smoke emissions can be measured. A significant portion of this research was devoted to studying smoke emissions and it is important for the reader to have some background in smoke measurement techniques. A discussion of secondary combustion and how it has been applied to reduce smoke emissions from residential coal-fired heaters is presented next. A section on efficiency measurement techniques is included to familiarize the reader with this area, since thermal performance assessment was also an important part of this research effort. Finally, a brief review of probe sampling and its limited application to furnace studies is presented.

### 2.1 Smoke Formation and Measurement

The term smoke is not precisely defined. However, it is generally considered to consist of particulate matter and condensed hydrocarbons. When a lump of coal is heated, the volatiles present in the coal are distilled. If the fuel bed temperatures are low and not enough oxygen is present, the smoke emitted by a coal stove consists mainly of condensed hydrocarbons (1). High fuel bed temperatures combined with insufficient combustion air causes the hydrocarbons emitted by the coal to crack and form carbon or soot. The interested reader is referred to the works of Ubhayakar, et al. (2) and Howard and Essenhigh (3) concerning the mechanisms of coal devolatilization and volatile combustion.

Detailed analyses concerning soot formation are presented by Calcote (4), Gaydon and Wolfhard (5), and Prado, et al. (6).

In general, the amount of smoke produced by a coal heater is directly related to the volatile content of the coal. Research conducted by Jaasma and Macumber (7), DeAngelis and Reznik (8), and Giammer, et al. (9) has indicated that high volatile coals (coals with a volatile content greater than 25% by mass) produce smoke emission factors up to four times greater than those produced by low volatile coals burned under identical conditions.

A number of techniques have been devised to quantify smoke emissions from residential coal stoves. However, if each method was used to measure the smoke emissions from a coal stove burning under identical conditions, it is unlikely that all of the measured smoke emission values would agree. The main reason for the discrepancies lies in the measurement of condensed organics. This will be discussed further with each method.

The simplest method of quantifying smoke emissions is through the use of a Ringlemann chart, basically a card with different shades of gray printed on it. By comparing the shade of the smoke issuing from a stack and the shades on the card, the user arrives at a number (from one to five) which characterizes the smoke density. Obviously, this method is quite subjective and only gives the user a rough estimate of the smoke emissions. This method had been used by Azbe (10) in 1927 and Landry and Sherman (1) in 1948 to estimate the smoke emissions from the "smokeless" stove designs they were testing.



The British have been using an electrostatic precipitator to measure smoke emissions from residential coal-fired appliances. The entire effluent from a stove being tested is passed through this device, and it is claimed that over 95% of the particulate matter is captured (11). The mass of collected particulates is determined by weighing the entire precipitator unit before and after each test. Since the gases which pass through the precipitator are hot (the precipitator is mounted just over the chimney exit), it is likely that the lower boiling point organics emissions are not captured. This could result in a lower estimate of smoke emissions than determined by another method. The British consider this technique to be quite adequate, and they have used it extensively in their smokeless fuel and heater research work (11,12,13).

Various versions of the EPA Method 5 sampling train have been used to quantify smoke emissions from residential coal stoves. This method uses a heated probe to isokinetically sample the flue gases. Particulates are captured on a heated filter and the condensible organics passing through the filter are captured by flowing the gases through a set of impingers held in an ice bath. Alternatively, a resin trap can be used in front of the ice bath to increase collection of the condensible organics. Disadvantages associated with this smoke collection method include high cost and difficulty in maintaining isokinetic sampling. (Determination of stack velocity is difficult due to the very low velocities involved.) Giammer, et al. (9) used the Method 5 sampling train to quantify the smoke emissions factors for two residen-

tial stoker-fired boilers. DeAngelis and Reznik (8) also used this method to measure smoke emissions from a stoker-fired boiler and warm air furnace.

Jaasma and Macumber (7) utilized a dilution tunnel to determine the smoke emissions from two hand-fired coal stoves. In this technique, all of the stack emissions, along with room air, are drawn into the dilution tunnel by a fan. Since the flow rate in the dilution tunnel is easily measured, a sampling probe can be used to isokinetically sample the dilution tunnel. Particulates and condensible organics were collected on fiberglass filters at room temperature. Advantages of this system include low cost and the ability of the coal stove being tested to operate under natural draft.

A similar system was utilized by Butcher and Ellenbecker (14) to measure smoke emissions factors from a small hand-fired coal heater. However, in this system the stove effluent was drawn into a large dilution tunnel ( $11 \text{ m}^3$ ) to more closely simulate the stove discharging into the atmosphere. A sampling probe was used to withdraw smoke samples from the tunnel and the particulates were captured in a cyclone and on fiberglass filters.

Toynbee (15) discusses a smoke measurement system used in New Zealand in which all the effluent leaving the stack, along with some dilution air, are drawn through a large Nomex<sup>\*</sup> bag ( $2.6 \text{ m}^2$  surface area) mounted in a plenum. The mass of collected particulates is

---

<sup>\*</sup>Trade Name, E. I. DuPont DeNemours Co.

determined by weighing the bag prior to and after each test. This system has the advantage of allowing the test stove to operate under natural draft conditions. However, the temperature of the stack gas/dilution air mixture entering the plenum may be high enough to allow some condensible organics to pass through the bag and escape collection.

In summary, different smoke measurement techniques determine smoke emissions differently. Collection methods such as the EPA Method 5 train are likely to capture more condensible organics emissions than a method such as the precipitator. Some caution must be used when comparing results determined by different methods.

## 2.2 Secondary Combustion and Smokeless Furnaces

Secondary combustion involves mixing the volatiles from the coal in the primary combustion zone with secondary air. This mixture then reacts, giving oxidation of the volatiles. In order to effect complete secondary combustion, three conditions are required: (1) the volatiles must contact a sufficient amount of air, (2) the temperature of the mixture must be kept sufficiently high, (3) the mixture must be kept at the required temperature for a sufficient time. Dickinson and Payne (12) of the National Coal Board (NCB) in England claim that a temperature of 550°C and a residence time of 0.5 s are needed for complete combustion of volatiles. However, they do not report oxygen concentrations needed for secondary combustion. Squires (16) discusses research at the NCB laboratory at Stoke Orchard which indicates that a residence time of 0.5 - 1 s is needed at 700°C. Indeed, there seems to be some

confusion about what conditions are needed for effective secondary combustion.

Hautman, et al. (17) studied hydrocarbon oxidation in a turbulent flow reactor at Princeton University and their results show that some aliphatic hydrocarbons can partially oxidize to CO in about 0.16 s at a temperature of 700°C. Judging from these results, the combustion requirements cited by Squires may be plausible.

The principle of secondary combustion can be applied to practical hand-fired furnaces. Successful designs generally incorporate down-draft combustion, in which the volatiles are drawn downward through the hot coal bed, and the addition of a secondary combustion zone with a separate air supply. The secondary combustion zone serves as an after-burner to further combust the volatiles.

The design of the secondary combustor chamber is critical to the smokeless operation of the unit. In order to maintain high gas temperatures in the secondary combustion zone, it is generally lined with insulating firebrick (13). Preheating the secondary air before introducing it into the chamber also helps to maintain high temperatures after the air and primary products mix.

A key problem associated with secondary combustion is achieving the proper mixing of the volatiles and the secondary air. Landry and Sherman (1) investigated a number of stove designs with various sizes, shapes, and placements of the secondary combustion chamber. Most of the designs indicated poor mixing between the volatiles and secondary air at the mouth of the secondary combustion chamber, resulting in a stratified

mixture with incomplete combustion. The final result of their work was a heater which used cross-flow primary air and had good mixing between volatiles and secondary air as a result of the use of a refractory arch at the entrance of the secondary combustion chamber. The unit was claimed to be smokeless in operation. However, no accurate smoke emissions tests were conducted and the determination of "smokeless" operation was only made using Ringlemann charts. An efficiency of 65%, determined with a calorimeter room, was stated for the unit.

In 1964, the NCB in England, in collaboration with manufacturers of residential heaters, began a program to incorporate effective secondary combustion in residential heating appliances (13). The goal of this program was to develop a series of domestic heating appliances that could smokelessly burn ordinary bituminous coals. A considerable savings could be realized by the homeowner burning ordinary bituminous coal over more expensive processed smokeless fuels such as anthracite and briquetted cokes. The smokeless heater development work was carried out using a "combustion box" in which the internal geometry of the unit, as well as the position, direction, and flow rates of the primary and secondary air streams could be varied (13). This work led to a series of practical smokeless appliances -- three room heaters with boilers rated at 8.0, 10.0, and 11.7 kW, a gravity-feed boiler rated at 17 kW, and an underfeed stoker rated at 23 kW. Efficiencies were claimed to range from 70 to 80 percent for these units. Smoke emissions, measured with an electrostatic precipitator, were reported to range from 1.2 - 5.9 g/h (approximately 1 - 12 g/kg). These emission rates were well

within the British smoke control standard in which the maximum allowable smoke emission rate is given by

$$W = \frac{\dot{H}}{3} + 5 \quad (1)$$

where

$W$  = maximum permitted smoke emissions (g/h)

$\dot{H}$  = mean heat output of appliance (kW)

The design of these early smokeless heaters (dubbed "smoke eaters") was similar to the stoves developed by Landry and Sherman (1). They were of down-draft design with refractory-lined secondary combustion zones. However, fans were needed to supply combustion air to these units in order to provide smokeless operation at higher burning rates. The ratio of primary to secondary air was designed to be approximately 1:1 in order to satisfy combustion air requirements when the volatiles in the fuel were distilling and not produce excessive sensible energy losses after the volatiles were driven off. These early units were sensitive to the caking properties of the coal and were only able to burn weakly caking coals in the singles sizes. (British coals are classified as singles (1/2 - 1 in.), doubles (1-2 in.) and trebles (2-3 in.)(12).)

A "second generation" of smoke eaters appeared on the British scene in the mid-nineteen seventies. These new units were simpler and more versatile than their predecessors. They relied on only natural draft for combustion air, thus eliminating the need for the potentially troublesome fans. It was claimed that these units were not sensitive to

the caking properties of the coals used and could burn both doubles and trebles sizes. Efficiencies for these units were reported to range from 50 to 80%. Smoke emissions were determined with a electrostatic precipitator and were found to range from 2.5 to 5.9 g/h (approximately 1 to 7 g/kg), again passing the British standard handily (12). The first of these new smoke eaters, the Rayburn Prince 76, was released to the public in 1975. This combination boiler/radiant heater, manufactured by the Aga-Rayburn Division of Glynwed Appliances Limited in Stirlingshire, has a rated output of 10.7 kW.

New Zealand has been developing a number of smokeless heaters since smoke from residential heaters has become a problem in some parts of that country. Intermittently-charged heaters have been developed which utilize secondary combustion to provide low smoke emissions ranging from 1.3 to 5.5 g/h (approximately 2 to 9 g/kg) (15). Efficiencies for these units are claimed to range from 50 to 65%. A magazine-fed domestic heater has also been developed in which the volatiles are slowly distilled from the fuel, eliminating the problem of large initial volatile release. The smoke emission for this unit is reported to be 1.6 g/hr (approximately 2 g/kg) and the claimed efficiency is 70 to 75%.

Work is continuing today at Stoke Orchard in England with the intended goal of producing a wide range of efficient, clean-burning, coal-fired appliances. Some ongoing work includes a hopper-fed high amenity boiler, a domestic scale fluidized bed boiler, and a very low output (3 to 4 kW) coal heater for well-insulated houses.

### 2.3 Efficiency Measurement Techniques

There are basically two ways to measure the efficiency of small coal stoves -- room calorimetry and the "stack loss" method. Room calorimetry, generally acknowledged to be the more accurate method, involves placing the stove to be tested in a well-insulated, air tight room. The heat given off by the stove is measured by the temperature rise of a known flow rate of air which is passed through the room. Alternatively, water is sometimes used as the heat transfer medium. This method yields a continuous record of heat output rate over time, which when integrated yields the total heat output of the stove during the test. Although this technique is very accurate, there is a large expense involved in building a well-designed calorimetry room. This technique was used by Landry and Sherman (1) in order to test the efficiency of a "smokeless" coal stove.

The stack loss method is an indirect technique for calculating efficiency in which it is assumed that the useful heat output of a heater is given by the difference in energy released by the fuel and the energy losses up the stack. The stack losses, which include the sensible, chemical, and latent heat losses, are found by determination of the temperature, composition, and flow rate of the stack gases. This method is inexpensive and widely used, but it is not without disadvantages. Chemical energy losses are often attributed to only CO emissions. However, to fully characterize the chemical losses, it is necessary to measure or calculate the hydrocarbon content in the gases, which is no easy task. Gas chromatographs or hydrocarbon analyzers must be used for



such measurements. Flow rates are difficult to measure because they are generally quite low. Finally, it is difficult to determine the energy release rate due to changes in the fuel's composition (and heating value) during a test (18).

Allen and Rowley (19) used this method in 1942 to determine the efficiency of two residential coal stoves. The composition of the flue gases was determined by Orsat analysis. However, they ignored energy losses due to particulate and hydrocarbon emissions, since means to determine these losses were not available.

In 1981, Jaasma and Macumber (7) determined the efficiency of two hand-fired coal stoves using the stack loss technique. CO and CO<sub>2</sub> concentrations in the stack gas were measured continuously using an infrared analyzer. Their use of a dilution tunnel and a CO<sub>2</sub> balance technique allowed for easy measurement of stack gas velocity. The mass burning rate of the fuel was found by determining the carbon flow in the stack or by the use of an electronic platform scale. Although chemical energy losses due to smoke were accounted for, losses due to volatile hydrocarbons were ignored. Their setup was relatively inexpensive and it allowed for highly repeatable efficiency determinations.

## 2.4 Probe Sampling Techniques

Probe sampling is a widely used method for obtaining gas temperatures and species concentrations in flames and post flame gases. Gas sampling probes can be broken up into two types -- sonic and water-cooled. In a sonic probe the sample enters the orifice at Mach 1 and

then becomes supersonic in the diverging section where its temperature and pressure drop rapidly. Water-cooled probes utilize heat transfer between the sample gas and the water to cool the sample. If the gas sample temperature reduction rate is substantially faster than the rate of concentration change of the species that are being measured, the sample is said to be quenched. In order to measure species concentrations accurately in a large system such as a furnace, the gases should be quenched in a time that when multiplied by the gas velocity in the furnace would result in the gases moving only a relatively small distance from the sampling point.

Some probe sampling work in furnaces has been reported. Thring (20) discusses sampling in industrial furnaces with single inlet water-cooled probes and multiple inlet probes which can continuously collect samples from various points over a cross-section to detect stratification. Stainless steel or silica lining was used in the probes to prevent corrosion due to the acid from the furnace gases. Electric heating of the sampling bore is suggested to prevent hydrocarbons from condensing within the probes and eventually clogging them. Thring also discusses methods of measuring gas temperatures in furnaces and presents a design of a suction pyrometer which basically consists of a thermocouple mounted near the inlet of a tube. Combustion gases are drawn past the bead at increasingly faster flow rates until no change in thermocouple output is seen. At this point, it is assumed that the radiation heat transfer between the thermocouple bead and the cool furnace walls is negated by the high convective heat transfer between

the product gases and the bead and the thermocouple output represents the actual gas temperature. Platinum/Rhodium thermocouples were suggested due to their ability to operate at the high temperatures experienced in furnaces.

Very little temperature and gaseous species probe sampling work in residential coal stoves has been reported. The author is aware of no published work which presents concentration and/or temperature data in the secondary combustion zone of a hand-fired coal heater.

Nicholls (21) used probe sampling in his work concerning the effect of preheated combustion air on overfeed fuel beds. Water-cooled sampling probes were inserted into the center of a burning coal bed and samples were withdrawn and analyzed for CO, CO<sub>2</sub>, and O<sub>2</sub> concentrations using Orsat equipment. Considerable difficulty was experienced with probe clogging.

Landry and Sherman (1) apparently used sampling probes to help them design a smokeless residential coal stove. The probes were used to detect stratification of the product gas/secondary air mixture in the combustion chambers of the various stove designs they tested. No quantitative results were presented regarding species concentrations or temperatures in the primary or secondary combustion chambers.

Although virtually no probe sampling work has been done in coal stoves, some measurements have been made in the secondary combustion zones of laboratory two-stage combustors. Howard, et al. (22) used a combustor of this type to measure the rate of CO oxidation. The fuel-rich products from a methane/air flame in the primary zone were mixed

with secondary air and flowed into a tubular, quartz-lined secondary combustion chamber. Axial temperature and gas composition measurements were made with a 0.5 mm diameter quartz-coated Platinum/Rhodium thermocouple and a water-cooled sampling probe, respectively. It must be emphasized, however, that probe sampling is significantly less difficult in this "clean" type combustor than in a coal furnace. Probes can clog very quickly in the particulate-laden streams in a coal furnace and temperature measurements can be inaccurate due to soot deposition on the thermocouple bead. (The soot coating decreases the thermocouple's response time and also increases radiation heat transfer from the bead, due to its increased diameter.)

### 3. EXPERIMENTAL APPARATUS AND PROCEDURES

#### 3.1 Experimental Apparatus

##### 3.1.1 Description of Test Heater

A cross-sectional view of the test heater, the Rayburn Prince 76, is shown in Figure 1. The unit is an inset coal burning heater providing both radiant heat and hot water to be used in a hydronic system or for providing sanitary hot water. (An inset heater is designed to fit into a fireplace recess.) The Rayburn Prince is of down-draft design and incorporates a separate refractory-lined secondary combustion chamber. The secondary air is preheated before being introduced into the chamber. The boiler body of the unit is constructed of mild steel while the firebox is of cast iron. The total boiler water content is 8.8 liters. The maximum rated output of the unit is 10.4 kW, of which 7.7 kW is supplied in the form of hot water.

Three burning rates can be obtained by varying the position of the closure plate located on the front of the unit. The maximum, intermediate, and low output burning rates as given in the operating manual are approximately 2.3, 1.1, and 0.4 kg/h, respectively. The burning rates can also be varied to a lesser extent by adjusting the draft regulator, a plate that slides across the flue outlet and limits the flow of air through the unit.

The Rayburn Prince is designed to use washed, double-screened bituminous coal in doubles and trebles sizes. Refueling is suggested when the firebox is 1/3 to 1/4 full. De-ashing, normally done before refueling, is accomplished by moving a lever on the front of the unit

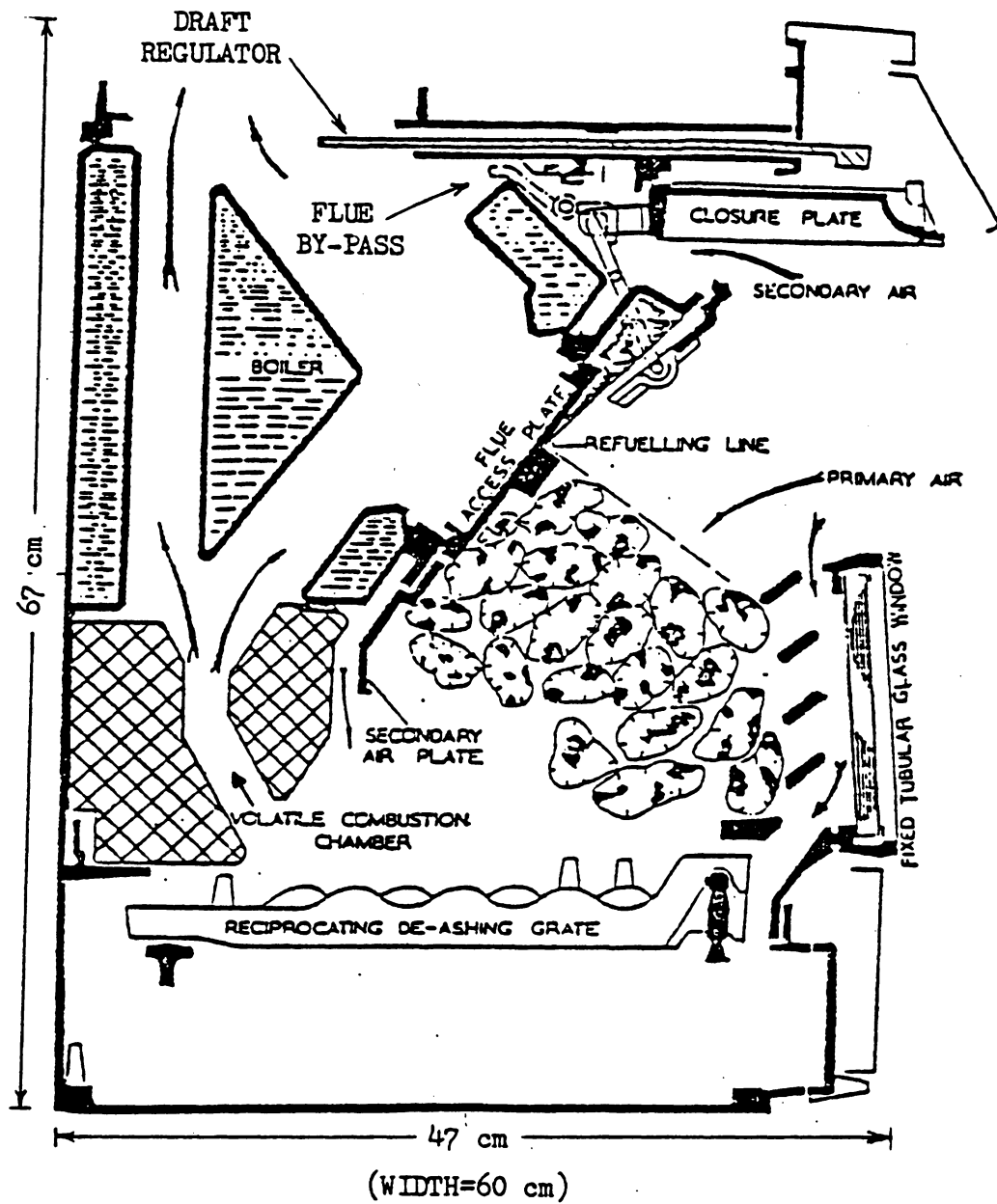


Figure 1. Cross-Section of Rayburn Prince 76.

which causes the grate bars to move back and forth. The linkage allows alternate bars to move forward while the others move in a reverse direction.

### 3.1.2 Description of Probe Sampling Apparatus

In order to extract gas samples from the secondary combustion zone of the Prince, two types of stainless steel, water-cooled gas sampling probes were developed. The probes were designed to be inserted into the secondary combustion zone through the back of the heater as shown in Figure 2. A tube was welded between the inner and outer walls of the boiler to facilitate insertion of the probes while not impeding the flow of cooling water.

The first type of probe developed, shown in Figure 3, was the axial sampling probe. This probe was used to obtain species concentrations along the probing axis, shown in Figure 2. The probe was constructed using three concentric stainless steel tubes. The sampled gases pass through the innermost tube and the cooling water enters between the inner and middle tubes and exits between the middle and outer tubes. This water path was chosen to keep the water contacting the inner tube as cool as possible to effect rapid quenching of the sample gases. The inside diameter of the innermost tube, 1.3 mm, was selected to be large enough to avoid clogging yet small enough to allow for a large Reynolds number to aid heat transfer. The overall diameter of the probe was kept small as possible to minimize interference on the product gas flow. An

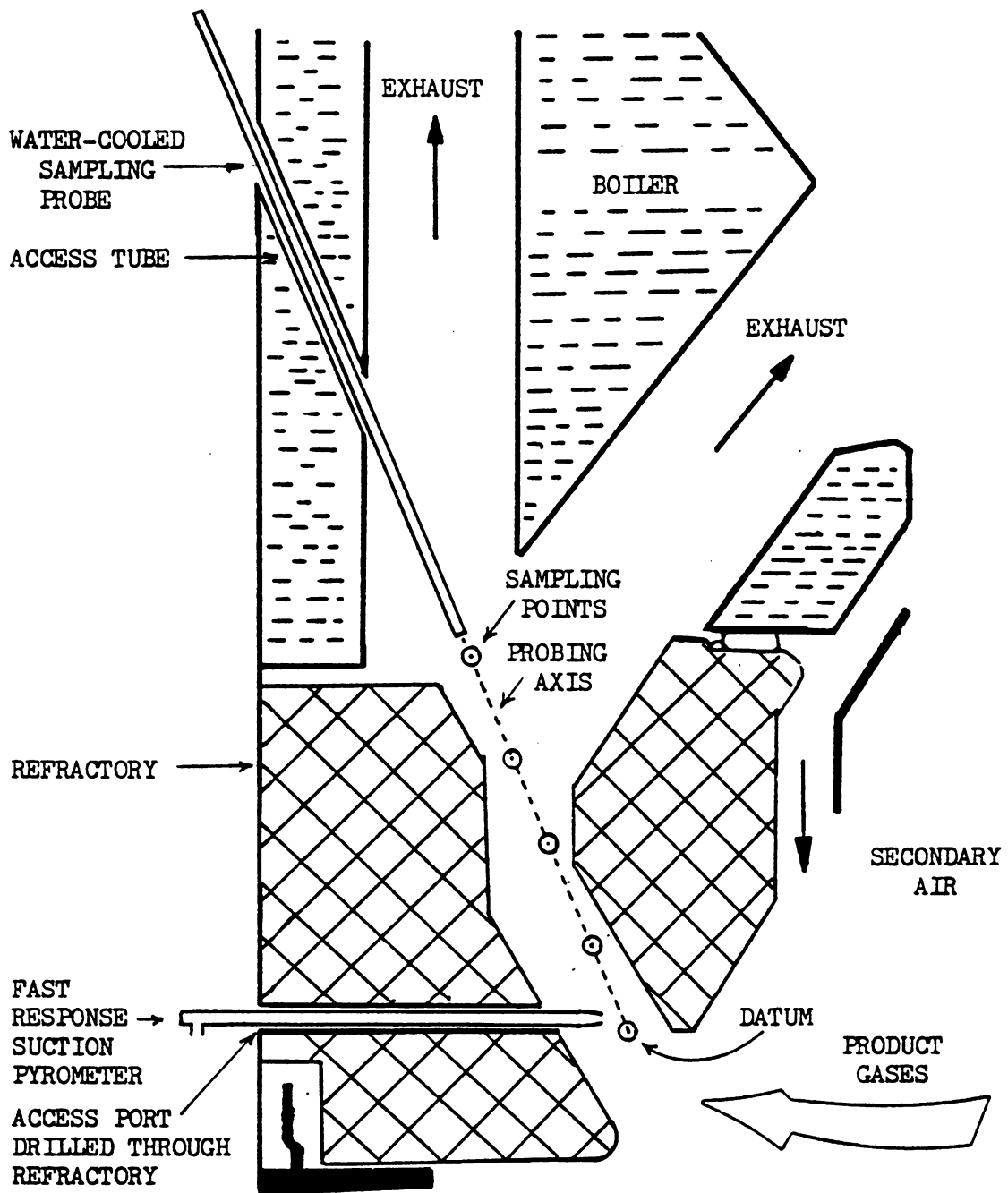


Figure 2. Orientation of Water-Cooled Sampling Probe and Fast Response Suction Pyrometer in Secondary Combustion Chamber.



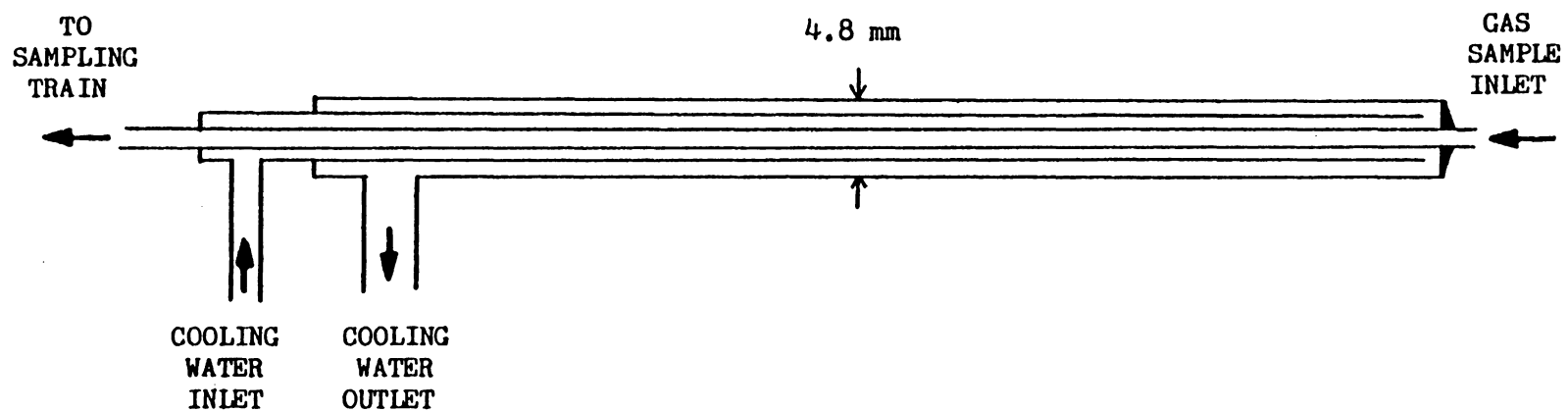


Figure 3. Water-Cooled Gas Sampling Probe.

analysis of the quenching capability of the probe is presented in Appendix A.

In order to obtain species concentrations over a cross-section in the secondary combustion zone, a "two-dimensional" probe was developed. A diagram of this probe is shown in Figure 4. The probe is similar in design to the axial probe with the exception of the inner tube, which extends 40 mm past the outer tube and is bent to form a 90° angle. This extension allows gas samples to be taken over the cross-section in the secondary combustion zone when the probe is rotated.

The sample gas was analyzed by the train shown in Figure 5. After leaving the sampling probe the sample passes through approximately 1.5 m of 1.6 mm I.D. Teflon tubing and then into a stainless steel 0°C condenser. The condenser was used to remove moisture which might damage the analyzers. Particulates were removed from the sample by a fiberglass filter. A diaphragm pump was used to move the sample to the infrared CO/CO<sub>2</sub> analyzer (Infrared Industries, Inc., Model IR-702), polarographic O<sub>2</sub> analyzer (Horiba Model POA-21), and the chemiluminescent NO<sub>x</sub> analyzer (Bendix Model 8102). Rotameters were used to measure sample flow rates to each analyzer. The train was designed for minimum sample residence time. In order to minimize sample adsorption, virtually all materials in contact with the sample are Teflon, stainless steel or glass.

Temperature measurements along the probing axis in the secondary combustion zone were made with a suction pyrometer. The suction pyrometer consists of a 130 micrometre Platinum/Platinum-10% Rhodium thermo-

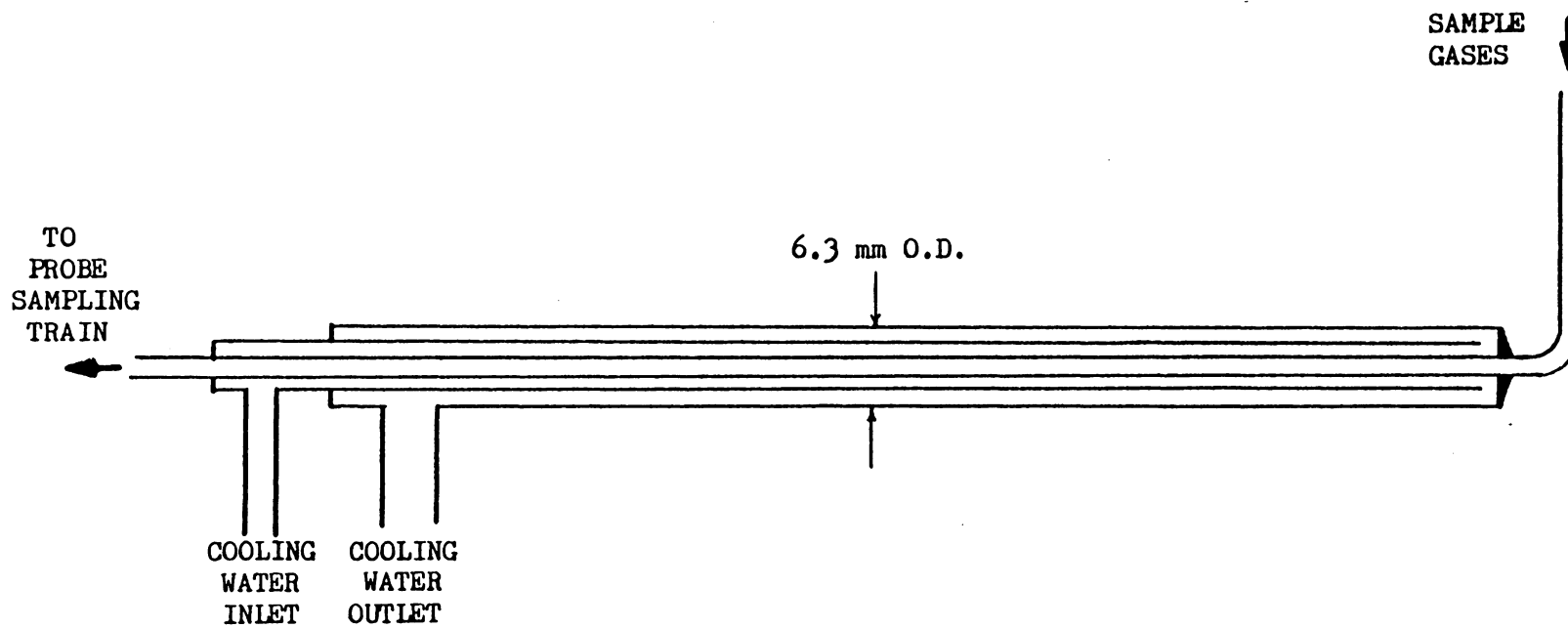


Figure 4. Two-Dimensional Stainless Steel Water-Cooled Sampling Probe.

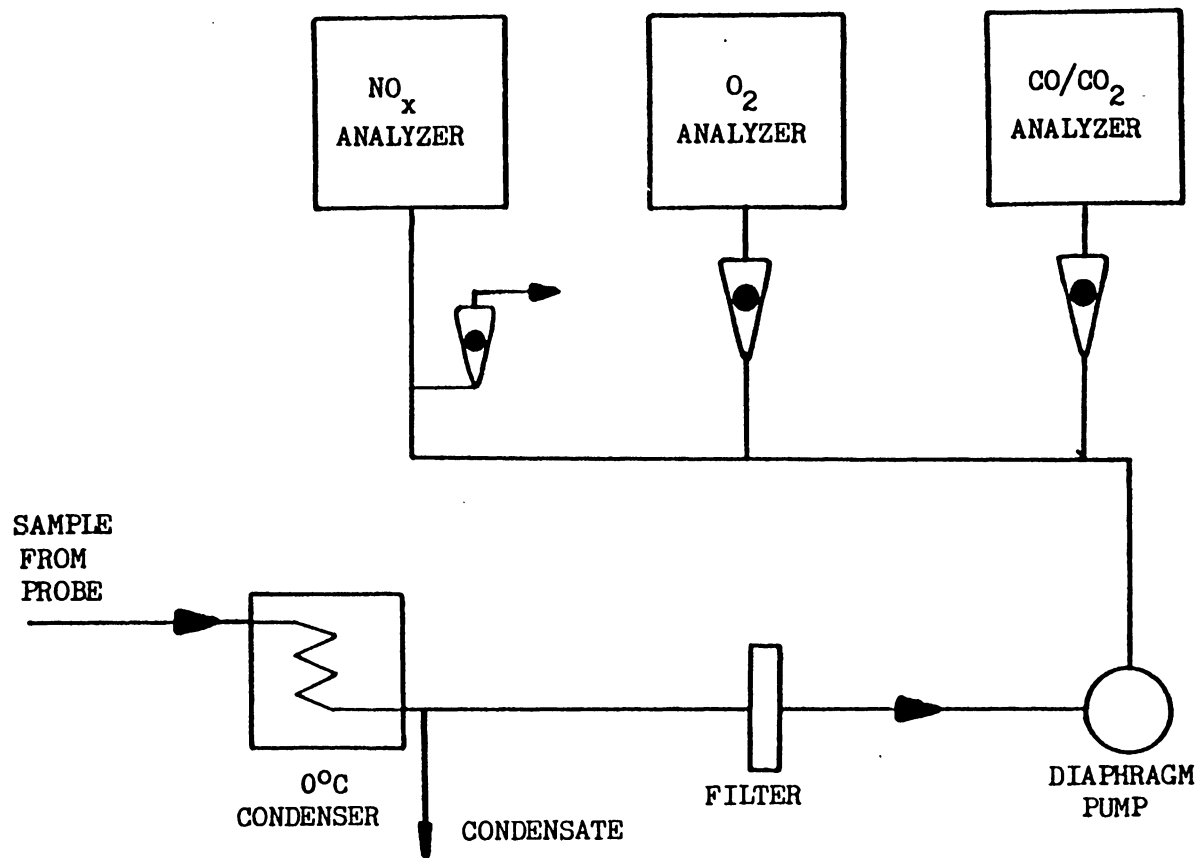


Figure 5. Probe Sampling Train.

couple, supported by a ceramic insulator and located near the inlet of a 4.9 mm I.D. stainless steel tube. Hexamethyldisiloxane was used to quartz-coat the thermocouple bead, following the method presented by Fristrom and Westenberg (23). This was done to prevent erroneous temperature readings caused by catalytic effects. A vacuum pump was used to pull the gases past the thermocouple bead. The high velocity of the gases past the thermocouple bead allowed for a response time of approximately 70 ms.

In order to determine the magnitude of the temporal temperature variations in the secondary combustion chamber, a faster response time suction pyrometer was developed. It was inserted into the mouth of the chamber through the back of the heater as shown in Figure 2. The pyrometer, shown in Figure 6, utilizes a 25 micrometre Platinum/Platinum-10% Rhodium thermocouple located near the inlet orifice of a quartz glass tube. The response time of the thermocouple was calculated to be approximately 6 ms at a flow rate of 0.4 l/min (room conditions). The thermocouple output was sent to a storage oscilloscope and a camera was used to take photographs of the traces.

### 3.1.3 Description of Emissions and Efficiency Measurement Apparatus

The flue gas handling system for the emissions and efficiency tests is shown in Figure 7. The Prince operates under natural draft conditions, with draft being provided by a 15 cm diameter, free-standing stack 5 m tall. The product gases leaving the stack are drawn, along with room air, into the collection hood at a ratio of approximately 1

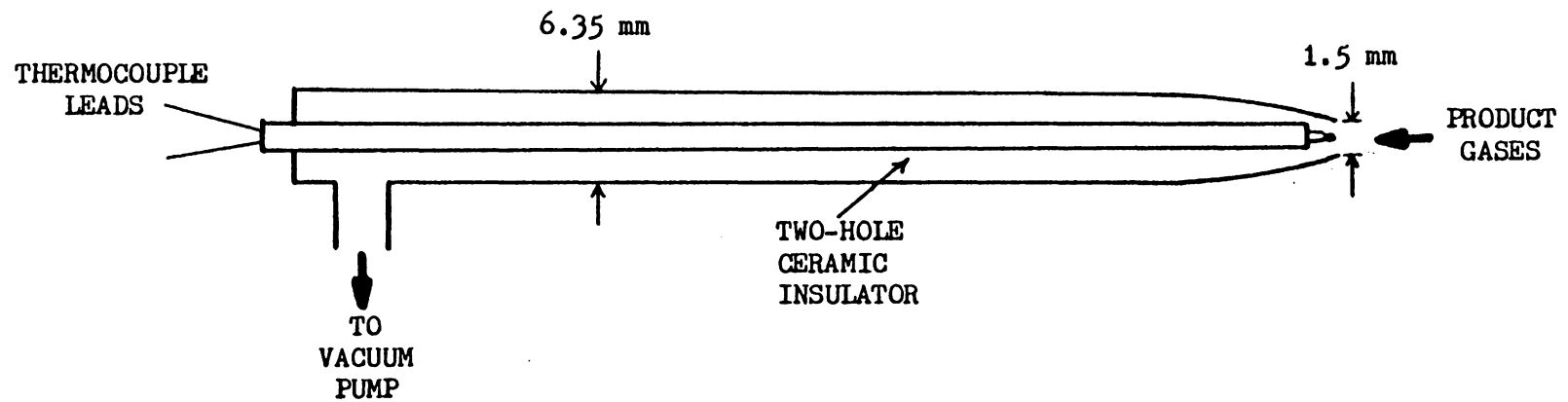


Figure 6. Fast Response Suction Pyrometer.

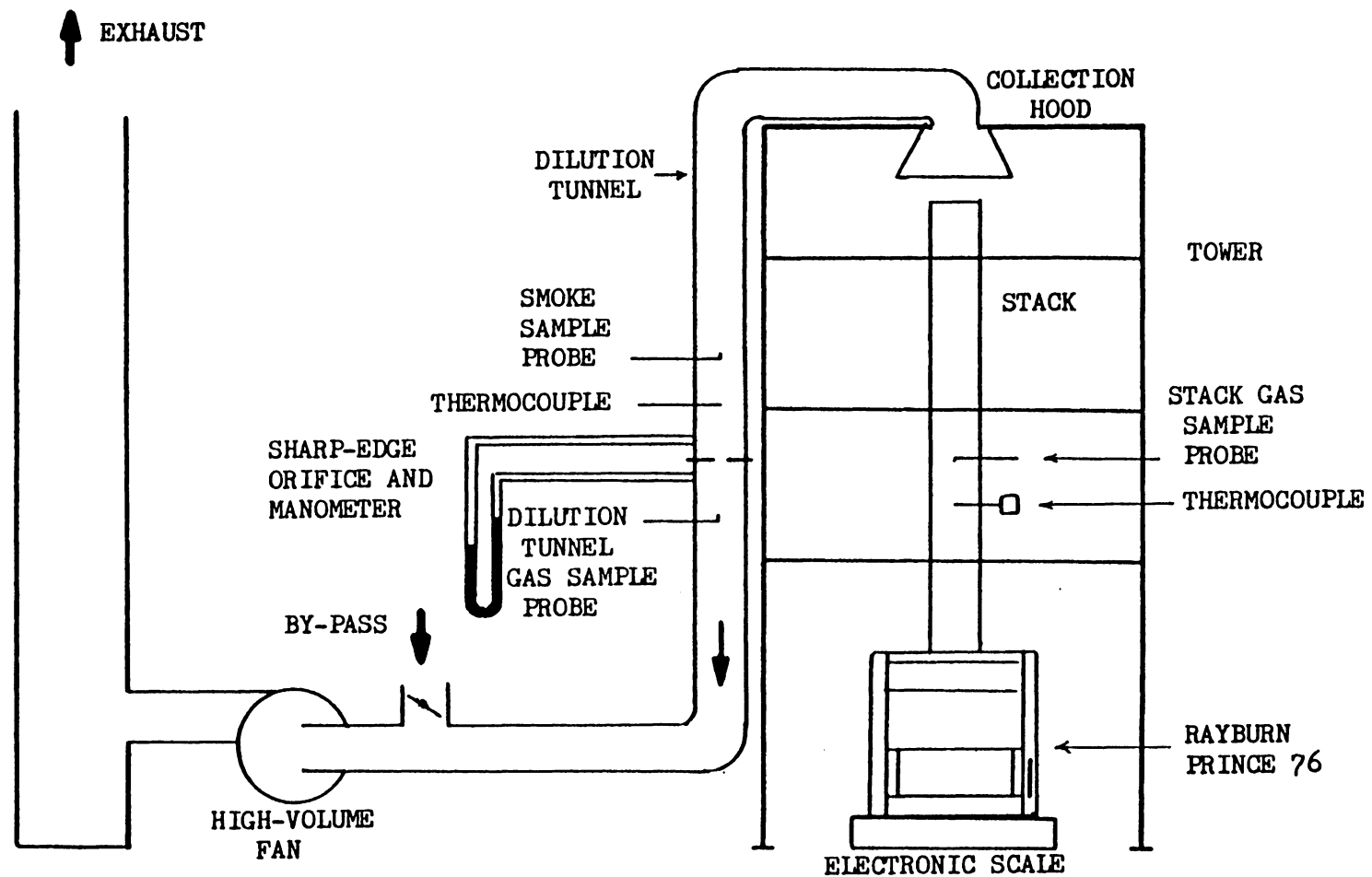


Figure 7. Flue Gas Handling System for Emissions and Efficiency Tests.

part flue gas to 2 parts room air. This mixture is pulled down the insulated dilution tunnel by a high volume fan. The entire stack--dilution tunnel system is supported by a steel tower 6.1 m in height. The flue gas/room air ratio in the dilution tunnel can be varied by a bypass valve located upstream of the fan. The flow rate in the dilution tunnel is determined by the pressure drop over a calibrated sharp-edge orifice.

The orifice plate was previously calibrated using a CO<sub>2</sub> dilution technique. The actual flow rate in the dilution tunnel (at room temperature) was calculated by injecting a known flow rate of pure CO<sub>2</sub> into the collection hood and measuring the CO<sub>2</sub> concentration near the orifice. A discharge coefficient was then found using the measured pressure drop across the orifice and the actual dilution tunnel flow rate.

Gas temperatures are measured by thermocouple probes located in the stack (1.2 m above the heater) and just upstream of the orifice. Gas samples are withdrawn from the stack and downstream of the orifice. A smoke sampling probe is located just upstream of the orifice.

The Prince is situated on an electronic scale with a resolution of 20 g. The scale is used to determine the mass of coal burned during a test. Flexible hoses connect the Prince to the heat rejection system shown in Figure 8. The heat from the boiler water is rejected to a cold water stream in the shell and tube heat exchanger. A centrifugal pump is used to circulate the cooling water. Its flow rate is measured with a rotameter and is varied using a globe valve.



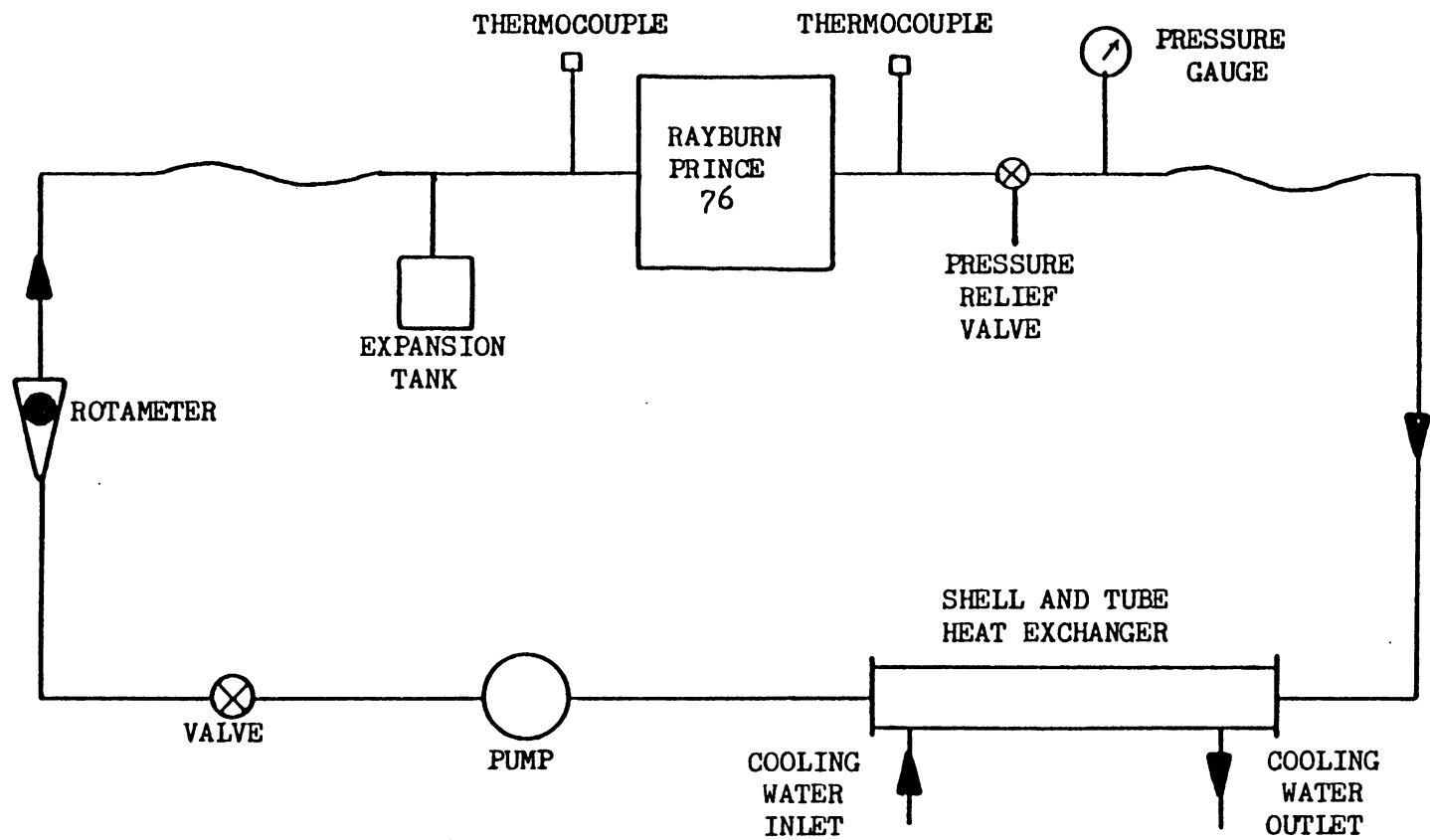


Figure 8. Boiler Water Flow Path.

A schematic of the gas sampling train is shown in Figure 9. The switching valve allows the train to sample in either the stack or dilution tunnel. After the moisture is removed from the sample in the 0°C condenser it passes through one of the two fiberglass filters arranged in parallel. This configuration allows for continuous sampling -- when one filter clogs, the other can be switched on line. A stainless steel bellows pump delivers the sample to the CO/CO<sub>2</sub> analyzer, O<sub>2</sub> analyzer, NO<sub>x</sub> analyzer, and flame photometric SO<sub>x</sub> analyzer (Bendix Model 8303). Flow bypasses are used to dilute the sample with room air before being sent to the SO<sub>x</sub> analyzer, whose measuring range is only 0-1 ppm (part per million).

A schematic of the smoke sampling train used to quantify smoke emissions from the Prince is shown in Figure 10. The sample was withdrawn isokinetically from the center of the dilution tunnel using the 7 mm I.D. smoke sampling probe. The smoke is collected at room temperature on a Gelman A/E 142 mm diameter, 0.3 micrometre, fiberglass filter. The 0°C condenser is used to prevent condensation problems in the vacuum pump and rotameter. The rotameter is used to set the isokinetic sampling rate, found using the pressure drop across the orifice and the gas temperature in the dilution tunnel.

Aerodynamic sizing of the particulate emissions was accomplished using a Sierra Model 226-K cascade impactor. A schematic of the particulate sizing train is shown in Figure 11. The impactor was mounted to sample the flue gases leaving the stack. The flow rate through the impactor, set for isokinetic sampling, was maintained by a

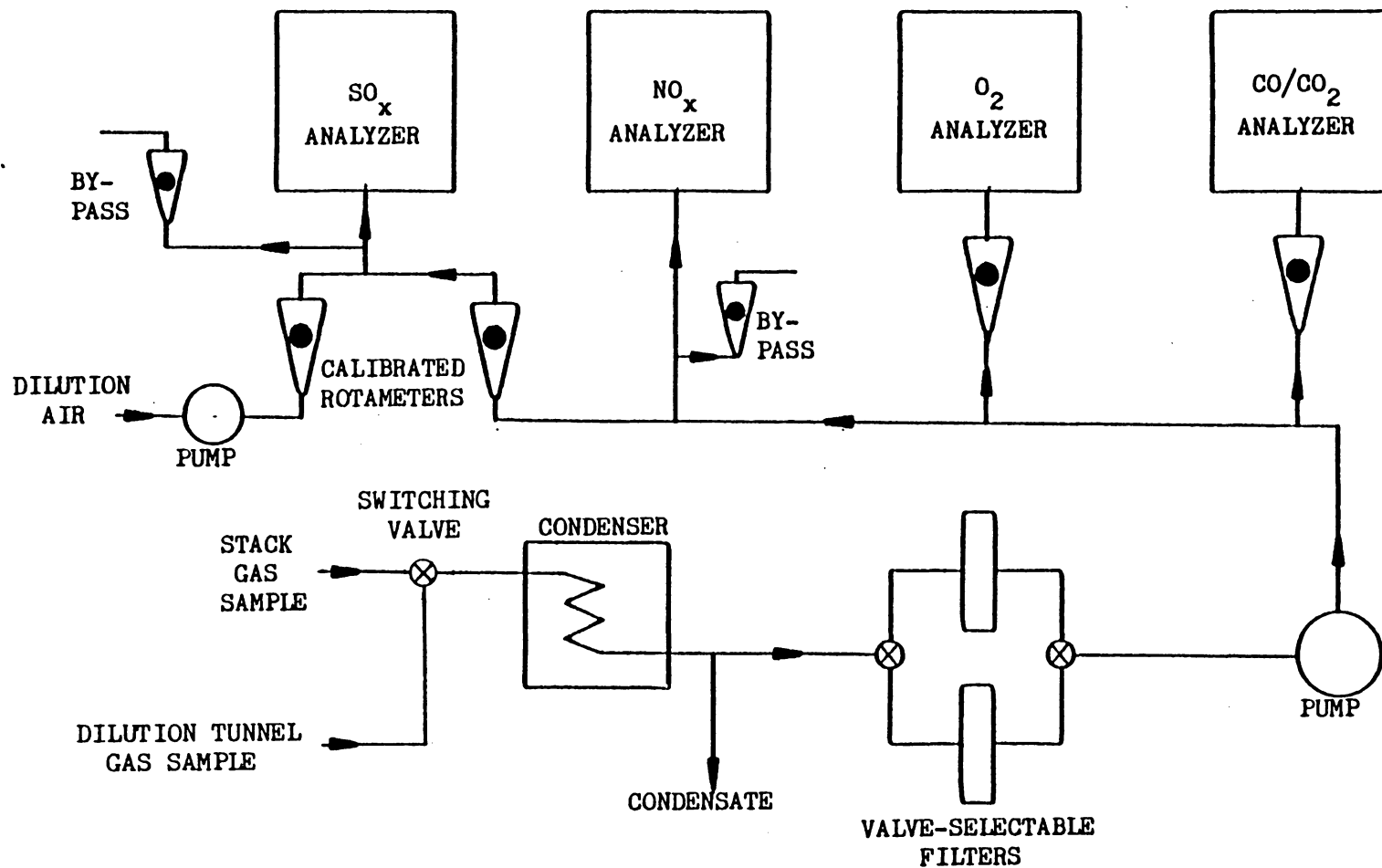


Figure 9. Stack Gas Sampling Train.

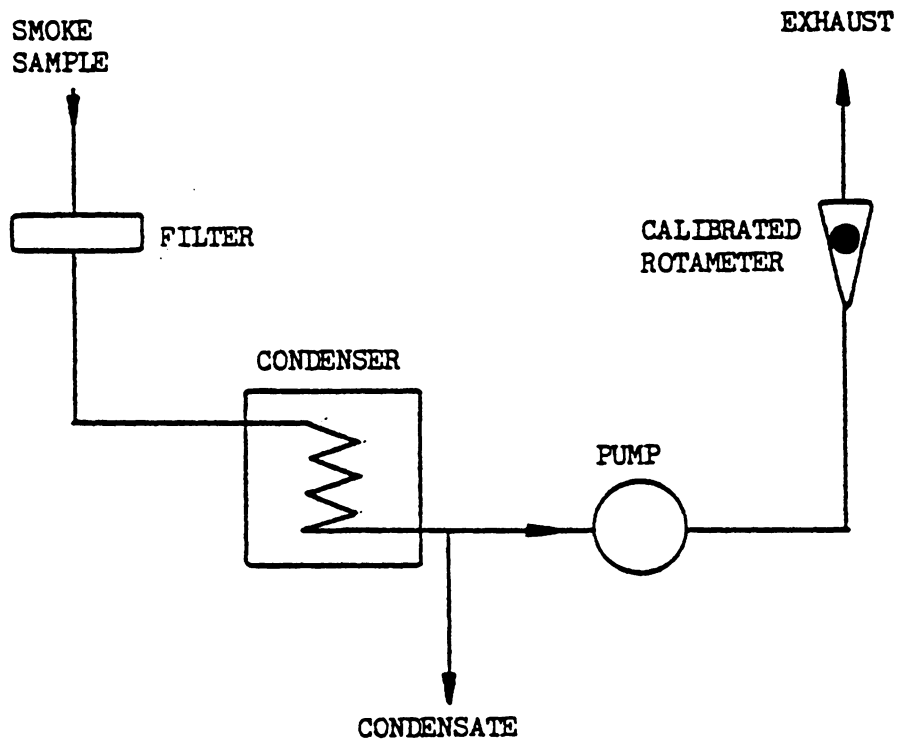


Figure 10. Smoke Sampling Train.

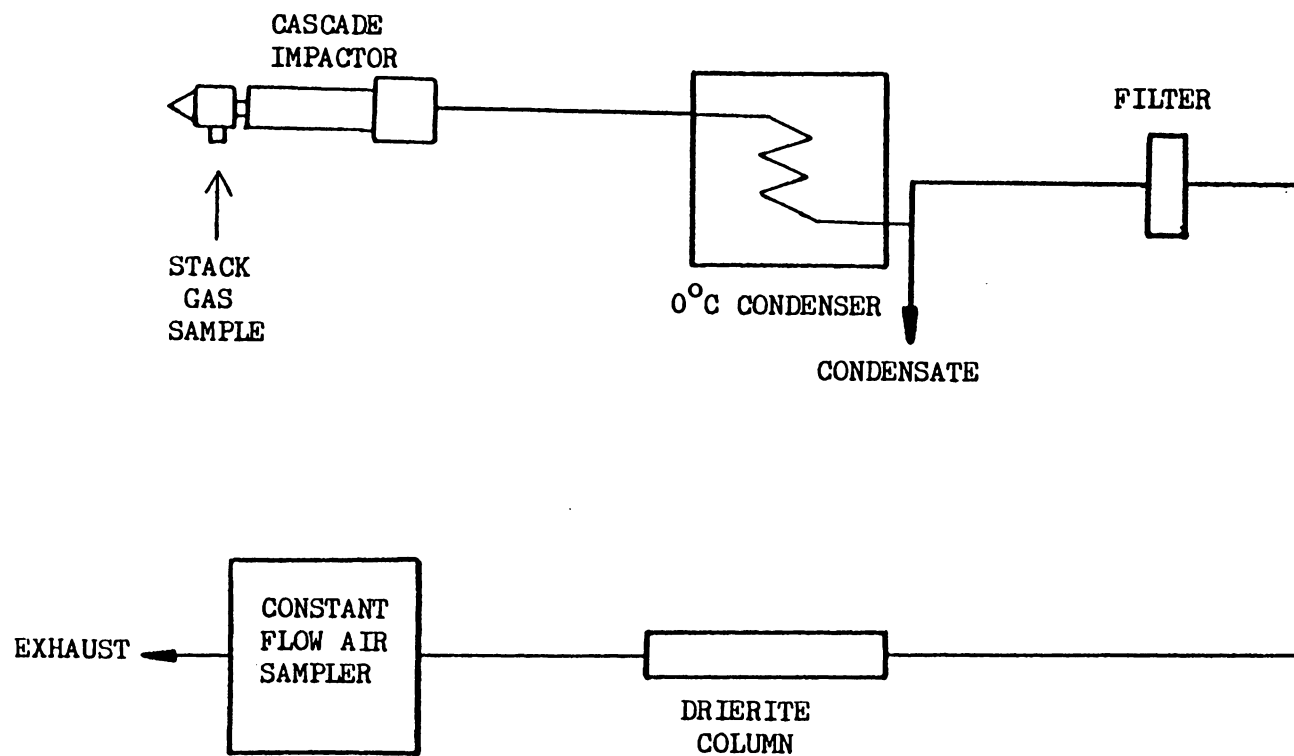


Figure 11. Cascade Impactor Sampling Train.

Sierra Model 110 Constant Flow Air sampler. (The stack gas velocity, needed to determine the isokinetic sampling flow rate, was determined using Eq. 2 in Section 4.1.) The 0°C condenser and the dessicator prevent moisture from reaching the air sampler. The impactor was wrapped with heat tape to keep it above the dew point of the water vapor in the flue gas.

### 3.2 Description of Test Coals

A high volatile Clinchfield coal and a low volatile Pocahontas coal were selected for testing. Data on these coals appear in Table I. Both coals were obtained at Bane Coal Company, Christiansburg, Virginia. The coals are classified as stove coals (double screened between 1 5/8 in. mesh and 2 7/16 in. mesh). The coals are quite similar, with low moisture and sulfur contents. Their major difference lies in their volatile content. The value of the free swelling index for the Clinchfield coal is in doubt since the value for a previous batch of Clinchfield coal with almost identical properties was 4.5.

The Pocahontas test coal was delivered with a large amount of fines, probable caused by rough handling during shipment. The fines were removed from the coal before it was burned.

TABLE I. Test Coal Data

	<u>Clinchfield Coal</u>	<u>Pocahontas Coal</u>
Volatile content (%)	32.76	23.95
Fixed carbon (%)	59.85	69.94
Moisture content (%)	0.54	0.87
Free swelling index	7	8
Heating Value (Dry, kJ/kg)	33,380	34,454
<u>Ultimate Analysis</u>		
Carbon (%)	80.54	84.54
Hydrogen (%)	5.12	5.08
Nitrogen (%)	1.45	1.11
Oxygen (%)	4.94	2.63
Sulfur (%)	0.56	0.54
Ash (%)	7.39	6.11

### 3.3 Experimental Procedures

#### 3.3.1 Axial Probe Sampling Test Procedure

Two axial probe sampling tests were conducted in the secondary combustion chamber. Local gas temperatures and species concentrations were measured in each test.

The probe sampling tests were begun when the coals were sufficiently ignited. The water-cooled axial probe was inserted into the secondary combustion chamber through the back of the heater, as shown in Figure 2. Samples were extracted at 5 points, each 3 cm apart, with the first point (datum) being approximately level with the lower edge of the inner refractory wall. The samples were sent to the probe sampling train where the concentrations of CO, CO<sub>2</sub>, O<sub>2</sub>, and NO<sub>x</sub> were measured.

After the species concentrations were recorded at the five sampling points, the axial probe was immediately withdrawn and replaced with the suction pyrometer. The thermocouple output potentials were recorded at the same five points. This procedure was repeated four times at fifteen minute intervals for each of the high, intermediate, and low burning rate conditions. At fifteen minute intervals between the probe sampling measurements, the pressure drop across the orifice, CO and CO<sub>2</sub> concentrations in the stack, CO<sub>2</sub> concentrations in the dilution tunnel, stack gas temperature, and dilution tunnel gas temperature were recorded.



### 3.3.2 Axial and Radial Probe Sampling Test Procedure

Prior to loading the coal into the Prince, the two-dimensional water-cooled probe was inserted into the secondary combustion zone and its tip was bent, forming a right angle. Probe sampling was started after the firebox was filled and the coals were well ignited. Samples were obtained at 6 stations, each 2 cm apart, along the probing axis. At each station, the probe was rotated in  $10^\circ$  increments, sampling six positions over the cross section of the secondary combustion zone. The samples were sent to the probe sampling train for determination of the  $\text{CO}$ ,  $\text{CO}_2$ ,  $\text{O}_2$ , and  $\text{NO}_x$  concentrations. This procedure was repeated three times at 25 minute intervals for each of the three burning rate conditions.

Temperature measurements were not made in the secondary combustion zone during this test. This was due to the extended tip of the two dimensional probe which prevented it from being withdrawn from the heater during the test.

### 3.3.3 Temperature Variation Test Procedure

The fast response time suction pyrometer was inserted into the entrance of the secondary combustion chamber after the coal bed was sufficiently ignited. The closure plate was kept in the open position for the duration of the test. Photographs of the thermocouple output traces on the oscilloscope screen were taken when the pyrometer tip was near the inner refractory wall, outer refractory wall, and the center of the passage.

### 3.3.4 Emissions and Efficiency Test Procedure -- Maximum Burning Rate

Two tests were conducted to determine the emissions and efficiency of the Rayburn Prince at maximum burning rate conditions, obtained by setting the closure plate and draft regulator in the fully opened positions. The Clinchfield coal was burned during one test while the Pocahontas coal was burned during the other.

Analyzer calibration was performed before each test. This consisted of spanning and zeroing the CO/CO<sub>2</sub>, O<sub>2</sub>, NO<sub>x</sub>, and SO<sub>x</sub> analyzers with Matheson Certified Standard span gases and zero gas. Calibration drift was determined by repeating this operation after each test. Ambient pressure, temperature, and humidity readings were recorded before and after each test.

The Prince was loaded with approximately 1 kg of wood and paper and ignited. A small load (approximately 3.5 kg) of coal was added and allowed to become sufficiently ignited. The firebox was then filled by adding two more loads (5 and 3 kg) for the Clinchfield test and one more load (4 kg) for the Pocahontas test. The coal bed was stirred whenever excessive caking of the coal caused the CO emissions to rise rapidly and the stack gas temperature to fall.

Data recording was started when the initial load of coal was added. The measurements, taken at five minute intervals, included the CO, CO<sub>2</sub>, and O<sub>2</sub> concentrations in the stack, the CO<sub>2</sub>, NO<sub>x</sub>, and SO<sub>x</sub> concentrations in the dilution tunnel, gas temperatures in the stack and dilution tunnel, pressure drop across the orifice, and the readings on the SO<sub>x</sub> dilution rotameters.

Smoke sampling in the dilution tunnel was initiated when the first load of coal was added and was continued for the entire duration of the test. The rotameter in the smoke sampling train was set to provide isokinetic sampling. The sampling flow rate was adjusted periodically to insure isokinetic sampling during the entire test.

Prior to each test, the fiberglass collection filters were dessicated for at least 12 hours and then weighed on a balance with a 0.1 mg resolution. The filters were again dessicated for at least 12 hours after each test and then reweighed. In addition, any matter which collected in the probe and Teflon sampling line was rinsed off with acetone, dried, and weighed in a tared dish.

When the initial charge had burned down so that the firebox was approximately one-third full, the Prince was de-ashed and reloaded to the fill line. Data recording continued during the refueling procedure. The total duration of the Clinchfield test was 635 minutes while that of the Pocahontas test was 525 minutes. Reloading during the Clinchfield and Pocahontas tests occurred at 295 and 205 minutes, respectively.

During the test, water was circulated through the Prince at a flow rate of approximately 6.3 l/min. The water temperature leaving the boiler was maintained at approximately 88°C by varying the flow rate of cooling water through the shell and tube heat exchanger.

### 3.3.5 Emissions and Efficiency Test Procedure -- Low Burning Rate

Two low burning rate tests were performed -- one using Clinchfield coal and the other using Pocahontas coal. The same instrument calibration procedure followed in the high burning rate tests was used in the low burning rate tests. In addition, the same ambient conditions were measured.

Both "banked" tests were run in an identical manner. A wood fire was used to ignite the initial coal charge. After the initial charge had burned down so that the firebox was approximately 1/3 full, a second charge was added, filling the firebox. The fire was allowed to burn for one hour with the closure plate in the open position, at which time it was set in the closed position and the draft regulator was set at an intermediate position. The closure plate was kept open for one hour to allow the fresh coal charge to ignite properly.

Data collection was initiated when the closure plate was set in the closed position. The same readings taken during the high burning rate tests were taken during these tests. However, no  $\text{SO}_x$  readings were taken during the Pocahontas test due to the  $\text{SO}_x$  analyzer being inoperative. The same smoke sampling procedure followed in the high burning rate tests was followed in these tests. Smoke collection was begun when the closure plate was set in the closed position. Data were collected for 450 minutes during the Clinchfield test and for 445 minutes during the Pocahontas test.

### 3.3.6 Particulate Sizing Procedure

The cascade impactor train was used to isokinetically sample the flue gases leaving the stack. Particulates were collected by impaction on six substrate media and a backup filter.

Prior to each test, the fiberglass substrates and backup filter were dessicated for at least 12 hours and then carefully weighed. The cascade impactor was used during each emissions and efficiency test. However, an adequate amount of particulate matter was collected only during the full output Pocahontas test and the low output Clinchfield test. This was due to an inadequate sampling time during the full output Clinchfield test and very low particulate emissions during the low output Pocahontas test. The sampling times for the full output Clinchfield and Pocahontas tests and the low output Clinchfield and Pocahontas tests were 35, 45, 222, and 355 minutes, respectively. At the end of each test, the substrates and back-up filter were again dessicated for 12 hours, then reweighed to determine particulate loading.

## 4. DATA REDUCTION

### 4.1 Emission Factor Calculations

The emission factors are expressed as grams of pollutant per kilogram of coal burned. They are found using measured values of species concentrations in the stack and dilution tunnel, mass of collected smoke, and the molar flow rate in the dilution tunnel.

The gaseous species concentrations measured by the analyzers are higher than the actual values due to most of the water vapor in the sample being condensed out before the sample reached the analyzers. The procedure used to convert the species concentrations from dry to wet basis is outlined in Appendix B. All species concentrations used in subsequent equations are on a wet basis.

The molar flow rate in the dilution tunnel is given by

$$\dot{n}_{DT} = C_d A_{or} \sqrt{\frac{2 \Delta P P_{DT}}{R T_{DT} MW_{DT}}} \quad (2)$$

where

- $\dot{n}_{DT}$  = dilution tunnel molar flow rate, kg mol/s
- $C_d$  = orifice discharge coefficient
- $A_{or}$  = orifice area, m<sup>2</sup>
- $\Delta P$  = pressure drop over orifice, kPa
- $P_{DT}$  = pressure in dilution tunnel, kPa
- $R$  = universal gas constant, 8.314 J/mol K
- $T_{DT}$  = gas temperature in dilution tunnel, K
- $MW_{DT}$  = molecular weight of gas in dilution tunnel, 29 g/mol

The molar flow rate in the stack is calculated using the method developed by Macumber and Jaasma (24). This method makes use of the fact that the molar flow rates of  $\text{CO}_2$  in the stack and dilution tunnel must be equal. The molar flow rate in the stack is then given by

$$\dot{n}_s = \frac{x_{\text{CO}_2})_{\text{DT}}}{x_{\text{CO}_2})_s} \dot{n}_{\text{DT}} \quad (3)$$

where

$\dot{n}_s$  = molar flow rate in stack, kg mol/s

$x_{\text{CO}_2})_{\text{DT}}$  = mole fraction of  $\text{CO}_2$  in dilution tunnel

$x_{\text{CO}_2})_s$  = mole fraction of  $\text{CO}_2$  in the stack

The total mass of smoke emitted by the stove during the entire test is given by

$$M_{\text{sm,em}} = \frac{\dot{n}_{\text{DT})_A}{\dot{n}_p} M_{\text{sm,col}} \quad (4)$$

where

$M_{\text{sm,em}}$  = total mass of smoke emitted by stove, g

$M_{\text{sm,col}}$  = total mass of smoke collected on filters and in sampling probe, g

$\dot{n}_p$  = average molar flow rate of gases in smoke sampling probe, kg mol/s

$\dot{n}_{\text{DT})_A}$  = average molar flow rate of gases in dilution tunnel, kg mol/s

The instantaneous mass burning rate of the coal is found by approximating the flow of carbon up the stack. This method uses the assumption

that the carbon present in the coal forms only CO, CO<sub>2</sub>, and smoke. Since a hydrocarbon analyzer was not available, the non-condensable hydrocarbon content in the flue gases was ignored. The instantaneous mass burning rate of the coal is then given by

$$\dot{m} = \frac{(\dot{X}_{CO})_S + \dot{X}_{CO_2})_S \dot{n}_S MW_C + \dot{M}_{sm} y_{C)sm}}{y_{C)coal}} \quad (5)$$

where

$\dot{m}$  = instantaneous burning rate of coal, kg/s

$\dot{X}_{CO})_S$  = mole fraction of CO in stack gases

$MW_C$  = molecular weight of carbon, 12 g/mol

$\dot{M}_{sm}$  = average mass emission rate of smoke kg/s

$y_{C)sm}$  = mass fraction of carbon in the smoke

$y_{C)coal}$  = mass fraction of carbon in the as-fired coal

The mass fraction of carbon in the smoke was assumed to be 0.80, approximately the same as the carbon content of the coal. This is consistent with approximations made by others (8,25). The average mass emission rate of smoke is found by dividing the total mass of smoke emitted during the test by the total test time.

The smoke emission factor is given by

$$EF_{sm} = \frac{M_{sm,em}}{M_{coal}} \quad (6)$$

where

$EF_{sm}$  = smoke emission factor, g smoke/kg coal

$M_{coal}$  = total mass of coal burned during test, kg

The total mass of coal burned during a test can be determined from the



scale readings or by summing the products of the instantaneous mass burning rate (given in Eq. 4) and the time interval between data recording.

The instantaneous CO emission factor is determined using the measured concentration of CO in the stack and the molar flow rate in the stack. It is given by

$$EF_{CO} = \frac{x_{CO})_S \dot{n}_S MW_{CO}}{\dot{m}} \quad (7)$$

where

$EF_{CO}$  = instantaneous CO emission factor, g CO/kg coal

$MW_{CO}$  = molecular weight of CO, 28g/mol

The instantaneous  $NO_x$  and  $SO_x$  emission factors are determined from the measured  $NO_x$  and  $SO_x$  concentrations in the dilution tunnel and the molar flow rate of the gases in the dilution tunnel. They are given by

$$EF_x = \frac{x_x)_{DT} \dot{n}_{DT} MW_x}{\dot{m}} \quad (8)$$

where

$EF_x$  = instantaneous  $NO_x$  or  $SO_x$  emission factor, g/kg coal

$x_x)_{DT}$  = mole fraction of  $NO_x$  or  $SO_x$  in the dilution tunnel

$MW_x$  = molecular weight of  $NO_x$  (46 g/mol) or  $SO_x$  (64 g/mol)

The average CO,  $NO_x$ , and  $SO_x$  emission factors were determined by mass-weighted averaging of the corresponding instantaneous emission factors.

## 4.2 Efficiency Calculations

The efficiency of the Rayburn Prince was calculated using the "stack loss" method. In this method the useful heat output from the heater was found by subtracting the losses up the stack from the energy given off by the burning coal. These losses are due to sensible energy, chemical energy, and the latent heat of vaporization of water vapor in the stack gases, and unburned combustibles in the smoke emissions.

The instantaneous rate of chemical energy release due to combustion of the coal is approximated by

$$\dot{E} = \dot{m} \text{HV}_{\text{coal}} \quad (9)$$

where

$\dot{E}$  = instantaneous energy release rate, kW

$\text{HV}_{\text{coal}}$  = heating value of the coal, kJ/kg (as-burned basis)

This energy release rate is only an approximation since the heating value of the coal is assumed constant for the duration of the test. In actuality, the heating value of the fuel changes due to devolatilization-induced changes in the chemical composition of the fuel.

The instantaneous sensible energy loss up the stack is given by

$$\dot{E}_{\text{sen}} = \dot{n}_S \bar{C}_p (T_S - T_r) \quad (10)$$

where

$\dot{E}_{\text{sen}}$  = instantaneous sensible energy loss, kW

$\bar{C}_p$  = constant pressure specific heat of air, 30 J/mol K

$T_s$  = temperature of stack gases, K  
(1.2 m above flue collar of heater)

$T_r$  = room temperature, K

Since the measured  $O_2$  concentration in the stack was generally about 18%, representing the specific heat of the stack gases by that of air is a very good assumption.

The chemical energy loss due to gaseous species was approximated as the loss due to CO in the stack gases. This was due to the inability to determine the non-condensable hydrocarbon content of stack gases, since a hydrocarbon analyzer was not available. The instantaneous gas-phase species chemical energy loss is approximated by

$$\dot{E}_{ch} = X_{CO})_S \dot{n}_S HV_{CO} \quad (11)$$

where

$\dot{E}_{ch}$  = instantaneous CO chemical energy loss, kW

$HV_{CO}$  = heating value of CO, 282, 993 kJ/kg

The instantaneous energy loss due to condensable hydrocarbons and soot in the smoke can be approximated by (25)

$$\dot{E}_{sm} = \dot{M}_{sm} HV_{coal} \quad (12)$$

where

$\dot{E}_{sm}$  = instantaneous energy loss due to smoke, kW

The instantaneous energy loss due to the latent heat of vaporization of water in the stack gases (from moisture present in the coal and water formed during the combustion process) is given by

$$\dot{E}_1 = \bar{h}_{fg} \left[ \frac{\dot{m} y_{H_2O}^c}{MW_{H_2O}} + \frac{\dot{n}_S (x_{CO}^S + x_{CO_2}^S)}{2r} + \frac{y_c^sm \dot{M}_{sm}}{2r MW_c} \right] \quad (13)$$

where

- $\dot{E}_1$  = instantaneous latent heat loss, kW  
 $y_{H_2O}^c$  = mass fraction of water in as-burned coal  
 $MW_{H_2O}$  = molecular weight of water, 18 g/mol  
 $h_{fg}$  = molar heat of vaporization of water, 43,740 J/kmol  
 $r$  = molar ratio of carbon to hydrogen in coal

The instantaneous percent efficiency is then given by

$$\eta = \frac{\dot{E} - (\dot{E}_{sen} + \dot{E}_{ch} + \dot{E}_{sm} + \dot{E}_1)}{\dot{E}} \cdot 100 \quad (14)$$

where

- $\eta$  = instantaneous efficiency, %

The efficiency calculation equations presented in this section and the emission factor equations presented in Section 4.1 were incorporated into a computer program, a listing of which is presented in Appendix C. This program enabled rapid reduction of the large amount of data collected.

#### 4.3 Calculation of Gas Residence Time in Secondary Combustion Chamber

The gas residence time in the secondary combustion chamber is found using the geometry of the chamber and the calculated local gas velocities. The flow rate of gases through the secondary combustion zone was

assumed to be much greater than the flow rate of air passing into the stack through the flue bypass. This assumption was substantiated by the measured  $\text{CO}_2$  concentrations just outside of the secondary combustion zone (determined with water-cooled probes) generally being within 15% of the  $\text{CO}_2$  concentrations measured in the stack. Then it can be assumed that the molar flow rate in the secondary combustion zone is equal to the molar flow rate in the stack.

The local volumetric flow rate in the secondary combustion chamber is given by

$$\dot{Q}_{sc} = \frac{\dot{n}_s RT_{sc}}{P_{sc}} \quad (15)$$

where

$\dot{Q}_{sc}$  = local volumetric flow rate in secondary combustion chamber,  $\text{m}^3/\text{s}$

$T_{sc}$  = local gas temperature in secondary combustion zone, K

$P_{sc}$  = pressure in secondary combustion zone, kPa

The local velocity in the secondary combustion zone is then given by

$$V_{sc} = \frac{\dot{Q}_{sc}}{A_{sc}} \quad (16)$$

where

$V_{sc}$  = local velocity in secondary combustion zone, m/s

$A_{sc}$  = cross sectional area of secondary combustion zone,  $\text{m}^2$

The gas residence time is the time taken by the flow to move from the entrance of the chamber to the exit. It can approximated by

$$t_{rs} = \frac{d}{\frac{V_{sc})_i + V_{sc})_o}{2}} \quad (17)$$

where

$t_{rs}$  = gas residence time, s

$d$  = distance between inlet and outlet of secondary combustion chamber, m

$V_{sc})_i$  = gas velocity at inlet of chamber, m/s

$V_{sc})_o$  = gas velocity at outlet of chamber, m/s

## 5. RESULTS AND DISCUSSION

### 5.1 Species Concentration and Temperature Measurements in Secondary Combustion Zone

Species concentration and temperature measurements were taken in the secondary combustion chamber at high, intermediate, and low burning rate conditions. Due to the large number of measurements taken, only a limited number are presented in this section. Additional species concentration measurements are tabulated in Appendix D.

Four secondary combustion zone gas temperature data sets taken along the probing axis are plotted as a function of probe position in Figure 12. Four data sets of  $\text{CO}_2$ ,  $\text{O}_2$ , and CO concentrations and  $\text{NO}_x/\text{CO}_2$  ratios, also taken along the probing axis, are plotted in Figure 13. The data sets were taken at 15 minute intervals with the Prince operating at the intermediate burning rate. They are numbered in chronological order. The probe position is referenced to the datum which, as previously mentioned, is approximately level with the lower edge of the inner refractory wall. The coals were not stirred during this test.

Probe-induced interference effects on the gases in the secondary combustion zone are considered negligible since the suction pyrometer and gas sampling probes withdrew less than 1% and 0.1%, respectively, of the total gas molar flow rate. Interference effects were also minimized by orienting the probe bodies (which may be cool as in the case of the water-cooled probes) downstream of the sample inlets.

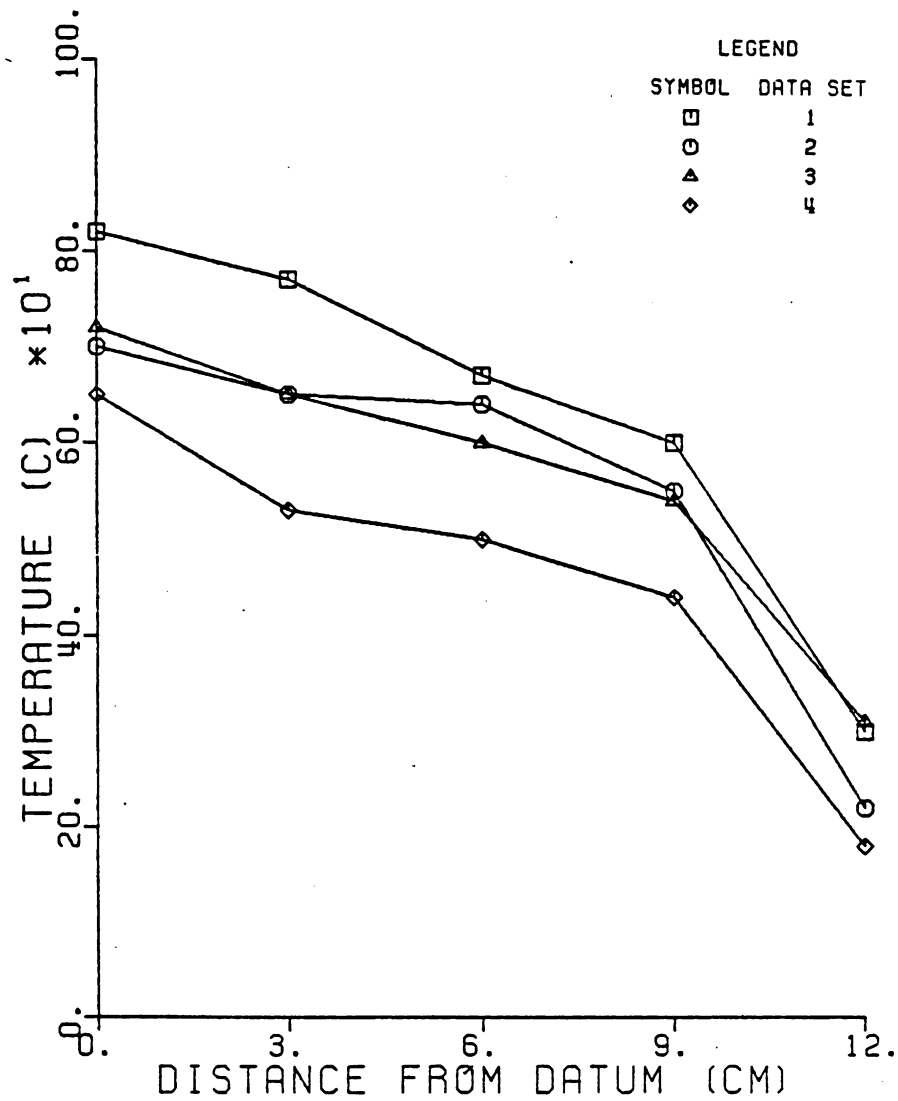


Figure 12. Axial Gas Temperature Measurements in Secondary Combustion Zone for Intermediate Burning Rate Test.



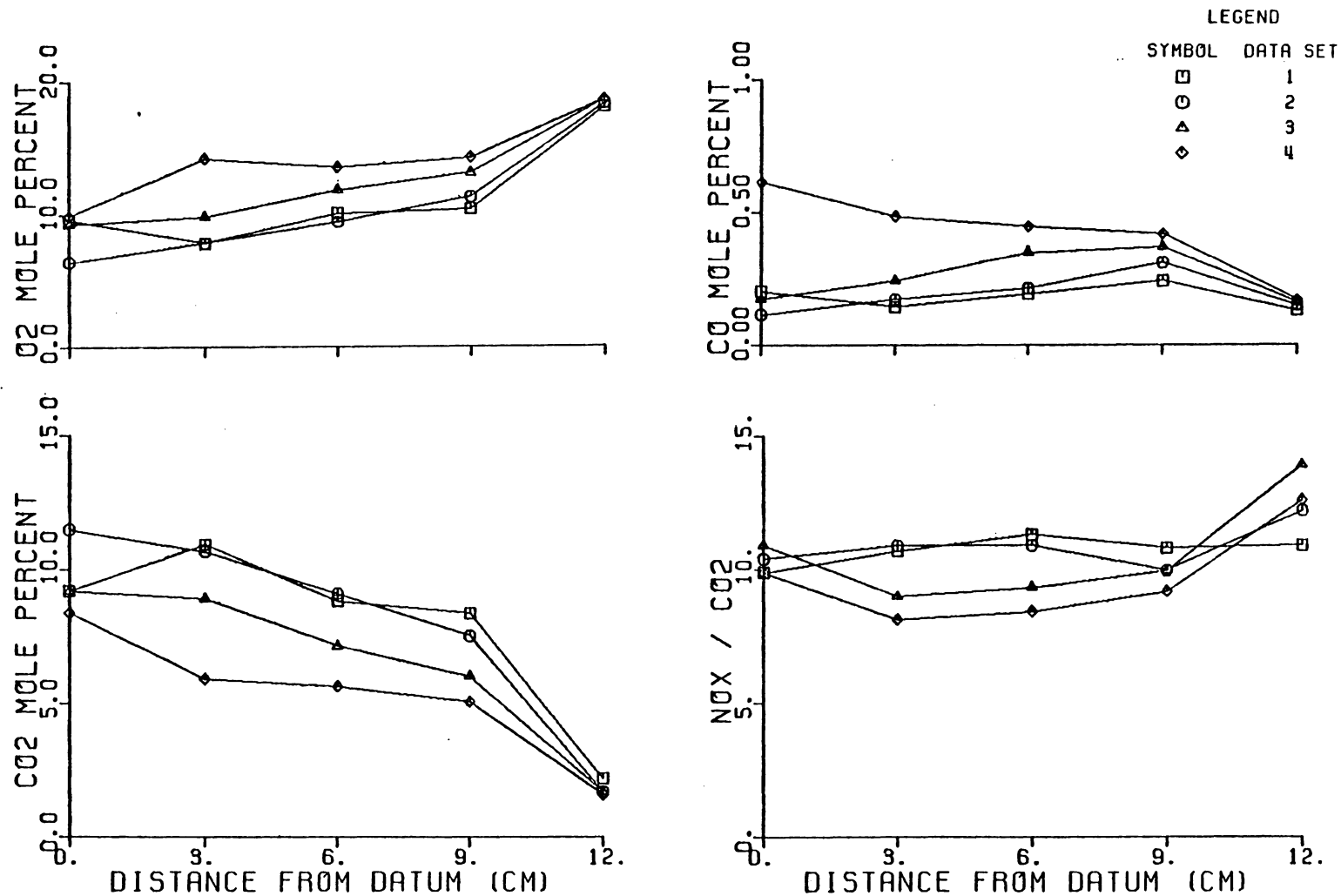


Figure 13. Axial Species Concentration Measurements in Secondary Combustion Zone for Intermediate Burning Rate Test.

The measured gas temperatures at each point generally fluctuated considerably, sometimes as much as  $150^{\circ}\text{C}$ . The temperatures presented in Figure 12 represent average values at each point. Since the measurements were obtained with the suction pyrometer, they are assumed to be free of radiation effects.

The secondary combustion zone gas temperatures decrease with increasing distance from the datum. This is most likely due to the introduction of dilution air (discussed shortly in greater detail). Heat transfer would also tend to lower the gas temperature. The large temperature drop occurring between 10 and 12 cm from the datum is due to the fact that the 12 cm sampling point lies just outside the refractory-lined zone and hence, heat transfer occurs between the gases at that point and the cool boiler walls. In addition, a recirculation may be occurring just outside of the secondary combustion chamber which brings relatively cold air from near the boiler walls into the center of the passage.

In general, the gas temperatures in the secondary combustion chamber tend to decrease with time unless the coal bed is stirred. This effect is attributed to caking of the coals, which causes less primary air to flow through the fuel bed, thus reducing the burning rate of the coal and the product gas temperatures. In addition, the air which passes around the fuel bed mixes in with the product gases and lowers its temperature.

The secondary combustion zone gas temperatures for the high, intermediate, and low burning rate tests ranged from  $550^{\circ}\text{C}$  to  $1040^{\circ}\text{C}$ ,

440°C to 970°C, and 360°C to 830°C, respectively. The gas residence times in the secondary combustion chamber were found to lie between 15 and 40 ms. These short residence times are attributed to the high volumetric flow rates, ranging from 35 to 90 l/s, in the chamber. The work of Hautman, et al. (17) indicates that some aliphatic hydrocarbons can partially oxidize at temperatures (approximately 700°C) which are similar to the temperatures measured in the Prince's secondary combustion zone. However, their data indicate that approximately 0.16 s is required for this to occur. Since the gas residence times are so short, it is uncertain if much hydrocarbon oxidation occurred in the secondary combustion zone.

Soot particles seem to require more time to oxidize compared to hydrocarbons. Extrapolating the results of Fenimore and Jones (26) to lower temperatures and assuming a mean soot particle diameter of 0.3 micrometre, the particle burning time in air at 725°C is found to be approximately 2.7 s. (This particle size is typical of soot emitted from wood burning stoves tested in the VPI&SU Solid Fuels Research Laboratory, and it is here assumed that soot from coal stoves is not too different in size from soot emitted by wood stoves.) However, since the particle burning time is directly proportional to its diameter, the burning time may be shorter if the soot particles are smaller. If the assumed soot particle diameter is correct, it seems that a negligible amount of soot oxidation would occur in the Prince's secondary combustion chamber because of the very short gas residence times.

Dickinson and Payne (12) suggest that the volatile/air mixture must be kept at 550°C for at least 0.5 s in order for coal volatiles to completely oxidize. Squires (16) indicates that a gas temperature and residence time of 700°C and 0.5 to 1 s, respectively, are required for volatile oxidation. These residence times are more than an order of magnitude larger than those measured in the Prince, again indicating that little volatile oxidation probably occurs in its secondary combustion chamber.

It is difficult to determine if CO oxidation was occurring in the Prince's secondary combustion chamber. Fenimore and Moore (26) found that CO could be quenched in a stratified mixture of lean product gases (primarily equivalence ratios ranging from 0.66 to 0.8) and air if the adiabatic mixing temperature was less than about 1000°C. They also found that CO was not quenched when a stratified mixture of rich primary products ( $\phi = 1.5$ ) and air mixed. These results show that CO oxidation in the Prince's secondary combustion zone may be possible if rich primary products mix with air. Since it was not possible to determine the primary equivalence ratio in the Prince, it is difficult to predict if CO oxidation could occur at the temperatures in the secondary combustion zone.

The CO<sub>2</sub> concentrations shown in Figure 13 tend to decrease with increasing distance from the datum. This trend was evident in the majority of the tests and seems to be caused by dilution of the product gases with air. Indeed, this hypothesis seems to be supported by the O<sub>2</sub> concentrations which increase as the probe tip is moved away from the

datum. This dilution can be from secondary air introduced through the secondary air supply system or it can be "primary" air which flows around the fuel bed. The axial and radial probing results (discussed later in this section) yield more information on the air flows in the secondary combustion chamber.

Presented in Table II is a comparison of measured  $\text{CO}_2$  concentrations and  $\text{CO}_2$  concentrations calculated by assuming only dilution (no reaction) occurs between adjacent sampling points. The changes in measured  $\text{O}_2$  concentrations were used to calculate these diluted  $\text{CO}_2$  concentrations. (This method is detailed in Appendix E.) Agreement between measured and calculated  $\text{CO}_2$  concentrations is quite good in most cases, indicating that dilution probably causes the changes in  $\text{CO}_2$  concentrations.

The  $\text{CO}_2$  concentrations decrease with time, probably due to caking of the fuel bed. The caking reduces the burning rate of the coal and lowers the  $\text{CO}_2$  concentrations in the product gases.

The measured CO concentrations in the first three data sets shown in Figure 13 tend to increase up to 9 cm from the datum and then decrease. Assuming only dilution occurs between sampling points, one would expect the CO concentrations to decrease with distance just as the  $\text{CO}_2$  concentrations have done. Since the CO concentrations increase, CO seems to be formed in the secondary combustion chamber. This formation is possibly due to partial oxidation of hydrocarbons. Indeed, Hautman, et al. (17) showed that CO can be formed by the partial oxidation of a lean aliphatic hydrocarbon-air mixture at a relatively low temperature

TABLE II. Comparison of Measured and Calculated CO<sub>2</sub> Concentrations  
(Based on Dilution) in the Secondary Combustion Chamber.

<u>Data Set</u>	<u>Dilution Occurring Between Points</u>	<u>Predicted CO<sub>2</sub> (Mole %)</u>	<u>Actual CO<sub>2</sub> (Mole %)</u>	<u>Percent Difference</u>
1	1-2	*		
	2-3	9.0	8.8	2.3
	3-4	8.6	8.4	2.4
	4-5	2.3	2.2	4.5
2	1-2	10.4	10.7	-2.8
	2-3	9.4	9.1	3.3
	3-4	7.6	7.5	1.3
	4-5	2.1	1.7	2.4
3	1-2	8.7	8.9	2.2
	2-3	7.3	7.1	2.8
	3-4	6.1	6.0	1.7
	4-5	1.8	1.7	5.9
4	1-2	5.2	5.9	13
	2-3	*		
	3-4	5.1	5.1	0
	4-5	1.8	1.6	12

\* Data did not indicate dilution occurring between these points

approximately 700°C. The trend of increasing CO concentrations with increasing distance from the datum was not observed in all cases, however. The CO at times seemed to decrease with distance, possibly due to the effects of dilution or oxidation. It is difficult to make generalizations concerning the CO concentrations in the secondary combustion zone.

The  $\text{NO}_x$  concentrations at each point are divided by the corresponding  $\text{CO}_2$  concentrations to eliminate the changes caused by the dilution with distance from the datum. The  $\text{NO}_x/\text{CO}_2$  curves are relatively flat, as one would expect, since the secondary combustion zone temperatures are too low for  $\text{NO}_x$  to form.

The measurements taken with the two-dimensional probe yield additional information concerning the species concentration gradients in the secondary combustion chamber. Presented in Figure 14 are the intermediate burning rate  $\text{CO}_2$ ,  $\text{O}_2$ , CO, and  $\text{NO}_x$  concentrations plotted as a function of probe rotation and distance from the datum. The position of the probe tip in the secondary combustion chamber is shown in Figure 15 (looking down the probe axis into the chamber). The zero probe rotation angle refers to the probe tip being approximately in the center of the passage. Positive and negative probe rotation angles refer to the probe tip being nearer the inner and outer refractory walls, respectively.

The measured  $\text{CO}_2$  concentrations decrease as the probe tip is moved further from the datum. This trend is probably caused by dilution, as the  $\text{O}_2$  concentrations increase with distance from the datum. Since the  $\text{O}_2$  concentrations increase for all radial positions at each axial

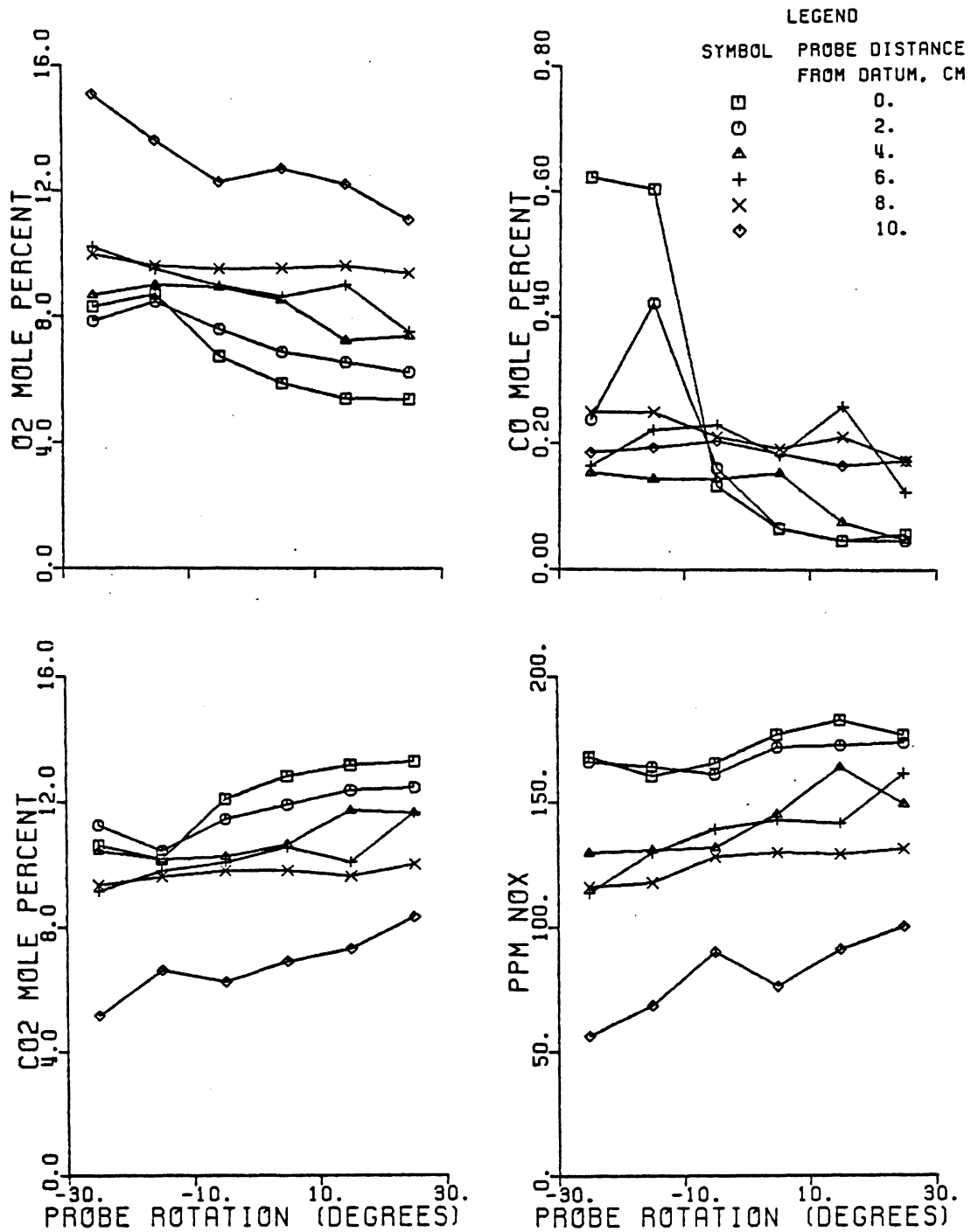


Figure 14. Species Concentrations over Six Cross-Sections in Secondary Combustion Zone for Intermediate Burning Rate Test.



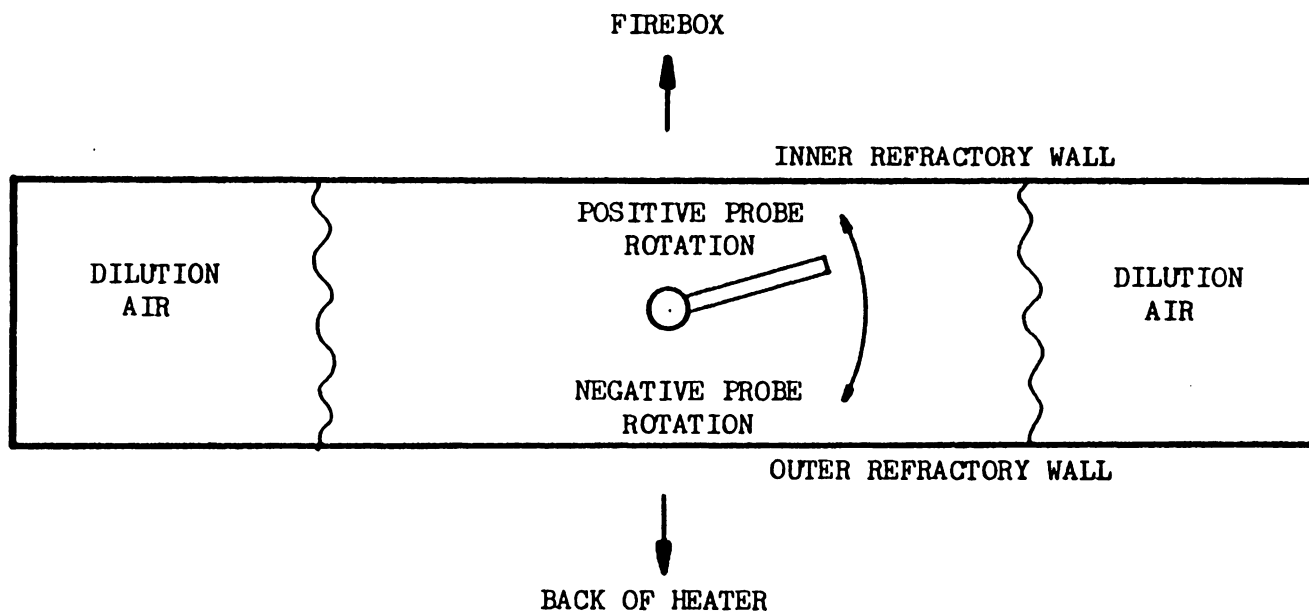


Figure 15. Position of Two-Dimensional Probe in Secondary Combustion Chamber.

position up the secondary combustion chamber, the dilution is probably due to air streams flowing beside the sampled region (see Figure 15). These air streams seem to mix with the product gases as they move up the chamber. However, this mixing may be occurring too late for effective secondary combustion, since the gas temperature becomes rather low (approximately 360°C to 500°C) by the time the  $O_2$  is well mixed in with the product gases.

The CO profiles indicate marked stratification of the flow at the entrance of the secondary combustion chamber, as the CO concentrations vary by a factor of 10 over the cross-section. The profiles tend to flatten as the probe is moved away from the datum, indicating mixing. The average CO concentrations over each cross-section seem to decrease little with increased distance from the datum. This may be due to CO formation in the secondary combustion chamber by partial oxidation of the hydrocarbons in the product gases. This would explain why the average CO concentration remains relatively constant while the average  $CO_2$  concentrations decrease with distance from the datum. Alternatively, it is possible that a stream of gases containing a small amount of CO is diluting the product gases in the secondary combustion zone. This would also allow the average CO concentration to remain constant with distance from the datum. However, some  $CO_2$  would probably also be mixed in with the CO in the dilution gases. Yet the  $CO_2$  concentrations only seem to be affected by dilution with pure air, as shown by Table II. Therefore, the relatively constant average CO concentrations are probably due to CO formation in the secondary combustion zone.

The  $\text{NO}_x$  concentrations decrease as the probe is moved upward in the secondary zone. This trend is similar to that shown by the  $\text{CO}_2$  concentrations and is again attributed to dilution air mixing with the combustion products.

A photograph of an oscilloscope trace displaying the output of the fast response suction pyrometer, which was inserted into the entrance of the secondary combustion zone, is shown in Figure 16. The temperature fluctuations, as great as  $290^\circ\text{C}$ , are indicative of poor mixing between the combustion products and the secondary air. The rapid fluctuations seem to show that the flow consists of hot "packets" of product gases mixed in with cooler secondary air. This poor mixing could inhibit effective combustion in the secondary zone.

## 5.2 Emissions Tests

### 5.2.1 Emission Factors for High Burning Rate Tests

The instantaneous  $\text{CO}$ ,  $\text{NO}_x$ , and  $\text{SO}_x$  emission factors for the high burning rate Clinchfield and Pocahontas tests are plotted as a function of time in Figures 17-22. The average  $\text{CO}$ ,  $\text{NO}_x$ ,  $\text{SO}_x$ , and smoke emission factors for these tests are given in Table III along with emissions factors determined by other researchers testing hand-fired coal stoves and oil and natural gas-fired domestic heaters.

The instantaneous  $\text{CO}$  emission factors for both the Clinchfield and Pocahontas tests were influenced by the caking of the fuel bed. As the coals agglomerated, allowing less primary air to flow through the fuel bed, the  $\text{CO}$  emission factors increased. Mackend (27) found that

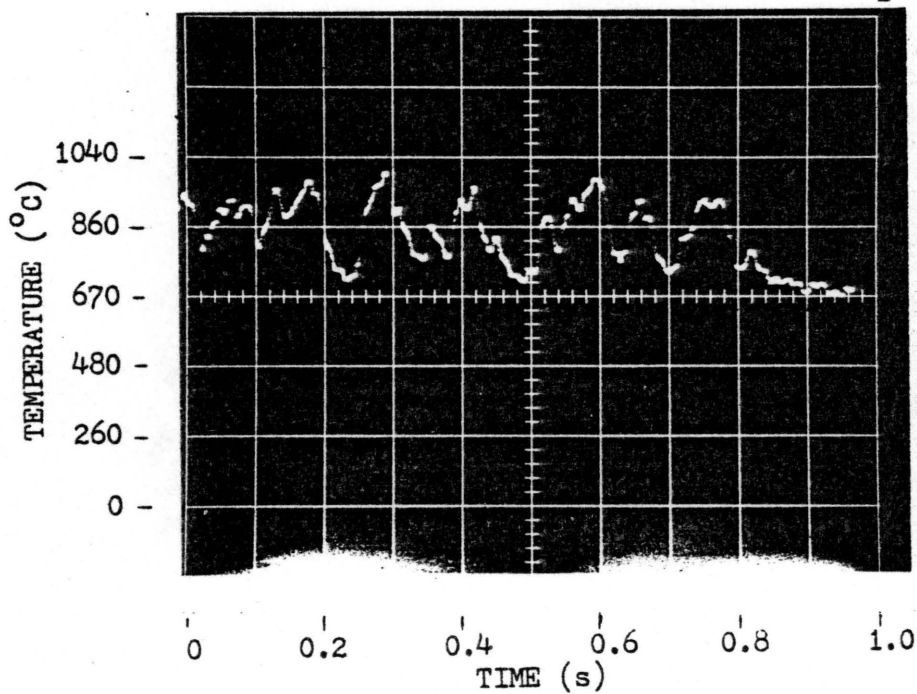


Figure 16. Oscilloscope Trace Displaying Temperature Variation at a Point Near the Entrance of the Secondary Combustion Chamber.

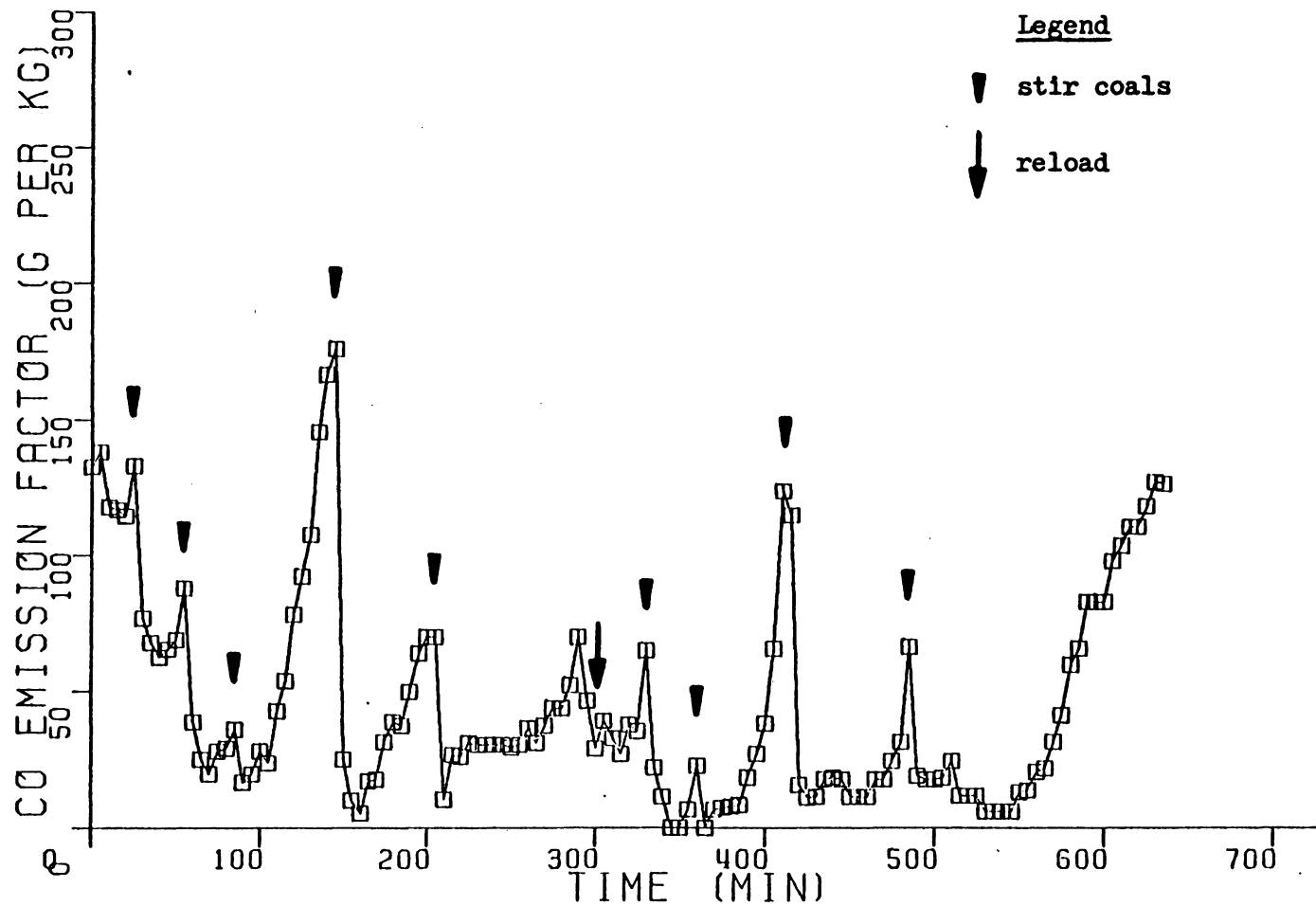


Figure 17. Instantaneous CO Emission Factor for the High Burning Rate Clinchfield Test.

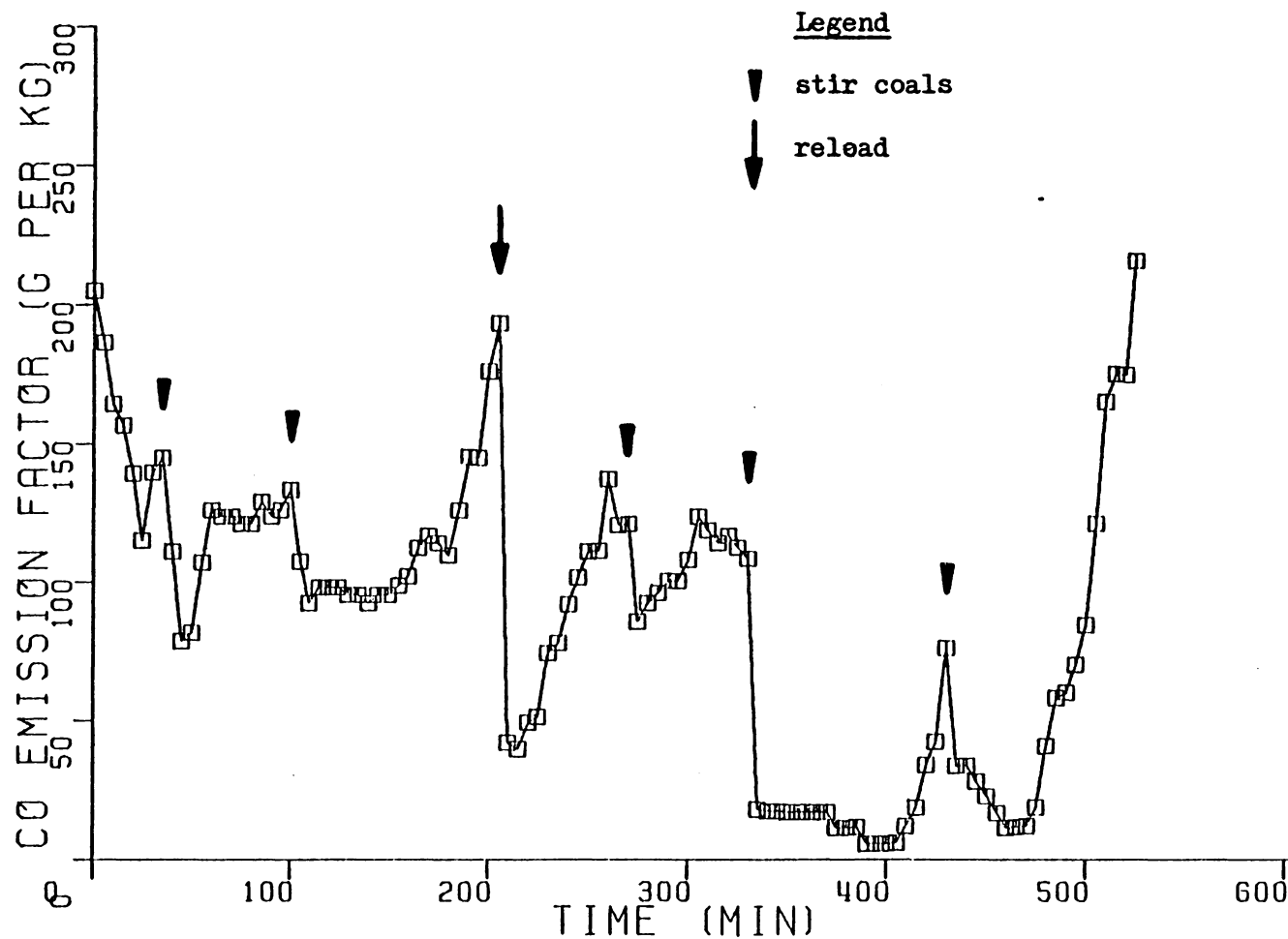


Figure 18. Instantaneous CO Emission Factor for the High Burning Rate Pocahontas Test.

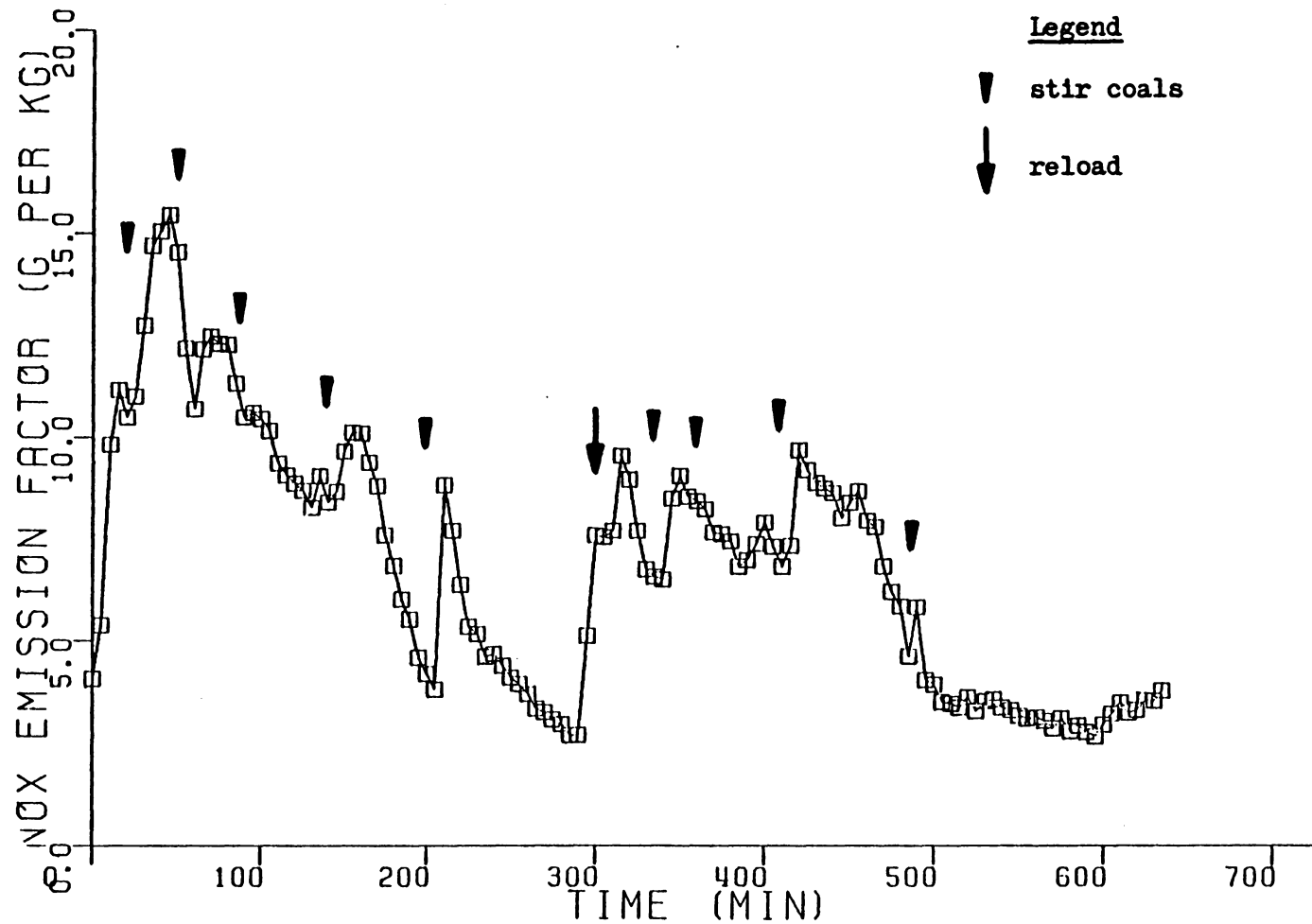


Figure 19. Instantaneous NO<sub>x</sub> Emission Factor for the High Burning Rate Clinchfield Test.

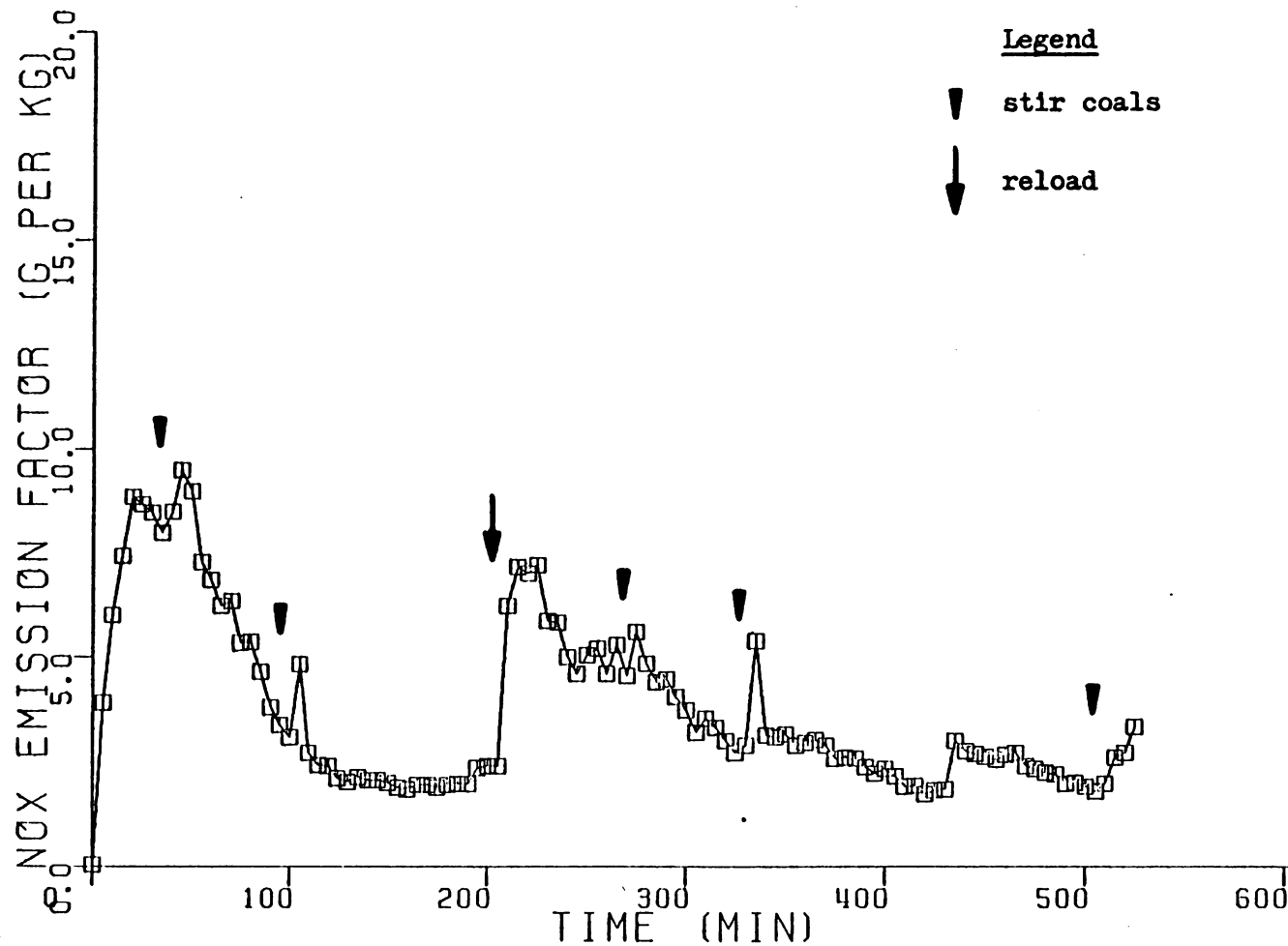


Figure 20. Instantaneous NO<sub>x</sub> Emission Factor for the High Burning Rate Pocahontas Test.



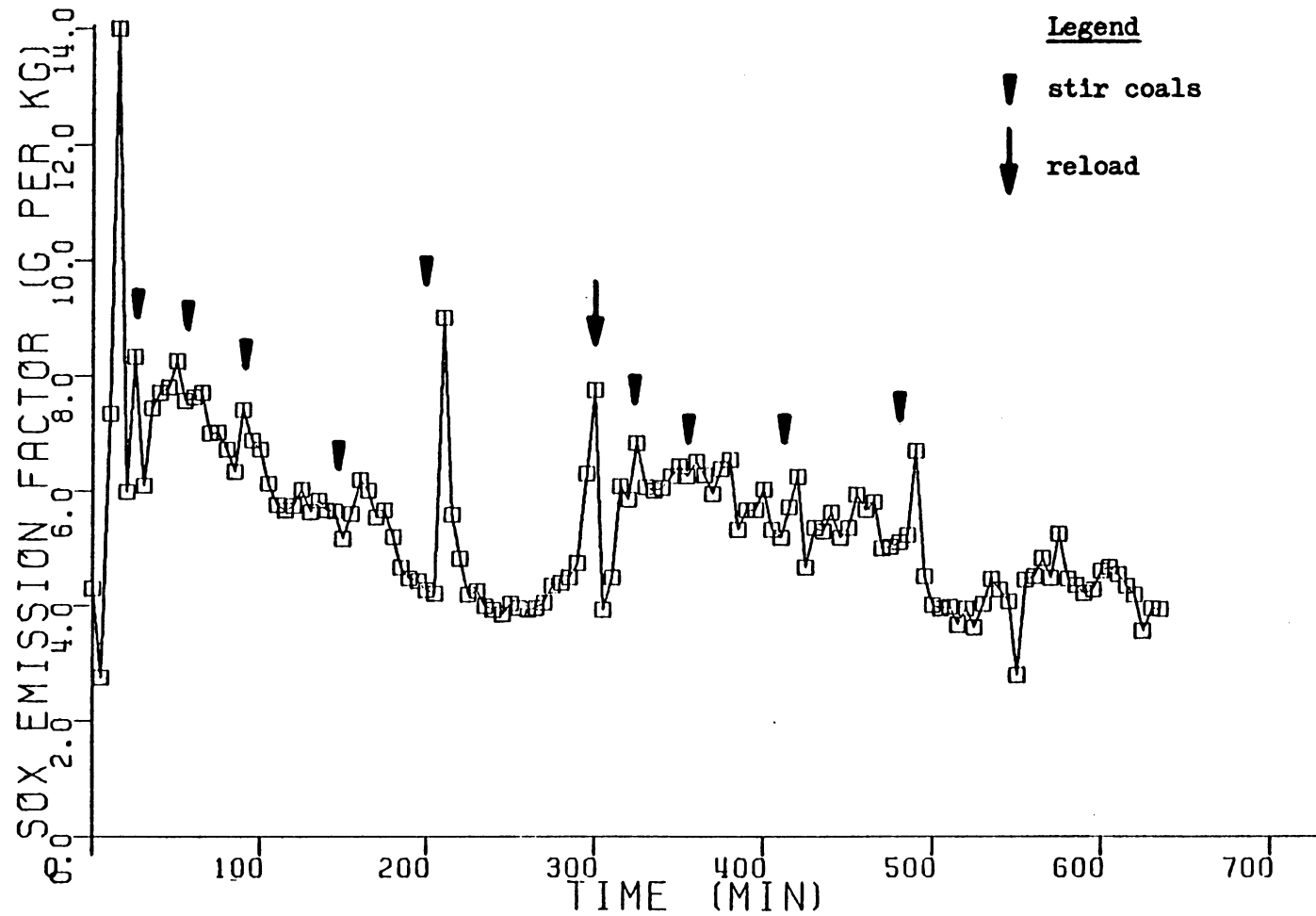


Figure 21. Instantaneous SO<sub>x</sub> Emission Factor for the High Burning Rate Clinchfield Test.

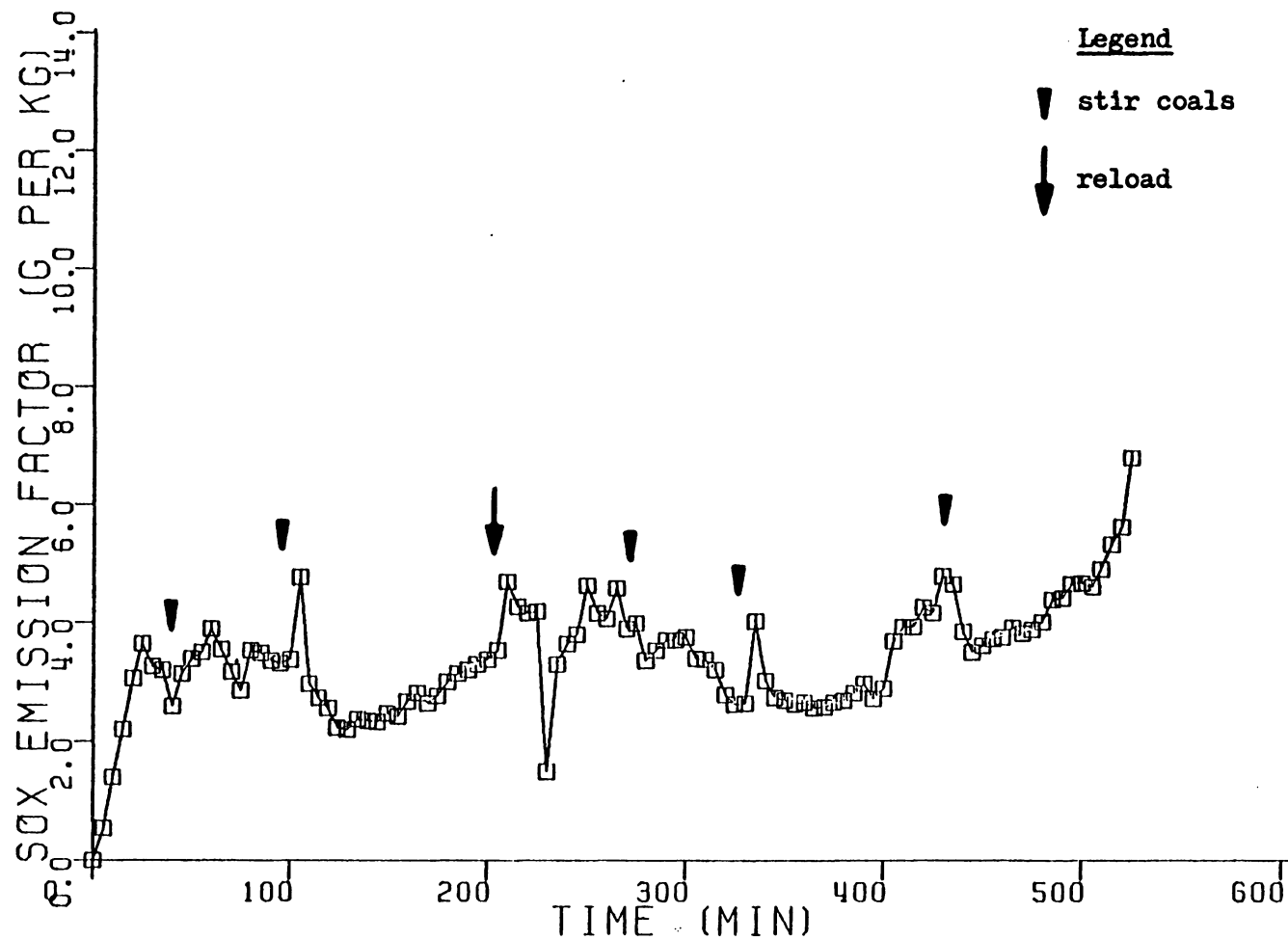


Figure 22. Instantaneous SO<sub>x</sub> Emission Factor for the High Burning Rate Pocahontas Test.

TABLE III. CO, NO<sub>x</sub>, SO<sub>x</sub>, and Smoke Emission Factors for High and Low Burning Rate Tests with Comparison to Other's Results

	CO (g/kg)	NO <sub>x</sub> (g/kg)	SO <sub>x</sub> (g/kg)	Smoke(g/kg)
High Burning Rate Test (Clinchfield Coal)	38	6.8	5.4	14 <sup>a</sup> 7.9 <sup>b</sup>
High Burning Rate Test (Pocahontas Coal)	81	3.6	3.3	16 <sup>a</sup> 4.4 <sup>b</sup>
Low Burning Rate Test (Clinchfield Coal)	55	3.1	5.1	7.3 <sup>b</sup>
Low Burning Rate Test (Pocahontas Coal)	120	1.2	-	2.3 <sup>b,c</sup>
Updraft Stove (7) (Clinchfield Coal)	96-151	3.3-5.1	3.3-3.6	54-79 <sup>a</sup>
Updraft Stove (7) (Pocahontas Coal)	105-157	2.6-4.2	2.8-2.9	17-31 <sup>a</sup>
Hand-Fired Coal Stoves (9,14,28)	2-120	1.6-6	7.5-58	10-19 <sup>d</sup>
Rayburn Prince (12)	-	-	-	2.3-6.8 <sup>b,c</sup>
Oil-Fired Domestic Boiler (28,29)	0.7	3.	-	0.4
Natural Gas-fired Domestic Heater (28,29)	0.5	2.	0.01	0.2

a - start-up smoke included

b - start-up smoke not included

c - no stirring of coal bed during test

d - not known if start-up smoke is included

reducing the primary air flow in a staged downdraft combustor caused the primary equivalence ratio to decrease from 1.5 to 0.92 and the CO emission factor to increase. It is possible that the same phenomenon is occurring within the Prince. The primary products may become fuel lean when the fuel bed cakes, thus forming a stratified mixture of air and lean primary products in the secondary combustion zone. The work of Fenimore and Moore (26) shows that it is possible for the CO to quench in such a mixture if the adiabatic mixing temperature is less than 1000°C (as it almost always is in the secondary combustion zone). The increases in CO emission factor when the coals agglomerate may be due to this CO quenching phenomenon.

Stirring the fuel bed caused the CO emission factors to drop rapidly. The stirring probably causes the primary equivalence ratio to increase, thus reducing the CO quenching. More frequent stirring was required during the Clinchfield test, as this coal seems to have a greater agglomerating tendency compared to Pocahontas coal. Although the Pocahontas coal was observed to cake less than the Clinchfield coal, the CO emission factor for the Pocahontas test was about twice as high as that for the Clinchfield test. The reason for this occurrence is unknown.

The "stepped" appearance of the CO emission factor curves is due to the fact that the CO concentrations were displayed on a digital readout. This, combined with relatively constant burning rates, caused the discrete jumps in the instantaneous CO emission factors.

The CO emission factors for the high burning rate tests are substantially lower than those found by Jaasma and Macumber (7), who used identical coals in "air-tight" updraft stoves. This is most likely due to decreased primary air flow rate in the "air-tight" stoves which tends to increase the CO emissions. The CO emission factors for the high output tests lie within the range of values determined by other researchers for hand-fired coal stoves. Since the CO emission factor is dependent on coal properties and stove design (unspecified in most of the references), these values can only serve as a guide for rough comparison.

The instantaneous  $\text{NO}_x$  emission factors for both tests were highest when the fresh coals devolatilized and burned. They decreased as less volatiles were being released from the coal. Stirring the fuel bed generally caused sharp increases in the  $\text{NO}_x$  emission factor. This is probably due to increased fuel bed and product gas temperatures and also allowing more oxygen to be present in the high temperature regions.

The average  $\text{NO}_x$  emission factor for the Clinchfield test was about twice as high as that for the Pocahontas test. The fuel nitrogen in the Clinchfield coal was about 30% greater than the fuel nitrogen in the Pocahontas coal. This might represent one cause for the higher emissions. In addition, the Clinchfield coal seemed to burn with a higher fuel bed temperature (as evidenced by a greater intensity of the fire) which could also increase the  $\text{NO}_x$  emissions. Finally, the more frequent stirring during the Clinchfield test may have contributed to the increase.

The  $\text{NO}_x$  emission factor for the Clinchfield test was about 33% greater than the highest value found by Jaasma and Macumber (7) using Clinchfield Coal. The  $\text{NO}_x$  emission factor for the Pocahontas test lies in the range of values they found using Pocahontas coal. The higher  $\text{NO}_x$  emission factor for the Clinchfield test is possibly due to the higher primary air flow rate (as evidenced by the higher burning rates) and hotter fuel bed temperatures in the Prince.

The instantaneous  $\text{SO}_x$  emission factors do not correlate with stirring as well as the CO and  $\text{NO}_x$  emission factors. However, some increases in  $\text{SO}_x$  emission factors do seem to be caused by stirring. The large peak occurring 15 minutes into the Clinchfield test is probably erroneous due to misadjustment of the dilution rotameter settings.

Sulfur balances conducted on the Clinchfield and Pocahontas tests indicate that 48 and 31% of the sulfur present in the respective coals forms  $\text{SO}_x$ . Results presented by DeAngelis and Reznik (8) show a 45-75% conversion of fuel sulfur to  $\text{SO}_x$ . There are several possible explanations concerning the fate of the sulfur during the high output tests. The  $\text{SO}_x$  emissions can form  $\text{H}_2\text{SO}_4$  and other sulfates on the particulate surfaces. It has been reported that these sulfates can account for 25 to 35% of the mass of particulates emitted from a hand-fired stove burning bituminous coal (30). Since a sulfur analysis of the particulate catch was not performed it was not possible to determine the amount of sulfates formed. Also, since  $\text{SO}_2$  is soluble in water, it is possible that some of the  $\text{SO}_x$  was absorbed by the condensate in the  $0^\circ\text{C}$  condenser before the sample reached the analyzer. Finally, it is

possible for the sulfur to react with elements in the coal (such as calcium) and form compounds which remain in the ashpit (8).

Two smoke emission factors are shown in Table III for each high burning rate test -- one for the initial charge of coal (start-up) and the other for the reload charge (no start-up smoke included). The smoke emission factors for the portions of the Clinchfield and Pocahontas which include start-up smoke are 77 and 260% greater, respectively, than those for the reload portion of the test. These large differences are attributed to low fuel bed temperatures during start-up which allow the volatiles, distilled from the coal and kindling wood, to pass up the stack without undergoing combustion. Since the Prince is intended to be kept continuously burning, the smoke emission factors for the reload portions of the test are perhaps the more realistic values to consider.

The smoke emission factor for the Clinchfield reload test is 80% larger than that for the Pocahontas reload test. This is probably due to the higher volatile content of the Clinchfield coal (33%) compared to that of the Pocahontas coal (24%). Others (7,8,9) have also found that high volatile coals produce greater smoke emissions than low volatile coals.

The smoke emission factors determined by Jaasma and Macumber (7), using identical coals in hand-fired coal stoves, are up to six times greater than the high firing rate emission factors for the Prince. The higher emission factors for their stoves are probably due to the updraft design and ineffective secondary combustion. The Princes' design seems to work well in terms of reducing smoke emissions. Although the

secondary combustion chamber seems to play only a small part in reducing the smoke, the refractory walls of the secondary combustion chamber inlet probably help to keep the fuel bed temperatures as high as possible. The volatiles distilled from the fresh coal are drawn through this hot, glowing fuel bed where they are rapidly combusted. This downdraft operation of the Prince leads to its low smoke emissions.

The smoke emission factor for the high burning rate Clinchfield test (without start-up) is somewhat greater than the Table III values determined by the National Coal Board of Great Britain for the Rayburn Prince. This may be due to the large amount of stirring required during the Clinchfield test or it may be due to differences between properties of this coal and British coals. However, the smoke emission factor for the Pocahontas test lies in the range of values determined by the National Coal Board.

The smoke emission rates for the Clinchfield and Pocahontas tests (start-up smoke not included) are shown in Table IV, along with emission rates allowed under British law (corresponding to the mean heat output of the heater during each test). The Pocahontas test meets the standard but the Clinchfield test fails. Again, this can be due to the "dirty" nature of Clinchfield coal or the large amount of fuel bed stirring during the test.

It should be noted that visible smoke emissions for the Prince were not observed under normal burning conditions. However, visible smoke emissions were noticed during the first half hour of start-up.



Table IV. Smoke Emission Rates for High and Low Burning Rate Tests with Comparison to British Results and Standards.

	<u>Measured Emission Rate (g/h)</u>	<u>Allowed Emission Rate Under British Standard (g/h)</u>
High Burning Rate <sup>a</sup> (Clinchfield - Reload)	11	7.7
High Burning Rate <sup>a</sup> (Pocahontas - Reload)	5.9	7.4
Low Burning Rate <sup>a</sup> (Clinchfield)	2.9	5.9
Low Burning Rate <sup>b</sup> (Pocahontas)	1.1	5.9
Values Obtained by <sup>b</sup> National Coal Board Burning Bituminous Coals in Rayburn Prince 76 (9)	2.4 - 6.0	5.8 - 8.4

a - coal bed stirred during test

b - coal bed not stirred during test

### 5.2.2 Emission Factors for Low Burning Rate Tests

The instantaneous CO and NO<sub>x</sub> emission factors for the low burning rate Clinchfield and Pocahontas tests are plotted in Figures 23-26. The instantaneous SO<sub>x</sub> emission factor for the low burning rate Clinchfield test is plotted in Figure 27. The average CO, NO<sub>x</sub>, SO<sub>x</sub>, and smoke emission factors for these tests appear in Table III.

Stirring of the coal bed during the Clinchfield test resulted in tremendous reductions in the instantaneous CO emission factor, as in the high burning rate tests. After the CO emission factor drops to a low value, however, it slowly rises to at least its original value before stirring. The "stepped" appearance of the CO emission factor curve is again due to the fact that the CO concentrations were displayed on a digital readout. The coal bed was not stirred during the Pocahontas test since steady burning conditions were achieved and the fire did not appear to be going out. The instantaneous CO emission factor for this test rose rapidly when the closure plate was put in the closed position. After reaching a peak value of about 280 g/kg, it declined slowly to about 200 g/kg.

The average CO emission factors for the low output tests are about 45% greater than those for the corresponding high burning rate tests. This increase in CO emission factor with lower burning rate correlates well with the results found by Mackend (27) and is attributed to the same quenching phenomenon that occurs during coal agglomeration (discussed in Sec. 5.2.1). The CO emission factors for the low burning rate tests are similar to those obtained by Jaasma and Macumber (7) for

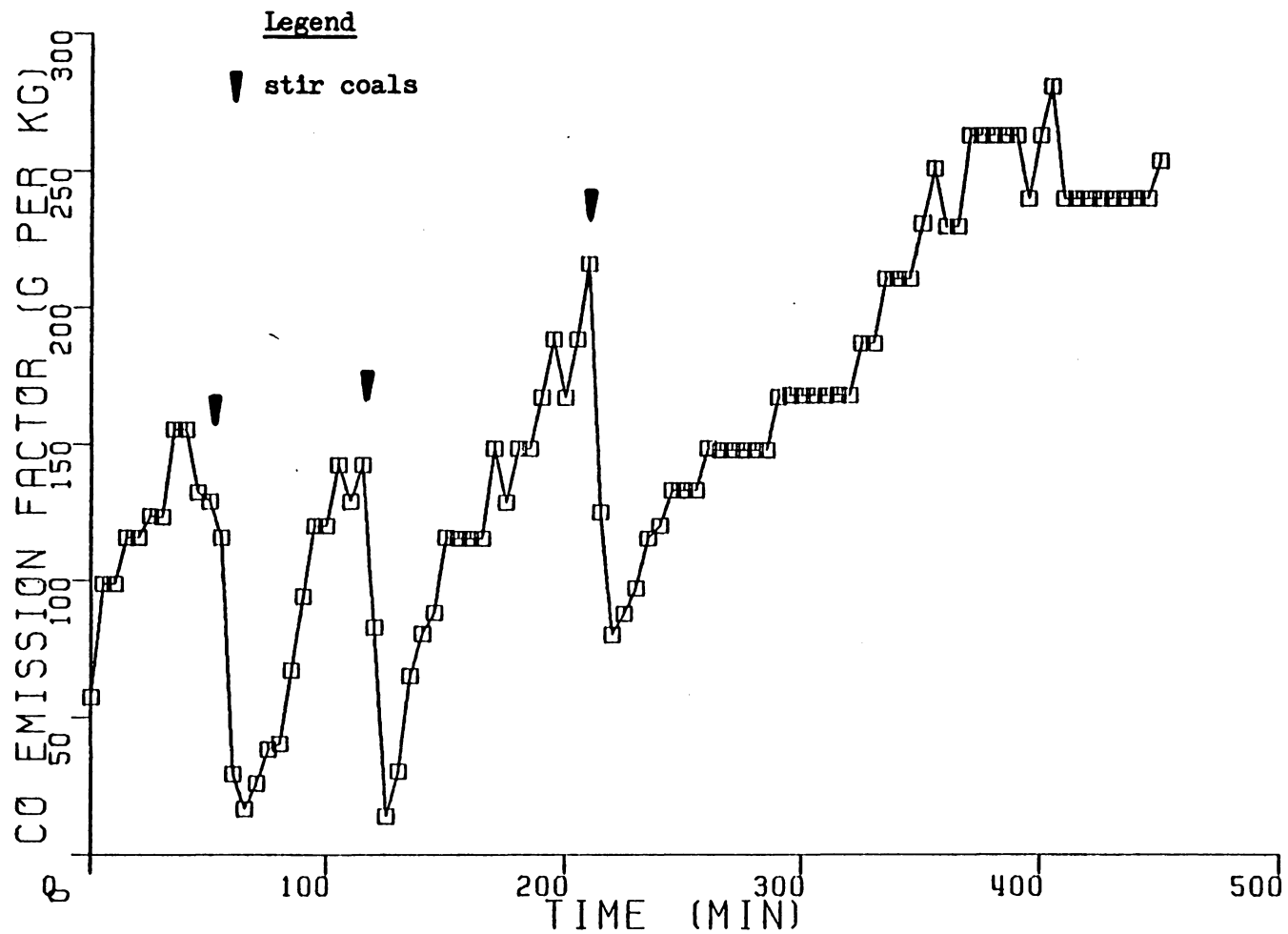


Figure 23. Instantaneous CO Emission Factor for the Low Burning Rate Clinchfield Test.

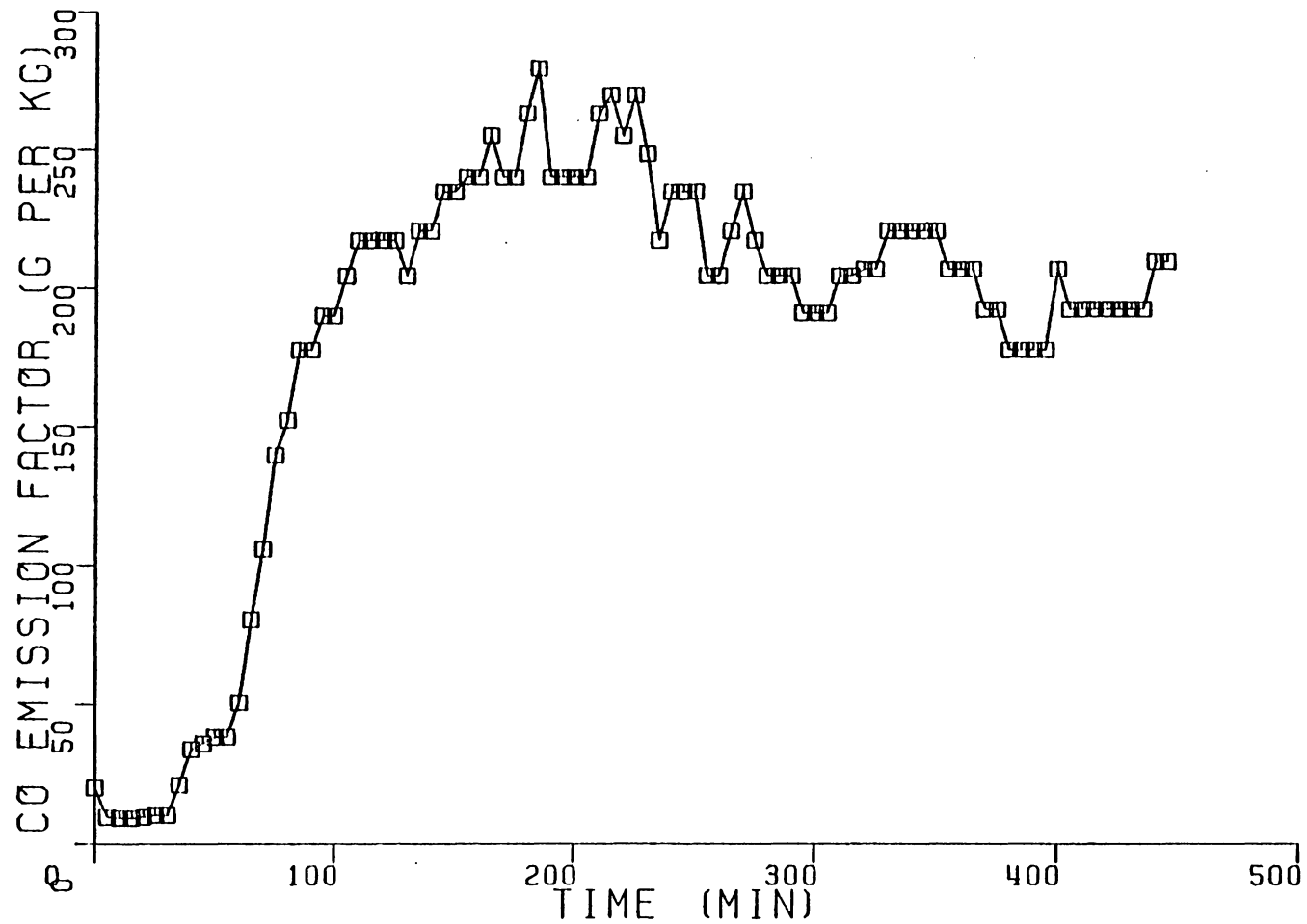


Figure 24. Instantaneous CO Emission Factor for the Low Burning Rate Pocahontas Test.

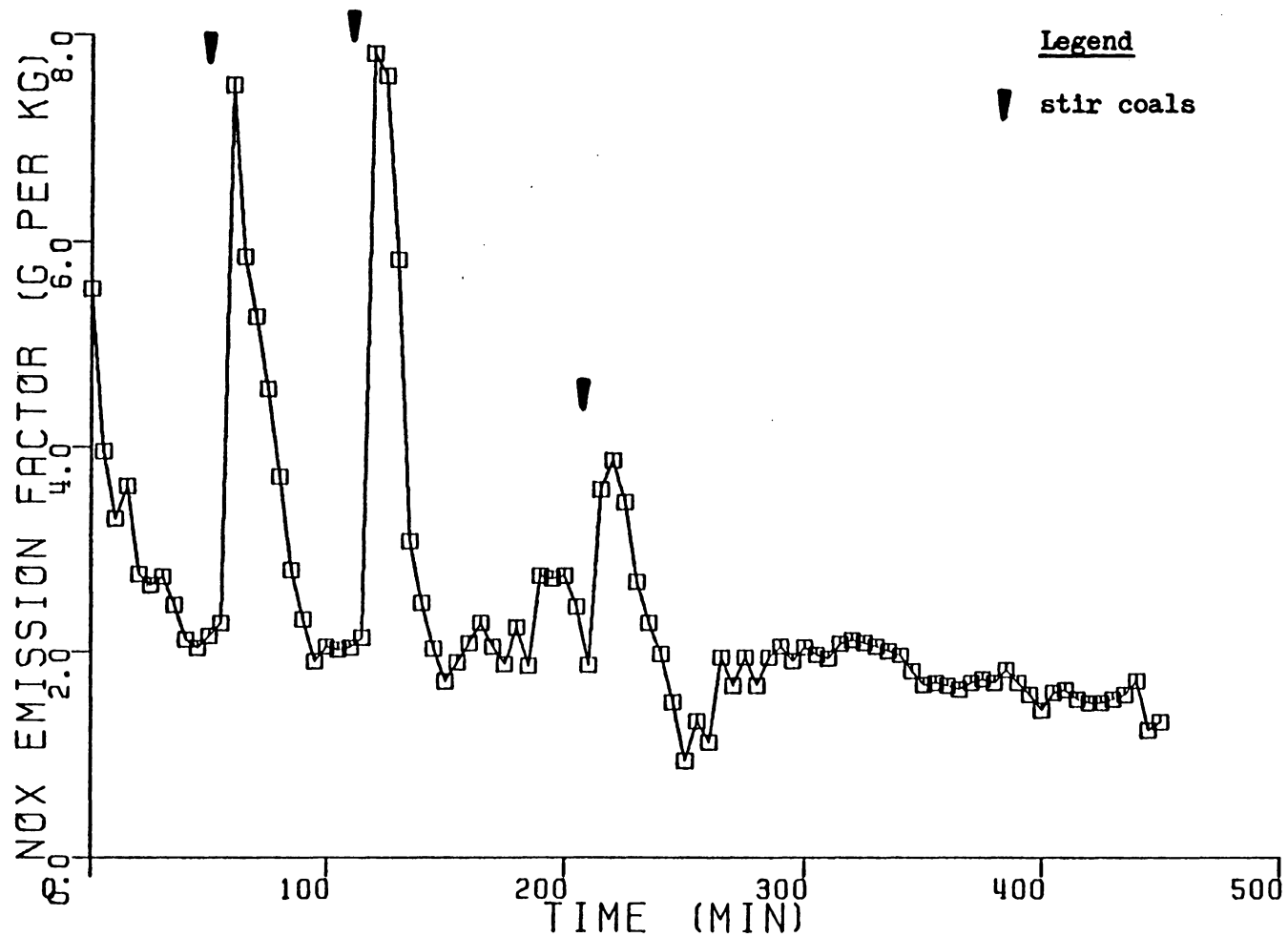


Figure 25. Instantaneous NO<sub>x</sub> Emission Factor for the -  
Low Burning Rate Clinchfield Test.

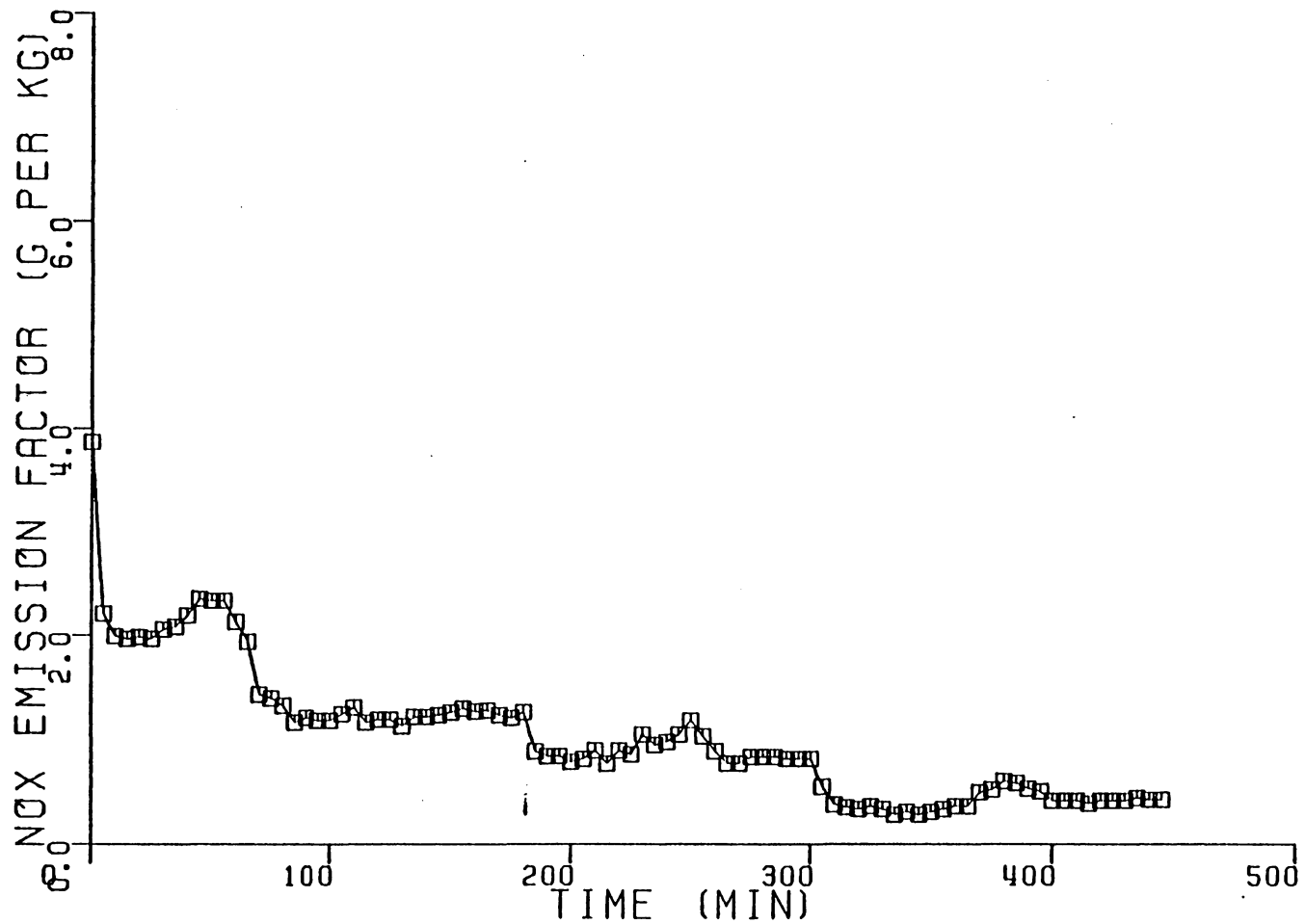


Figure 26. Instantaneous NO<sub>x</sub> Emission Factor for the Low Burning Rate Pocahontas Test.

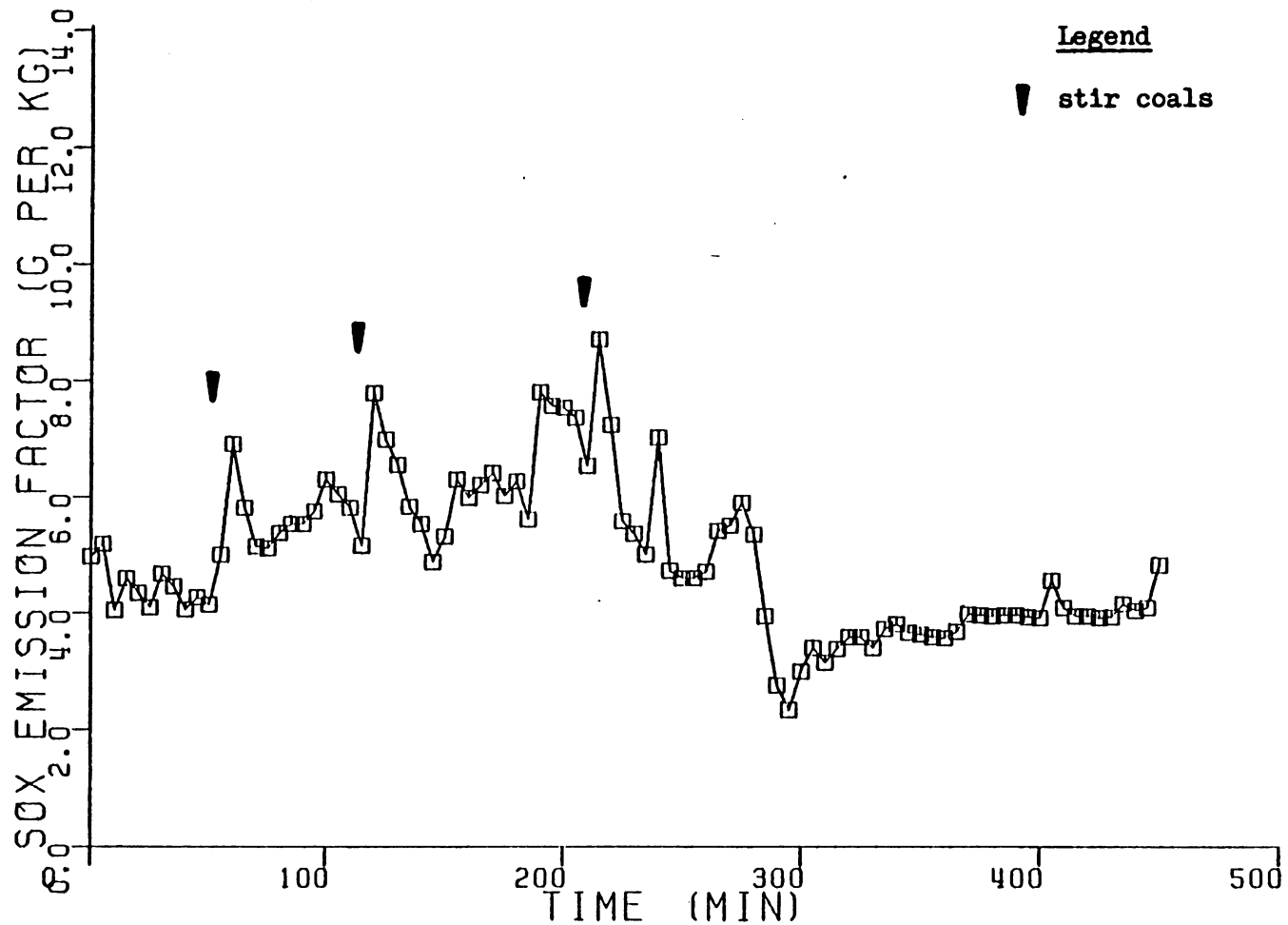


Figure 27. Instantaneous SO<sub>x</sub> Emission Factor for the Low Burning Rate Clinchfield Test.

updraft stoves using identical coals. The CO emission factors lie in the range of values reported by other researchers for hand-fired coal stoves. The values can only serve as a guide for comparison, however, due to the limitations discussed earlier.

The instantaneous  $\text{NO}_x$  emission factor for the Clinchfield test increased rapidly when the fuel bed was stirred, as in the high output tests after stirring. The  $\text{NO}_x$  emission factor for the Pocahontas test exhibits no peaks since the coal bed was not stirred. The  $\text{NO}_x$  emission factor for this test decreases very slowly with time. The higher average  $\text{NO}_x$  emission factor for the Clinchfield test over the Pocahontas test may be due to the higher fuel nitrogen content in the Clinchfield coal and/or the stirring of the fuel bed during the Clinchfield test. The  $\text{NO}_x$  emission factors were about 25 to 65% lower than those determined by Jaasma and Macumber (7). This is probably due to the lower burning rate condition (and lower fuel bed temperatures) that the Prince was operated at.

The instantaneous  $\text{SO}_x$  emission factor for the Clinchfield test shows some increases due to stirring. A sulfur balance performed on the test data indicated that 46% of the sulfur present in the coal forms  $\text{SO}_x$ . This is similar to the 48% value found for the high burning rate Clinchfield test.

The Table III smoke emission factors for the low-fire tests do not include start-up smoke. The smoke emission factor for the Clinchfield test is found to be approximately 220% greater than that for the Pocahontas test. This difference seems to be caused by the higher



volatile content of the Clinchfield coal and the fact that the coal bed was not stirred during the Pocahontas test.

The smoke emission factor for the Clinchfield test is somewhat higher than the range of values determined for the Prince by the National Coal Board. The Pocahontas test smoke emission factor is identical to the lowest value presented by the British researchers. The smoke emission rates for the low output tests are presented in Table IV and are observed to have passed the British standards handily.

### 5.2.3 Particulate Sizing

The size distributions of the particulates captured by the cascade impactor during the high burning rate Pocahontas test (start-up test) and the low burning rate Clinchfield test (no start-up) are presented in Table V. The cut diameters are different in each test since different isokinetic sampling flow rates were used. (The cut diameter refers to the smallest particle diameter that is collected with 50% efficiency.) The vast majority of particulate mass emitted during the Pocahontas test was in the sub-micrometre range, while a substantial amount of particulate mass greater than 1 micrometre was emitted during the Clinchfield test.

Butcher and Ellenbecker (14) used a cyclone to determine that 89% of the particulate mass emitted from a hand-fired coal stove burning high volatile bituminous coal had an aerodynamic diameter less than 4 micrometres. The results of the Clinchfield test, with 89% of the particulate mass having diameters less than 4 micrometres, compare

TABLE V. Particulate Size Distributions for the Rayburn Prince 76  
Operating on Pocahontas and Clinchfield Coals.

Full Output - Pocahontas Coal<sup>a</sup>

<u>Aerodynamically Equivalent Particle Diameter ( <math>\mu\text{m}</math> )<sup>c</sup></u>	<u>Percent of Particulates in this range (by mass)</u>
> 14	.5
8 - 14	.5
3.5 - 8	.6
2.0 - 3.5	.5
1.3 - 2.0	1.8
0.7 - 1.3	5.1
< 0.7	91.0

Low Output - Clinchfield Coal<sup>b</sup>

<u>Aerodynamically Equivalent Particle Diameter ( <math>\mu\text{m}</math> )<sup>c</sup></u>	<u>Percent of Particulates in this range (by mass)</u>
> 28	4.0
17 - 28	1.2
7 - 17	2.4
4 - 7	3.6
2.5 - 4.0	4.8
1.4 - 2.5	6.0
< 1.4	78.2

a - start-up test

b - reload test

c - at 50% collection efficiency

favorably to theirs. However, this agreement may be fortuitous. Measurements of wood stove particulate emissions at VPI&SU (using electron microscopy) indicate that the mean particulate diameter is about 0.3 micrometre. These particles seem to be similar in size to those emitted by coal stoves.

Particulates that are less than 10 micrometres in aerodynamic diameter are of interest because of their potential health hazard. Particulates in this size range have the longest atmospheric residence times and are most likely to be drawn deeply into the lung where removal by mucociliary transport is more difficult (31). In addition, these particulates are often coated with toxic compounds which can cause pulmonary damage (30).

### 5.3 Efficiency Test Results

The instantaneous efficiencies for the high and low burning rate tests are plotted in Figs. 28-31. The average efficiencies, energy loss distributions, and useful heat outputs for these tests are presented in Table VI. These values characterize the operation of the Prince on the coals tested. The values obtained on British coals (which the Prince was designed to burn) may be different due to differences between properties of the test coals and British coals.

The variations in the instantaneous efficiencies are a strong function of the CO chemical energy loss. When the coal begins to cake, the CO emission factor climbs rapidly, decreasing the instantaneous

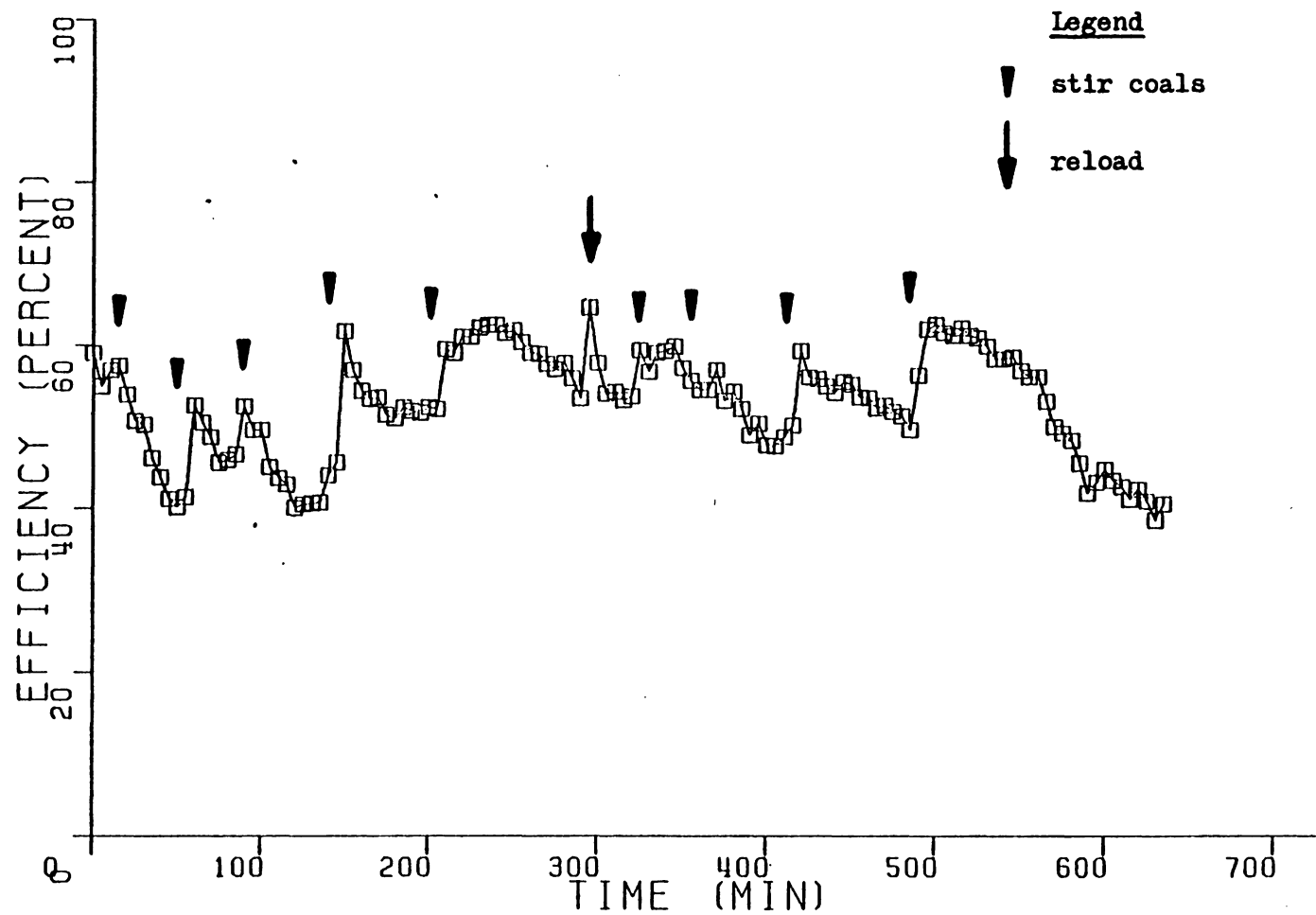


Figure 28. Instantaneous Efficiency for the High Burning Rate Clinchfield Test.

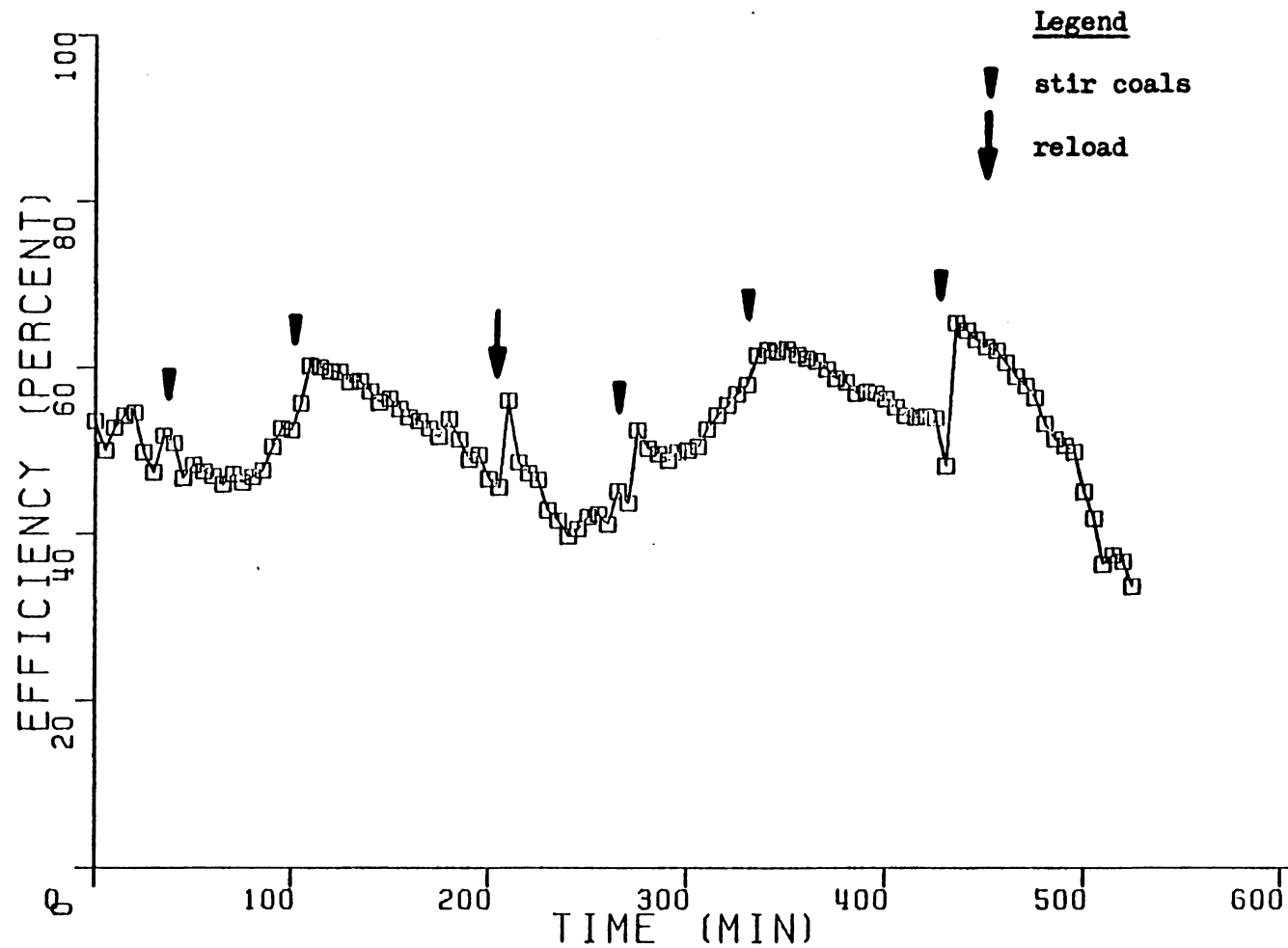


Figure 29. Instantaneous Efficiency for the High Burning Rate Pocahontas Test.

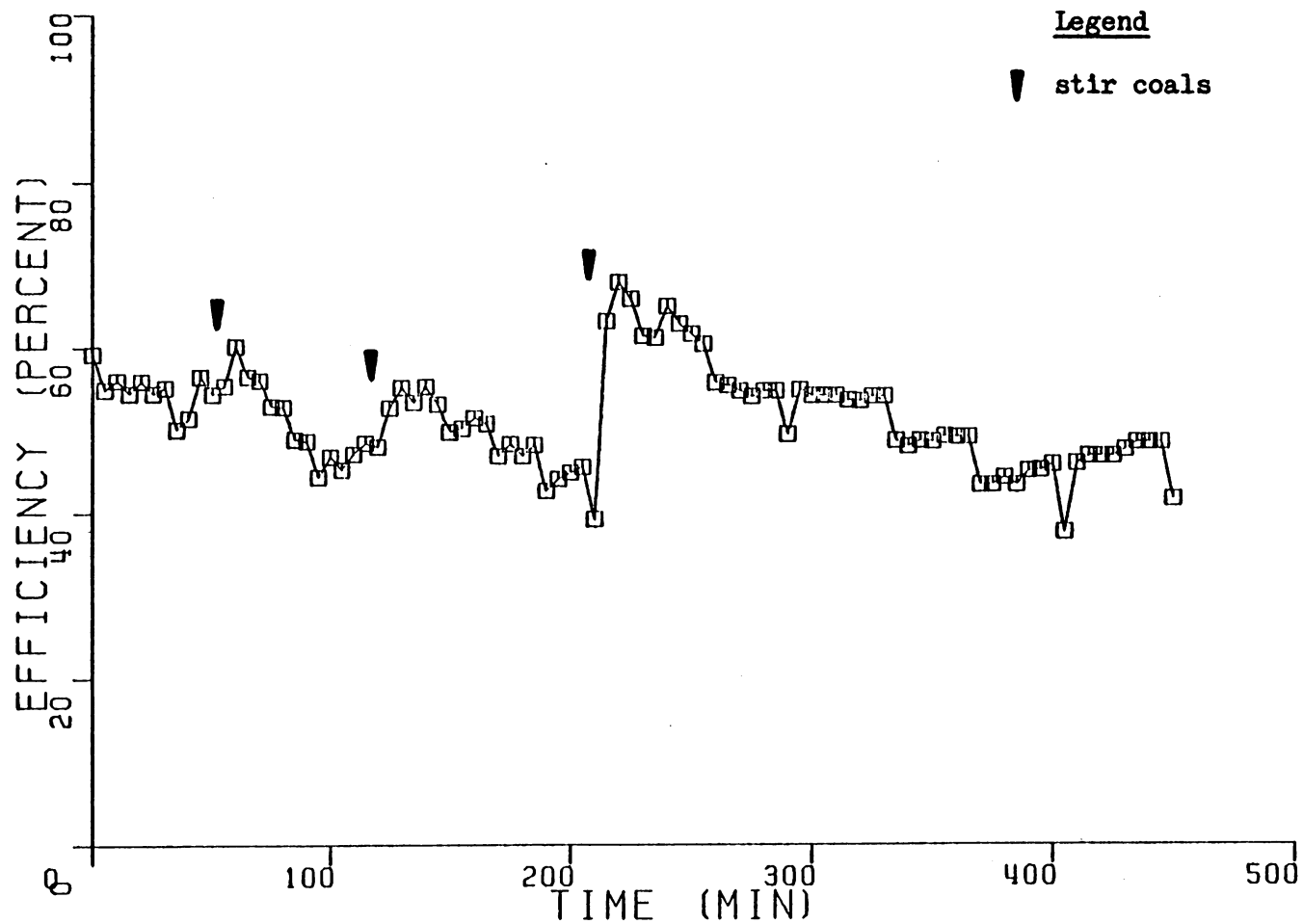


Figure 30. Instantaneous Efficiency for the Low Burning Rate Clinchfield Test.

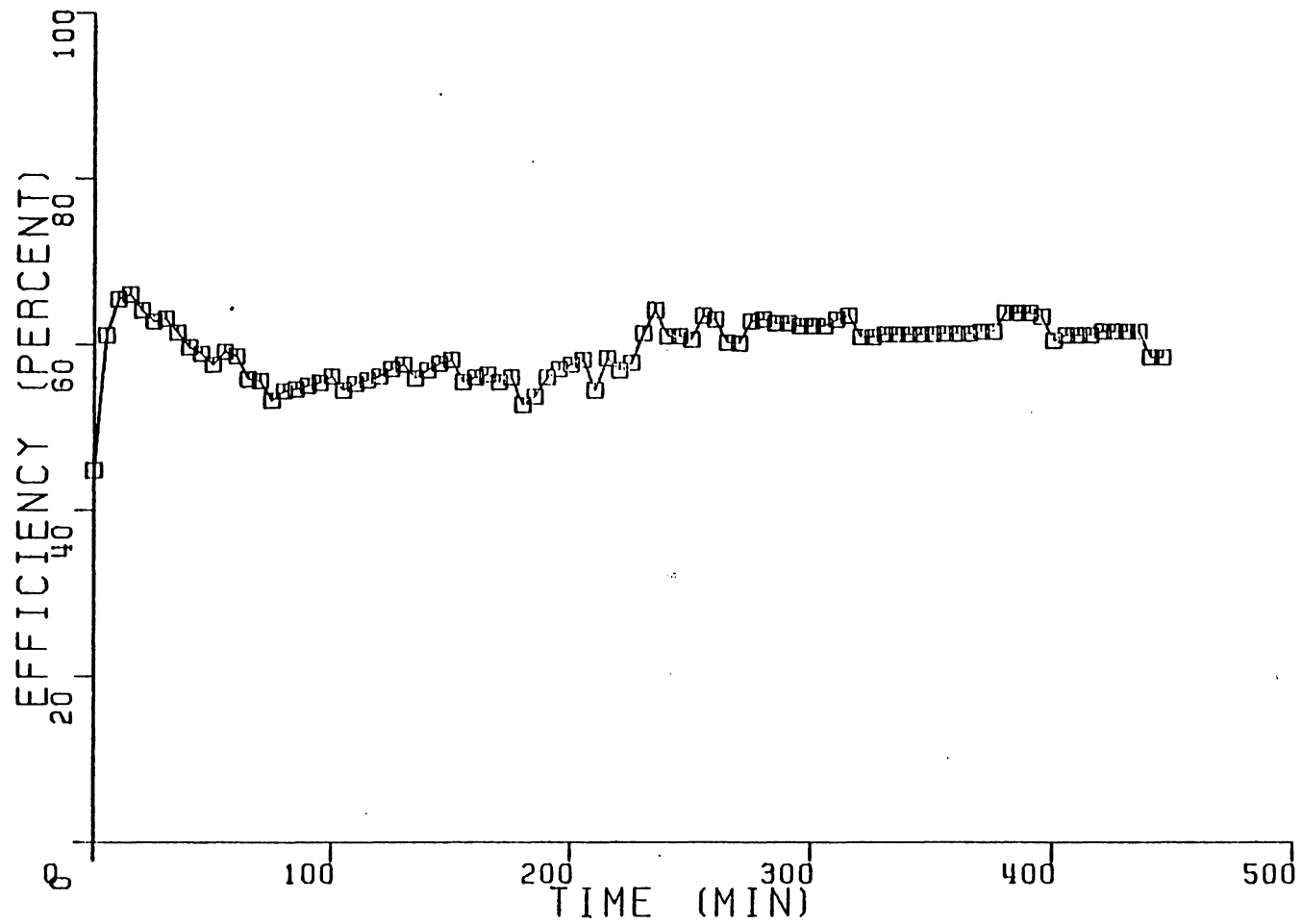


Figure 31. Instantaneous Efficiency for the Low Burning Rate Pocahontas Test.

TABLE VI. Energy Loss Distributions, Efficiencies, and Average Useful Heat Outputs for High and Low Burning Rate Tests.

<u>Test</u>	<u>Avg. Efficiency</u> %	<u>Avg. Sensible Energy Loss</u> %	<u>Avg. CO Energy Loss</u> %	<u>Avg. Energy Loss Due to Smoke</u> %	<u>Avg. Latent Energy Loss</u> %	<u>Avg. Useful Heat Output</u> (kW)
Full Output (Clinchfield) <sup>a</sup>	55	40	1.0	1.0	3.3	7.8
Full Output (Pocahontas) <sup>a</sup>	54	39	2.2	0.8	3.4	7.1
Low Output (Clinchfield) <sup>b</sup>	54	40	2.8	0.5	3.4	2.7
Low Output (Pocahontas) <sup>b,c</sup>	60	33	4.4	0.02	3.3	2.9
Updraft Stove (25) (Clinchfield) <sup>a</sup>	59-73	14-27	2.7-4.5	5.4-7.9	3.4-3.6	6.3-7.0
Updraft Stove (25) (Pocahontas) <sup>a</sup>	65-73	16-27	3.1-4.7	1.7-3.1	3.3	5.5-6.5

a - includes start-up

b - start-up not included

c - no stirring during test



efficiency. After the coal bed is stirred, the efficiency rises rapidly and the cycle then repeats itself.

The sensible energy losses from the Prince account for 81 to 88% of the total energy losses. The sensible energy losses are an order of magnitude greater than the other losses and seem to be caused by the 630 to 1800% excess air levels in the Prince.

The CO chemical energy losses are believed to be a function of primary air flow through the fuel bed. The CO emission factors for the low burning rate tests are higher than those for the high burning rate tests and seems to explain the higher CO chemical energy losses for the low burning rate tests. The chemical energy loss due to volatile hydrocarbon emissions was not considered because a hydrocarbon analyzer was not available. Volatile hydrocarbon emission factors have been reported to be 60% of the particulate emission factors for hand-fired coal furnaces (28). If this ratio holds true for the Prince, including the chemical energy loss due to the volatile organics would probably decrease its calculated efficiency by only one percentage point or less.

The energy loss due to smoke emissions is small, accounting for only about 1% or less of the total energy release rate. This is attributed to low smoke emissions, made possible by the Prince's design. Macumber (25) found the energy losses due to smoke to be as high as 8% of the total energy release rate, due to the substantially dirtier effluent from the updraft stoves he tested.

The average efficiencies are in fairly good agreement with the 50-55% values determined by the National Coal Board for the Prince. The

efficiencies are lower than those determined by Macumber (25). The "air-tight" stoves he tested have lower sensible energy losses than the Prince, but have somewhat higher chemical energy losses. However, the decrease in sensible energy loss is substantially greater than the increase in chemical energy loss. These stoves achieve higher efficiencies at the expense of higher CO emission factors.

Carbon balances conducted for the high burning rate Clinchfield and Pocahontas tests and the low burning rate Clinchfield and Pocahontas tests show that the total mass of coal burned during these tests, determined by integrating the instantaneous burning rates, are within 12, 10, 2.4, and 16%, respectively, of the scale-based values. This indicates that the orifice-calculated burning rates are reasonably consistent with the rates measured using the scale.

The useful heat output values for the high burning rate tests are considerably less than the 10.4 kW maximum rated output. It is possible that the Prince was tested at a lower draft than the unit was designed for. Also, differences in the properties of the test coals and the British coals may be responsible for the lower heat output.

#### 5.4 Uncertainty Analysis

Uncertainties in the results were determined using the method of Kline and McClintock (32). For the high burning rate tests, the average uncertainties in the mass burning rate, efficiency, CO, NO<sub>x</sub>, and SO<sub>x</sub> emission factors are 15%, 14%, 43%, 15%, and 18%, respectively. For the low burning rate tests, the average uncertainties in mass burning rate,

efficiency, CO, NO<sub>x</sub>, and SO<sub>x</sub> emission factors are 56%, 56%, 84%, 78%, and 56%, respectively. The uncertainties in the smoke emission factors are estimated at 20%.

The major contribution to the uncertainties in the results is attributed to the uncertainties in the CO and CO<sub>2</sub> readings. (CO/CO<sub>2</sub> analyzer uncertainties for the CO and CO<sub>2</sub> readings are  $\pm .03$  and  $\pm 0.2$  mole percent, respectively.) The average CO and CO<sub>2</sub> stack concentrations for the high and low burning rate tests were found to be 0.08 and 2.5 mole percent, and 0.10 and 1.1 mole percent, respectively. Since these values are small, the percent uncertainties in the readings become large -- up to 38%. However, the uncertainties in the CO and CO<sub>2</sub> readings are probably smaller due to accurate zeroing and spanning before each test and zero and span drift checks performed after each test. For these reasons, the uncertainty in the CO emission factor for the high burning rate tests is probably about 20% instead of 43%. The large uncertainties in the emission factors and efficiency for the low output tests are due to a large uncertainty in the mass burning rate, which is found using the measured CO and CO<sub>2</sub> concentrations. The carbon balance results show that the mass of coal burned during the test determined by the scale readings and from the carbon flow in the stack agree within 16%. This indicates that the uncertainty in mass burning rate is much smaller than 56%, probably about 20%. This lower burning rate uncertainty lowers the efficiency and emission factor uncertainties to probably 25% or less.

The  $\text{NO}_x$  and  $\text{SO}_x$  emission factors may be greater than reported due to possible absorption in the sampling train condenser. It is not known how much effect this had on the  $\text{NO}_x$  and  $\text{SO}_x$  emission factors.

It is not possible to determine the repeatability of the emission factors and efficiency for the complete (start-up and reload) tests, since duplicate tests were not run. However, there is good repeatability for the efficiency and emission factors (except smoke) between the start-up and reload portions of each test.

## 6. CONCLUSIONS

The flow in the secondary combustion chamber was found to be unsteady and three-dimensional. Thus, the probing results are difficult to interpret. The measurements do indicate, however, that the flow is quite stratified, which is indicative of poor mixing. Dilution of the product gases seems to be a major phenomenon affecting the species concentrations in the chamber. It is probable that very little soot or hydrocarbon oxidation occurs in the secondary combustion chamber due to short gas residence times and low gas temperatures of 440 - 1040°C.

The down-draft design of the Rayburn Prince 76 appears to be effective in reducing smoke emissions. This is evidenced by the smoke emission factors, which range from 2.3 to 7.8 g/kg without start-up smoke. The smoke emission factors are up to six times smaller than those found using identical coals in conventional updraft coal stoves. The smoke emission rates for the Prince operating on American bituminous coals generally meet the British smoke emission standards.

The instantaneous CO emission factors seem to be dependent on primary air flow rate. Reductions in primary air flow (caused by closing the closure plate or by coal agglomeration) resulted in higher CO emission factors, probably caused by CO quenching in the post flame gases. Reductions in primary air flow also seemed to lower the NO<sub>x</sub> emission factors. This was probably due to decreased fuel bed temperatures and allowing less primary air to be available in the high temperature regions.

The large air flow rates through the Rayburn Prince, indicated by excess air levels from 630-1800%, produced large sensible energy losses. However, the Prince's efficiency was found to be a respectable 54 to 60%.

## 7. RECOMMENDATIONS

1. The particulate concentrations at the inlet and outlet planes of the secondary combustion chamber could be determined simultaneously with several multi-inlet sampling probes. This technique might indicate the effectiveness of the secondary combustion chamber in reducing particulate emissions.
2. The use of a hydrocarbon analyzer in the probe sampling train would allow for hydrocarbon measurements in the secondary combustion chamber. These measurements could help determine if combustion of volatiles occurs in that zone.
3. Probe sampling should be conducted across the longitudinal dimension of the secondary combustion zone. This would yield additional information on species concentration gradients and dilution air flows in the chamber.
4. A CO/CO<sub>2</sub> analyzer with a higher resolution should be incorporated into the stack dilution tunnel gas sampling train. This would give less uncertainty in the calculated mass burning rates, emission factors, and efficiency values.
5. A hydrocarbon analyzer should be used to determine the hydrocarbon emissions from the Prince. This could be used to quantify the chemical energy losses due to volatile organics emissions.
6. An analysis of the sulfur content in the captured particulates should be performed. This would determine if the sulfur, unaccounted for as SO<sub>x</sub>, forms sulfates on the particulate surfaces.

7. The emissions and efficiency of the Rayburn Prince should be determined on a wide variety of American coals. This would determine the Prince's suitability for the American coal stove market.



## 8. REFERENCES

1. Landry, B. A., and R. A. Sherman, "The development of a design of a smokeless stove for bituminous coal," American Society of Mechanical Engineers Transactions, Vol. 72, 1948, Paper 48-A-119.
2. Ubhayakar, S. K., D. B. Stickler, C. W. Von Rosenberg, Jr., and R. E. Gannon, "Rapid devolatilization of pulverized coal in hot combustion gases", Sixteenth Symposium (International) on Combustion, The Combustion Institute, Pittsburg, PA (1976).
3. Howard, J. B., and R. H. Essenhigh, "Mechanism of solid particle combustion with simultaneous gas-phase volatiles combustion," Eleventh Symposium (International) on Combustion, The Combustion Institute, Pittsburg, PA (1967).
4. Calcote, H. F., "Mechanisms of soot nucleation in flames - a critical review", Combustion and Flame, Vol. 42, Sept. 1981, p. 215-242.
5. Gaydon, A. G., and H. G. Wolfhard, Flames, Chapman and Hall, London, 1979.
6. Prado, G. P., M. L. Lee, R. A. Hites, D. P. Hoult, and J. B. Howard, "Soot and hydrocarbon formation in a turbulent diffusion flame", Sixteenth Symposium (International) on Combustion, The Combustion Institute, Pittsburg, PA (1977).
7. Jaasma, D. R., and D. W. Macumber, "Measurement techniques and emission factors for hand-fired coal stoves", Proceedings of the Air Pollution Control Association Specialty Conference on Residential Wood and Coal Combustion, March 1-2, 1982. In press.
8. DeAngelis, D. G., and R. B. Reznik, "Source assessment: coal-fired residential combustion equipment field test", U.S. Environmental Protection Agency Report No. EPA 60012-78-004, June 1977.
9. Giammer, R. D., R. B. Engdahl, and R. E. Barret. "Emission from residential and small commercial stoker-coal-fired boilers under smokeless operation," U.S. Environmental Protection Agency Report No. EPA 60017-76-029, Oct. 1976.
10. Azbe, U. J., "Smokeless and efficient firing of domestic furnaces," American Society of Mechanical Engineers Transactions, Vol. 50, 1927, p. 223-238, Paper FSP-50-23.
11. British Standards Institute, "Method for the measurement of smoke from manufactured solid fuels for domestic open fires", British Standard 2841, 1972, 2 Park Street, London 2BS, England.

12. Dickinson, R., and R. C. Payne, "United Kingdom efficiency tests and standards for residential solid fuel heating appliances," in Residential Solid Fuels (J. Cooper and D. Malek, Eds.) Oregon Graduate Center, Beaverton, OR, 1982.
13. Kaye, W. G., "The development of smoke reducing coal-burning domestic appliances", 1971, Coal Research Establishment, National Coal Board, Stoke Orchard, Cheltenham Gos. GL42 4 RZ, England.
14. Butcher, S. S., and M. J. Ellenbecker, "Particulate emission factors for small wood and coal stoves", in Residential Solid Fuels, loc. cit.
15. Toynbee, P. A. "Domestic coal firing in smokeless zones," in Residential Solid Fuels, loc. cit.
16. Squires, A. M., Small Coal Furnaces: The Neglected Option, Virginia Polytechnic Institute and State University, Blacksburg, Virginia, 1981.
17. Hautman, D. J., F. L. Dryer, K. P. Schug, and I. Glassman, "A multiple-step overall kinetic mechanism for the oxidation of hydrocarbons", Department of Mechanical and Aerospace Engineering, Princeton University, Princeton, NJ.
18. Shelton, J. W., "Thermal performance testing of residential solid fuel heaters," in Residential Solid Fuels, loc. cit.
19. Allen, J. R., and E. F. Rowley, "Tests to determine the efficiency of coal stoves," American Society of Mechanical Engineers Transactions, Vol. 26, 1920, p. 115-122.
20. Thring, M. W. The Science of Flames and Furnaces, Wiley, New York, 1952.
21. Nicholls, P. "Underfeed combustion, effect of preheat, and distribution of ash in fuel beds, U.S. Bureau of Mines Bulletin 278, 1934.
22. Howard, J. B, G. C. Williams, and D. H. Fine, "Kinetics of carbon monoxide oxidation in postflame gases", Fourteenth Symposium (International) on Combustion, The Combustion Institute, Pittsburg, PA (1972).
23. Fristrom, R. M., and A. A. Westenberg, Flame Structure, McGraw-Hill, New York, 1965.

24. Macumber, D. W. and D. R. Jaasma, "Efficiency and emissions of a hand-fired residential coal stove," in Residential Solid Fuels, loc. cit.
25. Macumber, D. W. "Efficiency and emissions of hand-fired residential coal stoves," M.S. Thesis, Virginia Polytechnic Institute and State University, 1981.
26. Fenimore, C. P. and J. Moore, "Quenched carbon monoxide in fuel-lean flame gas," Combustion and Flame, Vol. 22, 1974, p. 343-351.
27. Mackend, J. "The effect of operating conditions on emissions from a two-stage lump coal combustor", M.S. Thesis, Virginia Polytechnic Institute and State University, 1982.
28. Hangebrauck, R. P., D. J. Von Lehnder, and J. E. Meeker, "Emissions on polynuclear hydrocarbons and other pollutants from heat generation and incineration processes", Journal of the Air Pollution Control Association, Vol. 14, No. 7, 1964.
29. Compilation of Air Pollutant Emission Factors, U.S. Environmental Protection Agency Publication No. AP-42 (Third Edition), 1977.
30. Beck, D. B., and J. D. Brain, "Prediction of the pulmonary toxicity of respirable combustion products from residential wood and coal stoves," Proceedings of the Air Pollution Control Association Specialty Conference on Residential Wood and Coal Combustion, March 1-2, 1982, In press.
31. Fischer, G. L., B. A. Prentice, D. Silberman, J. M. Ovpov, A. H. Biermann, R. C. Ragaini, and A. R. McFarland, "Physical and morphological studies of size-classified coal fly ash," Environmental Science and Technology, Vol. 12, April 1978, p. 447-451.
32. Holmann, J. P., Experimental Methods for Engineers, McGraw-Hill, New York, 1978.
33. Kays, W. M., and M. E. Crawford, Convection Heat and Mass Transfer, McGraw-Hill, New York, 1980.
34. Kramlich, H. C., and P. C. Malte, "Modeling and measurement of sample probe effects on pollutant gases drawn from flame zones," Combustion Science and Technology, Vol. 12, 1978, p. 91-104.

## APPENDIX A

### HEAT TRANSFER IN WATER-COOLED PROBE

In order to determine the quenching capability of the water-cooled probe it was necessary to calculate the temperature-time history of the gas sample. The temperature of the inner wall of the probe was assumed to be uniform and equal to the cooling water temperature. The temperature of the gas sample entering the probe was assumed to be 1300 K and the temperature profile was assumed to be developing along the probe axis. The flow in the probe had a calculated Reynolds number of 590 and was assumed to be laminar. The solution for this type of convective heat transfer problem is presented by Kays and Crawford (33). Their solution yields the axial distance from the probe tip needed to lower the gas temperature to any value lower than the entering temperature. This gives the temperature-distance history for the gas sample, and from the gas temperatures and molar flow rate in the probe the temperature-time curve can be found. The gas temperature as a function of distance and time from the probe tip is presented in Figure 32. The sample gas temperature is reduced from 1300 K to 700 K in only about 0.5 ms. This quenching time is adequate to prevent significant changes from occurring in the CO and NO<sub>x</sub> concentrations (34).

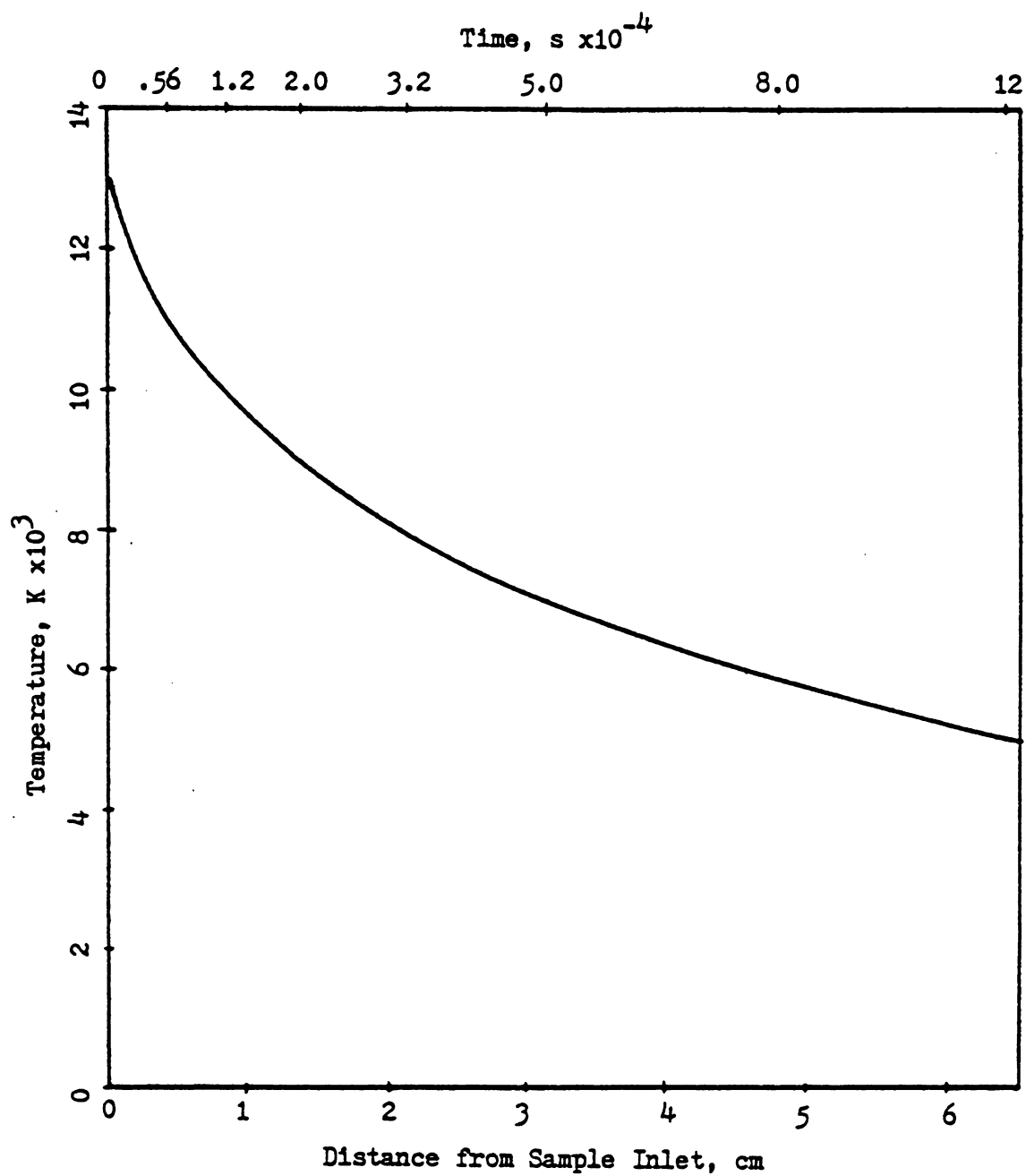


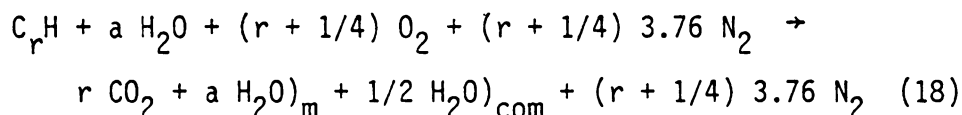
Figure 32. Sample Gas Temperature vs. Distance and Time from Tip of Water-Cooled Sampling Probe.

## APPENDIX B

### CONVERSION OF SPECIES CONCENTRATIONS FROM DRY TO WET BASIS

All species concentrations measured by the analyzers were on a dry basis due to most of the water vapor in the sample being condensed out. In order to correct the species concentrations to their true values, the mole fraction of water in the sample must be calculated. The water vapor in the gases leaving the Prince is due to moisture in the coal, water vapor formed by combustion, and moisture present in the combustion air.

Representing dry coal as  $C_rH$ , where  $r$  is the carbon to hydrogen ratio in the coal, a reaction equation for the stoichiometric combustion of coal can be written as



where

$a$  = molar ratio of water to hydrogen in coal

$H_2O)_m$  = water vapor in product gas due to moisture in coal

$H_2O)_{com}$  = water vapor in product gas formed by combustion

The mole fractions of water vapor in the sample gas due to the moisture in the coal and the moisture formed by combustion (assuming all the hydrogen in the coal forms water) are given by

$$x_{\text{H}_2\text{O}})_m = \frac{a}{r} x_{\text{CO}_2})_w \quad (19)$$

$$x_{\text{H}_2\text{O}})_{\text{com}} = \frac{1}{2r} x_{\text{CO}_2})_w \quad (20)$$

where

$x_{\text{H}_2\text{O}})_m$  = mole fraction of water in sample gas from moisture in coal

$x_{\text{CO}_2})_w$  = mole fraction of  $\text{CO}_2$  in sample gas (wet basis)

$x_{\text{H}_2\text{O}})_{\text{com}}$  = mole fraction of water in sample gas formed by combustion

If the gas sample leaving the condenser is just above  $0^\circ\text{C}$  and is saturated, the partial pressure of the water is 0.61 kPa. The mole fraction of water vapor in the gas sample (from humidity in combustion air) that was removed in the condenser is given by

$$x_{\text{H}_2\text{O}})_h = \frac{\phi P_{\text{sr}} - 0.61}{P} \quad (21)$$

where

$\phi$  = relative humidity of combustion air

$x_{\text{H}_2\text{O}})_h$  = mole fraction of water in sample gas from humidity in the air

$P_{\text{sr}}$  = saturation pressure of moisture in air at room temperature, kPa

$P$  = atmospheric pressure, kPa

The mole fraction of  $\text{CO}_2$  in the moist flue gases is given by

$$x_{\text{CO}_2})_w = x_{\text{CO}_2})_D \left[ 1 - \frac{a}{r} x_{\text{CO}_2})_w - \frac{1}{2r} x_{\text{CO}_2})_w - \frac{\phi^P_{sr} - 0.61}{P} \right] \quad (22)$$

where

$x_{\text{CO}_2})_D$  = measured  $\text{CO}_2$  mole fraction (dry basis)

Rearranging the above equation, the dry to wet basis correction factor,  $C_{DW}$ , is given by

$$C_{DW} = \frac{x_{\text{CO}_2})_w}{x_{\text{CO}_2})_D} = \frac{1 - \frac{\phi^P_{sr} - 0.61}{P}}{1 + \left( \frac{a}{r} + \frac{1}{2r} \right) x_{\text{CO}_2})_D} \quad (23)$$

The wet-basis  $\text{CO}$ ,  $\text{CO}_2$ ,  $\text{O}_2$ ,  $\text{NO}_x$ , and  $\text{SO}_x$  concentrations are given by

$$x_{x})_w = C_{DW} x_{x})_D \quad (24)$$

where:

$x_{x})_w$  = mole fraction of gas species (wet basis)

$x_{x})_D$  = mole fraction of gas species (dry basis)



## APPENDIX C

### DATA REDUCTION PROGRAM LISTING

```
C *****
C * THIS PROGRAM CALCULATES THE INSTANTANEOUS AND *
C * AVERAGE EFFICIENCY, CO,NOX, AND SOX EMISSION *
C * FACTORS FOR A COAL STOVE SET UP IN THE *
C * VIRGINIA TECH SOLID FUELS FURNACE TESTING *
C * FACILITY. IN ADDITION, THE ENERGY LOSSES DUE *
C * TO SENSIBLE HEAT PASSING UP THE STACK, *
C * INCOMPLETE CO OXIDATION,LATENT HEAT OF *
C * VAPORIZATION OF WATER, AND SMOKE FORMATION *
C * ARE CALCULATED. *
C *****
C
C NOMENCLATURE
C A = MOLAR RATIO OF WATER TO HYDROGEN IN COAL
C AREA = THE ORIFICE AREA , M**2
C AEFCO = AVERAGE CO EMISSION FACTOR , G CO/KG FUEL
C AEFNOX = AVERAGE NOX EMISSION FACTOR , G NOX/KG FUEL
C AEFSOX = AVERAGE SOX EMISSION FACTOR , G SOX/KG FUEL
C AESEN = AVERAGE SENSIBLE ENERGY LOSS , KW
C AEEO = AVERAGE CO CHEMICAL ENERGY LOSS , KW
C AEH2O = AVERAGE LATENT ENERGY LOSS , KW
C AESM = AVERAGE ENERGY LOSS DUE TO SMOKE EMISSIONS , KW
C AEFFIC = AVERAGE MASS- WEIGHTED EFFICIENCY , %
C CD = THE ORIFICE DISCHARGE COEFFICIENT
C CDWS = DRY TO WET CORRECTION FACTOR FOR MEASURED
C CONCENTRATIONS IN STACK
C CDWD = DRY TO WET CORRECTION FACTOR FOR MEASURED
C CONCENTRATIONS IN DILUTION TUNNEL
C ECO = INSTANTANEOUS CO ENERGY LOSS , KW
C EDOT = INSTANTANEOUS CHEMICAL ENERGY RELEASE RATE, KW
C EFCO = INSTANTANEOUS CO EMISSION FACTOR ,
C G CO/KG FUEL BURNED
C EFFIC = INSTANTANEOUS EFFICIENCY , %
C EFNOX = INSTANTANEOUS NOX EMISSION FACTOR ,
C G NOX/KG FUEL BURNED
C EFSOX = INSTANTANEOUS SOX EMISSION FACTOR ,
C G SOX/KG FUEL BURNED
C EH2O = INSTANTANEOUS LATENT ENERGY LOSS , KW
C ESEN = INSTANTANEOUS SENSIBLE ENERGY LOSS , KW
C ESM = INSTANTANEOUS ENERGY LOSS DUE TO SMOKE , KW
C HFGW = ENTHALPY OF VAPORIZATION OF H2O , J/MOL
```

```

C      HVC = HEATING VALUE OF THE COAL , KJ/KG
C      HVCO = HEATING VALUE OF CO , KJ/KG
C      II = NUMBER OF LINES OF DATA POINTS
C      MASST = TOTAL MASS OF COAL BURNED DURING TEST
C              (CALCULATED FROM BURNING RATE EQ.) , KG
C      MDOT(I) = INSTANTANEOUS BURNING RATE OF COAL , KG/S
C      MFCC = THE MASS FRACTION OF CARBON IN THE COAL
C      MFCSM = THE MASS FRACTION OF CARBON IN THE SMOKE
C      MFH2O = THE MASS FRACTION OF WATER IN THE COAL
C      MSMC = MASS OF SMOKE COLLECTED DURING TEST , G
C      MSME = MASS OF SMOKE EMITTED DURING TEST , G
C      NDOTD(I) = MOLAR FLOW RATE IN DILUTION TUNNEL , MOL/S
C      NDOTP = MOLAR FLOW RATE IN SMOKE PROBE , MOL/S
C      NDOTS = MOLAR FLOW RATE IN STACK , MOL/S
C      NOXSCL = SCALE USED ON NOX ANALYZER
C      PB = AMBIENT PRESSURE , MM HG
C      PHI = RELATIVE HUMIDITY OF ROOM AIR
C      PSR = SATURATION PRESSURE OF WATER AT ROOM TEMP. , KPA
C      Q600 = SOX SAMPLE ROTAMETER FLOW RATE , L/S
C      Q603 = SOX DILUTION ROTAMETER FLOW RATE , L/S
C      Q604 = SMOKE TRAIN ROTAMETER FLOW RATE , M**3/S
C      QD = VOLUMETRIC FLOW RATE IN DILUTION TUNNEL , M**3/S
C      QS = VOLUMETRIC FLOW RATE IN STACK , M**3/S
C      R = MOLAR RATIO OF CARBON TO HYDROGEN IN COAL
C      TD = DILUTION TUNNEL GAS TEMPERATURE , K
C      TR = ROOM TEMPERATURE , K
C      TS = STACK GAS TEMPERATURE , K
C
C      DIMENSION B(200,12),MDOT(200),NDOTD(200)
C      REAL NDOTS,MFH2O,MDOT,MFCC,MSMC,MFCSM,HVC,NDOTD
C      REAL MCO,MCOT,MNOX,MNOXT,MSOX,MSOXT,MASST
C      REAL MSME,NDOTT,NDOTDA,NDOTP
C      THE VALUES OF HVC,MFCC,MFCSM,MFH2O,MSMC,R,A
C      ARE READ IN.
C      READ (5,*) HVC, MFCC, MFCSM, MFH2O, MSMC, R, A
C      THE VALUES OF II, TR, PB, PHI, PSR, Q604 ARE READ IN.
C      READ (5,*) II, TR, PB, PHI, PSR,Q604
C      HFGW = 43749.
C      AREA = 0.00212
C      CD = 0.608
C      HVCO = 282993.0
C      NOXSCL = 200.
C      INITIALIZE VARIABLES:
C      EFFICT=0.0
C      MASST=0.0
C      EDOTT=0.0
C      MCOT=0.0
C      MNOXT=0.0
C      MSOXT=0.0

```

```

ESENT=0.0
EH2OT=0.0
ESMT=0.0
ECOT=0.0
NDOTT=0.0

C
PRINT 110
C
THE DATA IS READ IN TO THE PROGRAM
READ(5,*) ((B(I,K),K=1,12),I=1,II)
C
WHERE
C
B(I,1) = TIME OF READING (MINUTES, STARTING FROM ZERO)
C
B(I,2) = PRESSURE DROP ACROSS ORIFICE , IN H2O
C
B(I,3) = CO READING IN STACK , MOLE %
C
B(I,4) = CO2 READING IN STACK , MOLE %
C
B(I,5) = O2 READING IN STACK , DVM READING
C
B(I,6) = CO2 READING IN DILUTION TUNNEL , MOLE %
C
B(I,7) = NOX READING IN DILUTION TUNNEL , DVM READING
C
B(I,8) = SOX READING IN DILUTION TUNNEL , DVM READING
C
B(I,9) = SOX SAMPLE ROTAMETER READING
C
B(I,10)= SOX DILUTION ROTAMETER READING
C
B(I,11)= STACK GAS TEMPERATURE , C
C
B(I,12)= DILUTION TUNNEL GAS TEMPERATURE , C
C
C
THE PROGRAM IS RUN FOR THE VARIOUS DATA POINTS.
C
DO 5 I=1,II
C
THE DILUTION TUNNEL TEMPERATURE IS CONVERTED TO
C
DEGREES KELVIN.
B(I,12)=B(I,12)+273.
C
THE MOLAR FLOW RATE IN THE DILUTION TUNNEL IS GIVEN BY
NDOTD(I)=CD*AREA*SQRT((2*B(1,2)*PB*33.14)/
X      (8.315*B(I,12)*29))
NDOTT=NDOTT+NDOTD(I)
5
CONTINUE
C
DO 10 I=1,II
C
THE STACK GAS TEMPERATURE IS CONVERTED TO DEGREES K
TS=B(I,11) + 273.
C
CHANGE BAROMETRIC PRESSURE UNITS FROM MM HG TO KPA
PA=PB*0.13333
C
THE CORRECTION FACTOR FOR CONVERTING STACK
C
CONCENTRATIONS FROM DRY TO WET BASIS IS GIVEN BY
CDWS=(1.-(PHI*PSR-.61)/PA)/(1.+(A/R+1./(2*R))
X      *(B(I,4)/100.))
C
THE CORRECTION FACTOR FOR CONVERTING DILUTION TUNNEL
C
CONCENTRATIONS FROM DRY TO WET BASIS IS GIVEN BY
CDWD=(1.-(PHI*PSR-.61)/PA)/(1.+(A/R+1./(2.*R))
X      *(B(I,6)/100.))

```

```

C      THE CO,CO2 AND O2 READINGS IN THE STACK ARE CORRECTED
C      TO WET BASIS AND CONVERTED TO MOLE FRACTIONS.
      B(I,3) = B(I,3) * CDWS/100.
      B(I,4) = B(I,4) * CDWS/100.
      B(I,5) = B(I,5) * CDWS/4.

C
C      THE CO2,NOX AND SOX READINGS IN THE DILUTION TUNNEL
C      ARE CORRECTED TO WET BASIS AND CONVERTED TO MOLE
C      FRACTIONS.
      B(I,6) = B(I,6)*CDWD/100.
      B(I,7) = B(I,7)*CDWD*NOXSCL*1.0E-06
      B(I,8) = B(I,8)*1.0E-06*CDWD

C
C      THE MOLAR FLOW RATE IN THE STACK IS GIVEN BY
      NDOTS=NDOTD(I)*B(I,6)/B(I,4)

C
C      THE AVERAGE MOLAR FLOW RATE IN THE DILUTION TUNNEL
C      IS GIVEN BY
      NDOTDA=NDOTT/II
C      THE MOLAR FLOW RATE IN THE SMOKE PROBE IS GIVEN BY
      NDOTP=Q604*PA/(8.315*TR)
C      THE TOTAL MASS OF SMOKE EMITTED DURING THE TEST IS
C      GIVEN BY
      MSME=MSMC*NDOTDA/NDOTP

C
C      THE INSTANTANEOUS MASS BURNING RATE IS GIVEN BY
      MDOT(I)=((B(I,3)+B(I,4))*NDOTS*12.+MSME*MFCSM
X      /(300000*II))/MFCC
      MASST=MDOT(I)*300.+MASST

C
C      THE MASS OF CO EMITTED DURING A DATA INTERVAL IS
C      GIVEN BY
      MCO=B(I,3)*NDOTS*28.*300.*1000.
C      THE INSTANTANEOUS CO EMISSION FACTOR IS GIVEN BY
      EFCO=MCO/(MDOT(I)*300.)
      MCOT=MCO +MCOT

C
C      THE MASS OF NOX EMITTED OVER A DATA INTERVAL IS
C      GIVEN BY
      MNOX=B(I,7)*NDOTD(I)*46.*300.*1000.
C      THE INSTANTANEOUS NOX EMISSION FACTOR IS GIVEN BY
      EFXOX=MNOX/(MDOT(I)*300.)
      MNOXT=MNOX+MNOXT

C
C      THE DILUTION RATIO OF THE SOX SAMPLE IS CALCULATED
C      FROM THE SAMPLE AND DILUTION FLOW RATES.
      C600 = 2.85714E-02*B(I,9)-2.28571
      Q600 = (2.42519E-02+1.42164E-02*C600+2.22656E-03
X      *C600*C600)*1/60

```

```

C603 = 2.85714E-02*B(I,10)-2.28571
Q603 = 2.84586E-02+1.03191E-02*C603-1.19544E-03
X      *C603*C603

C
C      THE MOLE FRACTION OF SOX IN THE DILUTION TUNNEL
C      IS GIVEN BY
C      B(I,8) = B(I,8)*(Q600+Q603)/Q600
C      THE MASS OF SOX EMITTED DURING A DATA INTERVAL
C      IS GIVEN BY
C      MSOX=B(I,8)*NDOTD(I)*64.*300.*1000.
C      THE INSTANTANEOUS SOX EMISSION FACTOR IS GIVEN BY
C      EFSOX=MSOX/(MDOT(I)*300.)
C      MSOXT=MSOX+MSOXT

C
C      THE INSTANTANEOUS ENERGY RELEASE RATE IS GIVEN BY
C      EDOT=HVC*MDOT(I)
C      EDOTT=EDOT+EDOTT

C
C      THE INSTANTANEOUS SENSIBLE ENERGY LOSS IS GIVEN BY
C      ESEN=NDOTS*30.*(TS-TR)
C      ESENT=ESEN*MDOT(I)*300.+ESENT

C
C      THE INSTANTANEOUS ENERGY LOSS DUE TO CO EMISSIONS
C      IS GIVEN BY
C      ECO = NDOTS*B(I,3)*HVCO
C      ECOT=ECO*MDOT(I)*300.+ECOT

C
C      THE INSTANTANEOUS LATENT ENERGY LOSS IS GIVEN BY
C      EH2O=(MDOT(I)*MFH2O/18.+NDOTS*(B(I,3)+B(I,4)))/(2.*R)
X      +MFCSM*MSME/(2.*R*12.*300000*II))*HFGW
C      EH2OT=EH2O*MDOT(I)*300.+EH2OT

C
C      THE INSTANTANEOUS ENERGY LOSS DUE TO SMOKE EMISSIONS
C      IS GIVEN BY
C      ESM = HVC*MSME/(300000*II)
C      ESMT=ESM*MDOT(I)*300.+ESMT

C
C      THE INSTANTANEOUS EFFICIENCY IS GIVEN BY
C      EFFIC=(1.0-((ESEN+ECO+EH2O+ESM)/EDOT))*100.0
C      EFFICT=EFFIC*MDOT(I)*300.+EFFICT

C
C      TIME = 5*(I-1)
C      WRITE (6,100) TIME,EFFIC,EFCO,EFNOX,EFSOX,MDOT(I)
110  FORMAT(8X,4HTIME,6X,5HEFFIC,6X,4HEFCO,7X,5HEFNOX,6X,
X      5HEFSOX,6X,4HMDOT)
100  FORMAT(1X,F11.0,4F11.3,F11.6)
10  CONTINUE

```

```
AEFCO=MCOT/MASST
AEFNOX=MNOXT/MASST
AEFSOX=MSOXT/MASST
AEDOT=EDOTT/I I
AECO=ECOT/MASST
AESEN=ESENT/MASST
AEH2O=EH2OT/MASST
AESM=ESMT/MASST
AEFFIC=EFFICT/MASST
EFSM=MSME/MASST
PRINT 190
WRITE(6,200) AEFCO,AEFNOX,AEFSOX,EFSM
190  FORMAT(6X,5HAEFCO,6X,6HAEFNOX,5X,6HAEFSOX,5X,4HEFSM)
200  FORMAT (1X,4F11.3)
PRINT 210
WRITE(6,220) AEFFIC,AESEN,AEH2O,AECO,AESM,AEDOT
210  FORMAT(6X,6HAEFFIC,6X,5HAESEN,6X,5HAEH2O,7X,4HAECO,
X      5X,4HAESM,6X,5HAEDOT)
220  FORMAT (1X,6F11.3)
STOP
END
```

## APPENDIX D

### MEASURED AXIAL SPECIES CONCENTRATIONS IN THE SECONDARY COMBUSTION ZONE FOR THE HIGH, INTERMEDIATE, AND LOW BURNING RATE TESTS

TABLE VII. Measured Axial Species Concentrations (Wet Basis) in Secondary Combustion Zone for High Burning Rate Test.

<u>Run</u>	<u>Probe Position (cm from Datum)</u>	<u>CO (mole %)</u>	<u>CO<sub>2</sub> (mole %)</u>	<u>O<sub>2</sub> (mole %)</u>	<u>NO<sub>x</sub> (PPM)</u>
1	0	.34	7.5	10.9	127
	3	.43	6.2	12.9	86.8
	6	.45	6.1	12.8	70.8
	9	.45	6.3	12.7	67.3
	12	.20	3.4	16.6	45.6
2	0	.51	5.8	14.0	57.8
	3	.46	6.0	13.0	61.6
	6	.38	6.6	12.1	73.6
	9	.28	7.1	11.2	87.9
	12	.21	2.7	17.4	32.4
3	0	.51	4.8	14.8	60.0
	3	.43	5.8	13.3	67.5
	6	.39	6.0	13.0	66.0
	9	.30	6.9	12.2	73.5
	12	.23	2.9	16.9	35.8
4	0	.22	2.9	16.8	40.8
	3	.13	8.1	10.3	97.7
	6	.11	8.5	9.9	108
	9	.09	9.8	8.1	121
	12	.08	9.3	9.2	66.1



TABLE VIII. Measured Axial Species Concentrations (Wet Basis) in Secondary Combustion Zone for Intermediate Burning Rate Test.

<u>Run</u>	<u>Probe Position (cm from Datum)</u>	<u>CO (mole %)</u>	<u>CO<sub>2</sub> (mole %)</u>	<u>O<sub>2</sub> (mole %)</u>	<u>NO<sub>x</sub> (PPM)</u>
1	0	.20	9.2	9.6	91.0
	3	.14	10.9	7.8	117
	6	.19	8.8	10.1	99.3
	9	.24	8.4	10.4	90.8
	12	.13	2.2	18.1	24.1
2	0	.11	11.5	6.4	120
	3	.17	10.7	7.9	117
	6	.21	9.1	9.4	99.2
	9	.31	7.5	11.3	74.7
	12	.15	1.7	18.3	20.7
3	0	.17	9.2	9.2	101
	3	.24	8.9	9.8	80.1
	6	.35	7.2	11.8	67.1
	9	.37	6.0	13.1	59.7
	12	.16	1.7	18.6	23.7
4	0	.61	8.4	9.8	83.1
	3	.48	5.9	14.2	48.0
	6	.45	5.6	13.6	47.1
	9	.42	5.1	14.3	46.7
	12	.17	1.6	18.6	20.2

TABLE IX. Measured Axial Species Concentrations (Wet Basis) in Secondary Combustion Zone for Low Burning Rate Test.

<u>Run</u>	<u>Probe Position (cm from Datum)</u>	<u>CO (mole %)</u>	<u>CO<sub>2</sub> (mole %)</u>	<u>O<sub>2</sub> (mole %)</u>	<u>NO<sub>x</sub> (PPM)</u>
1	0	.29	9.4	8.85	153
	3	.40	11.5	6.52	176
	6	.43	11.0	7.20	153
	9	.25	9.5	8.94	132
	12	.10	1.8	18.3	23.7
2	0	.46	6.4	12.9	66.8
	3	.67	9.4	8.97	117
	6	.66	9.1	9.41	102
	9	.51	7.0	11.4	78.3
	12	.09	1.7	18.1	17.8
3	0	.52	5.9	13.2	61.6
	3	.68	8.5	10.1	98.0
	6	.64	8.5	10.0	92.7
	9	.61	7.3	11.8	71.4
	12	.15	1.6	18.2	17.8
4	0	.54	5.2	13.6	60.3
	3	1.03	7.3	11.2	76.7
	6	1.01	6.9	11.8	68.6
	9	.78	5.5	12.9	51.0
	12	.14	2.0	18.3	18.7

## APPENDIX E

### CALCULATION OF DILUTED CO<sub>2</sub> CONCENTRATIONS

In order to calculate the concentration of CO<sub>2</sub> at a position in the secondary combustion zone if only dilution effects are considered, the O<sub>2</sub> concentration at that position and the CO<sub>2</sub> and O<sub>2</sub> concentration at the previous position are needed. The gas at the initial position, i, was assumed to be a 1 mole mixture of CO<sub>2</sub>, O<sub>2</sub>, and N<sub>2</sub>. The amount of dilution air added between point i and the next sampling point, i + 1, can be calculated from the measured O<sub>2</sub> concentrations at each point by

$$x_{O_2)_{i+1}} = \frac{x_{O_2)_{i}} + 0.21 n_{air}}{1 + n_{air}} \quad (25)$$

where

$x_{O_2)_{i+1}}$  = measured O<sub>2</sub> mole fraction at point i+1

$x_{O_2)_{i}}$  = measured O<sub>2</sub> mole fraction at point i

$n_{air}$  = number of moles of dilution air added between points i and i+1

The concentration of CO<sub>2</sub> at i + 1, based on dilution effects, can be calculated by

$$x_{CO_2)_{i+1}} = \frac{x_{CO_2)_{i}}}{1 + n_{air}} \quad (26)$$

where

$x_{\text{CO}_2}^{i+1}$  = calculated  $\text{CO}_2$  mole fraction at point  $i+1$

$x_{\text{CO}_2}^i$  = measured mole fraction of  $\text{CO}_2$  at point  $i$

**The vita has been removed from  
the scanned document**

EMISSIONS, EFFICIENCY,  
AND COMBUSTION CHAMBER CONDITIONS  
OF A SMOKELESS, HAND-FIRED COAL HEATER

by

Daniel Waslo

(ABSTRACT)

The emissions, efficiency, and combustion chamber conditions of the Rayburn Prince 76, a clean-burning, hand-fired coal heater developed by the British have been studied. It was desired to determine if the downdraft design of the Prince would lead to low emissions when operated on American coals.

Temperature and species concentrations were measured in the unit's secondary combustion chamber. Temperatures and gas residence times in the secondary combustion chamber were found to range from 440 to 1040°C and 15 to 40 ms, respectively. Little soot and volatile oxidation probably occurred in the chamber, due to the relatively low temperatures and short residence times.

The emissions and efficiency of the heater were determined for operation on two bituminous coals at both high and low firing rates. The CO, NO<sub>x</sub>, SO<sub>x</sub>, and smoke emission factors were found to range from 38 to 120 g/kg, 1.2 to 5.8 g/kg, 3.3 to 5.4 g/kg, and 2.3 to 16 g/kg, respectively. The smoke emission factors for the Prince were found to be up to six times lower than those found using identical coals in

updraft stoves. The overall efficiency of the unit was determined to range from 54 to 60%. The sensible energy losses were found to represent the majority of the total energy losses.